Astrocyte-specific function of OTUD7B in experimental autoimmune encephalomyelitis

Thesis

for the degree of

doctor rerum naturalium

(Dr. rer. nat.)

approved by the Faculty of Natural Sciences of Otto von Guericke University Magdeburg

by M.Sc. Wenjing Yi

born on 13.10.1986 in Shaanxi, China

Examiner: Prof. Dr. med. Dirk Schlüter

PD Dr. Fred Lühder

submitted on: 20.12.2021

defended on: 16.06.2022

PUBLICATIONS

Yi W, Schlüter D, Wang X. Astrocytes in multiple sclerosis and experimental autoimmune encephalomyelitis: Star-shaped cells illuminating the darkness of CNS autoimmunity. Brain Behav Immun. 2019 Aug;80:10-24. doi: 10.1016/j.bbi.2019.05.029.

Wang X, Mulas F, Yi W, Brunn A, Nishanth G, Just S, Waisman A, Brück W, Deckert M, Schlüter D. OTUB1 inhibits CNS autoimmunity by preventing IFN-γ-induced hyperactivation of astrocytes. EMBO J. 2019 May 15;38(10):e100947. doi: 10.15252/embj.2018100947.

Mulas F, Wang X, Song S, Nishanth G, Yi W, Brunn A, Larsen PK, Isermann B, Kalinke U, Barragan A, Naumann M, Deckert M, Schlüter D. The deubiquitinase OTUB1 augments NF-κB-dependent immune responses in dendritic cells in infection and inflammation by stabilizing UBC13. Cell Mol Immunol. 2020 Feb 5. doi: 10.1038/s41423-020-0362-6.

SUMMARY (IN GERMAN)

Multiple Sklerose (MS) ist eine chronische demyelinisierende Krankheit, die das Zentralnervensystem (ZNS) befällt. Bei der MS handelt es sich um eine Autoimmunerkrankung mit Beteiligung von T-Zellen, jedoch sind die Mechanismen, die zur Neuroinflammation und Demyelinisierung führen, noch nicht vollständig geklärt. Astrozyten, die am weitesten verbreitete Gliazellpopulation des ZNS, sind wichtig für die Homöostase des ZNS und können bei der MS sowohl schädliche als auch schützende Funktionen haben. Die genauen molekularen Mechanismen der Regulierung der Astrozytenfunktion bei der Autoimmerkrankungen des ZNS sind noch weitgehend unbekannt. In GEO-Datenbanken publizierte Genexpressionsanalysen indizieren eine signifikante Verringerung der Expression von OTUD7B im Gehirn von MS-Patienten im Vergleich zu gesunden Probanden, was auf eine mögliche Rolle von OTUD7B bei der MS hinweist. Daher untersuchten wir die Funktion des deubiquitinierenden Enzyms OTUD7B in Astrozyten im Modell der experimentellen murinen autoimmunen Enzephalomyelitis (EAE), einem Tiermodell der MS. Mäuse mit einer Deletion von *OTUD7B* in Astrozyten (GFAP-Cre OTUD7B$^{fl/fl}$-Mäuse) entwickelten im Vergleich zu OTUD7B$^{fl/fl}$-Kontrollmäusen eine schwerere EAE mit verstärkter Neuroinflammation und ZNS-Schäden, was die schützende Rolle von astrozytärem OTUD7B bei Autoimmunerkrankungen des ZNS unterstreicht. Die Histologie des Rückenmarks von Mäusen mit EAE zeigte, dass die Astrozyten von GFAP-Cre OTUD7B$^{fl/fl}$-Mäusen hyperaktiviert und teilweise aus den entzündeten Bereichen verschwunden waren. Die Stimulation kultivierter Astrozyten zeigte, dass der Mangel an OTUD7B zu einer verstärkten Aktivierung der NF-κB- und MAPK-Signalwege sowie zu einer erhöhten Expression von Zytokinen und Chemokinen bei Stimulation mit Tumornekrosefaktor (TNF) führte. OTUD7B-defiziente Astrozyten waren auch anfälliger für den TNF- und CHX-induzierten Zelltod, was durch erhöhte Werte von gespaltener Caspase-8 und Caspase-3 belegt wird. Mechanistisch gesehen entfernte OTUD7B zunächst K63-gebundene Ubiquitinketten von RIPK1, indem es bei TNF-Stimulation an TRAF2 rekrutierte und so die Aktivierung der NF-κB- und MAPK-Signalwege einschränkte. Anschließend interagiert OTUD7B mit RIPK1 und TRAF2, um deren Degradation zu verhindern, indem es die K48-gebundene Ubiquitinierung hydrolysiert, was wiederum die Spaltung von Pro-Caspase 8 verhindert. Insgesamt haben unsere Studien OTUD7B als protektiven Faktor in Astrozyten während EAE identifiziert und gezeigt, dass OTUD7B die TNF-vermittelte proinflammatorische Reaktion und Apoptose von

Astrozyten unterdrückt und dadurch die Demyelinisierung und die klinischen Symptome der EAE begrenzt.

SUMMARY

Multiple sclerosis (MS) is a chronic demyelinating disease affecting the central nervous system (CNS). Although MS is an autoimmune disease with the involvement of T cells, the mechanisms leading to neuroinflammation and demyelination are incompletely understood. Astrocytes, the most prevalent glial cell population of the CNS, are important for the homeostasis of the CNS, but are also considered to play both detrimental and protective functions in MS. However, the precise molecular mechanisms on the regulation of astrocyte function in CNS autoimmunity are still largely unknown. GEO databases report a significant reduction in the expression of OTUD7B in the brains of MS patients compared to healthy subjects, indicating the potential role of OTUD7B in MS. Therefore, we studied the function of the deubiquitinating enzyme OTUD7B in astrocytes during murine experimental autoimmune encephalomyelitis (EAE), an animal model for MS. Mice with deletion of *OTUD7B* in astrocytes (GFAP-Cre OTUD7B$^{fl/fl}$ mice) developed more severe EAE compared to control OTUD7B$^{fl/fl}$ mice, with enhanced neuroinflammation, underlying the protective role of astrocytic OTUD7B in CNS autoimmune diseases. Histology of the spinal cord from mice with EAE showed that astrocytes of GFAP-Cre OTUD7B$^{fl/fl}$ mice were hyperactivated and partially lost from areas with inflammation. Stimulation of cultivated astrocytes revealed that OTUD7B deficiency resulted in enhanced activation of the NF-κB and MAPK pathways, as well as increased expression of cytokines and chemokine upon stimulation with tumor necrosis factor (TNF). OTUD7B-deficient astrocytes were also more vulnerable to TNF and CHX induced cell death, as indicated by increased levels of cleaved caspase 8 and caspase 3. Mechanistically, OTUD7B first removed K63-linked ubiquitin chains from RIPK1 via recruiting to TRAF2 upon TNF stimulation, thereby limiting the activation of the NF-κB and MAPK pathways. Subsequently, OTUD7B interacts with RIPK1 and TRAF2 to prevent its degradation by hydrolyzing K48-linked ubiquitination, which in turn prevented the processing of pro-caspase 8. Collectively, our studies identified OTUD7B as a protective factor in astrocytes during EAE and revealed that OTUD7B suppressed the TNF-mediated proinflammatory response and apoptosis of astrocytes, thereby limiting demyelination and clinical signs of EAE.

TABLE OF CONTENTS

PUBLICATIONS II

SUMMARY (IN GERMAN) III

SUMMARY V

TABLE OF CONTENTS VI

LIST OF FIGURES IX

LIST OF TABLES X

..... X

ABBREVIATIONS XI

1. INTRODUCTION 1

1.1 Multiple sclerosis and experimental autoimmune encephalomyelitis 1

1.2 Astrocytes 4

1.2.1 Astrocytes 4

1.2.2 Astrocytes in EAE and MS 5

1.2.3 Signaling in astrocytes during EAE 8

1.3 TNF signaling 10

1.4 Ubiquitination and deubiquitination 14

1.5 Ubiquitination and deubiquitination in TNF signaling 17

1.6 OTUD7B 20

2. AIMS 23

3. MATERIALS AND METHODS 24

3.1 Materials 24

3.1.1 Materials for animal experiments 24

3.1.2 Materials for cell culture 24

3.1.3 Primers 25

3.1.4 Materials for molecular biology 26

3.1.5 Materials for proteomics 26

3.1.6 Antibodies for western blot and immunoprecipitation 28

3.1.7 Antibodies for flow cytometry 29

3.1.8 Kits 30

3.1.9 Consumables 30

3.1.10 Instruments 31

3.1.11 Software 32

3.1.12 Animals 32

3.2 Methods 33

3.2.1 Genotyping of the mouse strains 33

3.2.2 EAE induction and assessment 33

3.2.3 Isolation of leukocytes 34

3.2.4 Flow cytometry 35

3.2.5 Magnetic-activated cell sorting (MACS) of astrocytes 36

3.2.6 Transcriptome 36

3.2.7 Primary astrocyte culture 36

3.2.8 Immunohistochemistry 37

3.2.9 Astrocyte treatment 37

3.2.10 Quantitative real time-PCR (RT-PCR) 37

3.2.11 Immunoprecipitation 38

3.2.12 Western blot 38

3.2.13 Statistics 39

4. RESULTS 40

4.1 Anti-inflammatory function of OTUD7B in astrocytes during EAE 40

4.1.1 OTUD7B expression is reduced in MS and increased in EAE 40

4.1.2 Generation and characterization of mice with astrocytic deletion of OTUD7B 42

4.2 Astrocytic OTUD7B ameliorates EAE 44

4.2.1 Aggravated EAE in GFAP-Cre OTUD7B$^{fl/fl}$ mice 44

4.2.2 Increased infiltration of immune cells in the spinal cord of GFAP-Cre OTUD7B$^{fl/fl}$ mice 45

4.2.3 Increased transcription of proinflammatory factors in the spinal cord of GFAP-Cre OTUD7B$^{fl/fl}$ mice 47

4.2.4 OTUD7B suppressed TNF-induced expression of proinflammatory cytokines in astrocytes 49

4.2.5 OTUD7B impairs TNF-induced NF-κB and MAPK pathways 50

4.2.6 OTUD7B deficiency leads to increased ubiquitination of RIPK1 51

4.3 Pro-survival function of astrocytic OTUD7B in EAE 53

4.3.1 OTUD7B deficiency renders astrocytes susceptible to TNF and CHX induced cell death 54

4.3.2 OTUD7B protects RIPK1 and TRAF2 from degradation 57

4.3.3 OTUD7B stabilizes TRAF2 and RIPK1 via removing K48-linked ubiquitin chains 59

4.3.4 OTUD7B interacts with TRAF2 and RIPK1 in a time-dependent manner 60

5. DISCUSSION 61

REFERENCES 68

DECLARATION OF ORIGINALITY 84

DECLARATION OF HONOR 85

LIST OF FIGURES

Figure 1. Clinical courses of MS and EAE 3

Figure 2. Schematic illustration of astrocyte functions in EAE and MS 8

Figure 3. Signaling in astrocytes regulated by T cell-derived cytokines 10

Figure 4. General information of TNF signaling 14

Figure 5. Ubiquitination 16

Figure 6. Ubiquitin system in TNF signaling 19

Figure 7. Structure of OTUD7B (human) 20

Figure 8. OTUD7B protein expression in mice and mRNA in MS brains 40

Figure 9. OTUD7B expression is increased in astrocytes during EAE. 41

Figure 10. Characterization of GFAP-Cre OTUD7B$^{fl/fl}$ mice under homeostatic conditions .. 43

Figure 11. GFAP-Cre OTUD7B$^{fl/fl}$ mice developed more severe EAE. 45

Figure 12. Increased infiltration of leukocytes and encephalitogenic CD4^{+} T cells in the spinal cord of GFAP-Cre OTUD7B$^{fl/fl}$ mice 46

Figure 13. Increased cytokines and chemokines in spinal cord of GFAP-Cre OTUD7B$^{fl/fl}$ mice during EAE 48

Figure 14. OTUD7B suppresses TNF-induced expression of pro-inflammatory factors. 50

Figure 15. OTUD7B deficiency upregulates TNF signaling in astrocytes 51

Figure 16. OTUD7B interacts with TRAF2 upon TNF stimulation 52

Figure 17. GFAP-Cre OTUD7B$^{fl/fl}$ mice have more astrocyte loss 54

Figure 18. OTUD7B-deficient astrocytes undergo increased TNF-induced apoptosis. 55

Figure 19. OTUD7B protects astrocytes from TNF-induced apoptosis. 56

Figure 20. OTUD7B deficiency destabilizes RIPK1 and TRAF2 58

Figure 21. OTUD7B removes K48-linked ubiquitin chains from RIIPK1 and TRAF2 59

Figure 22. OTUD7B removes K48-linked ubiquitin chains from RIPK1 and TRAF2 60

Figure 23. Summary of the study 67

LIST OF TABLES

Table 1. Primers for Genotyping 25

Table 2. Primers for real-time PCR 25

Table 3. Antibodies for western blot and immunoprecipitation 28

Table 4. Antibodies for flow cytometry 29

Table 5. PCR program 33

Table 6. EAE score 34

Table 7. Recipe for AKR lysis buffer 35

Table 8. PCR program 38

Table 9. OTUD7B deficiency in astrocytes reduces disease incidence and symptoms 44

ABBREVIATIONS

7-AAD	7-aminoactinomycin D
A	
AD	Alzheimer's disease
APC	antigen-presenting cell
B	
BBB	blood brain barrier
bFG	basic fibroblast growth factor
BSA	bovine serum albumin
C	
CCL	C-C motif chemokine ligand
CHX	cycloheximide
cIAP	cellular inhibitor of apoptosis protein
CIS	clinically isolated syndrome
CNS	central nervous system
CSF	cerebrospinal fluid
CXCL	C-X-C motif ligand
CXCR	C-X-C motif chemokine receptor
CYLD	cylindromatosis
D	
DC	dendritic cell
DUBs	deubiquitinating enzymes
E	
EAE	experimental autoimmune encephalomyelitis
EGFR	epidermal growth factor receptor
ERK	extracellular-signal-regulated kinase
F	
FADD	fas associated via death domain
FasL	Fas Ligand

FCS	fetal calf serum
FLIP	FLICE-like inhibitory protein
G	
GFAP	glial fibrillary acidic protein
GM-CSF	granulocyte-macrophage colony-stimulating factor
H	
HPRT	hypoxanthine-guanine phosphoribosyltransferase
I	
ICAM1	intercellular adhesion molecule 1
IFN	interferon
IKK	IκB kinase
IL	interleukin
J	
JAMM	JAB1/MPN/MOV34 metalloenzymes
JNK	c-Jun N-terminal kinases
L	
LPS	lipopolysaccharides
M	
MACS	magnetic-activated cell sorting
MAPK	mitogen-activated protein kinase
MBP	myelin basic protein
MJD	machado-Josephin domain
MOG	myelin oligodendrocyte glycoprotein
MS	multiple sclerosis
N	
Nec1s	necrostatin 1s
NEMO	NF-κB essential modulator
NF-κB	nuclear factor κB
NK	natural killer
NLS	nuclear localization signal
NO	nitric oxide

NOS2	nitric oxide synthase 2
O	
OPCs	oligodendrocyte progenitor cells
OTU	ovarian tumour
OTUD7B	OTU domain-containing 7B
P	
PD	Parkinson's disease
PFA	paraformaldehyde
PLP	proteolipid protein
PMSF	phenylmethanesulfonylfluoride
PPMS	primary progressive multiple sclerosis
Q	
qRT-PCR	quantitative real-time polymerase chain reaction
R	
RIPK1	receptor-interacting protein kinase 1
RRMS	relapsing-remitting multiple sclerosis
S	
Sox2	sex determining region Y-box 2
SPMS	secondary progressive multiple sclerosis
STAT1	signal transducer and activator of transcription 1
T	
TAB	TGFβ activated kinase 1 (MAP3K7) binding protein
TAK1	TGFβ-activated kinase 1
TCR	T cell receptor
TGFβ	transforming growth factor-β
TLR	Toll-like receptor
TNF	tumor necrosis factor
TRAF	TNF receptor-associated factor
TRAIL	TNF-related apoptosis-inducing ligand
U	
Ub	ubiquitin

UBA	ubiquitin-associated
UCH	ubiquitin C-terminal hydrolases
USP	ubiquitin-specific proteases

V

VCAM1	vascular cell adhesion molecule 1

W

WB	western blot

Z

ZnF	zinc finger domain

1. INTRODUCTION

1.1 Multiple sclerosis and experimental autoimmune encephalomyelitis

Multiple sclerosis (MS) is a chronic autoimmune disease of the central nervous system (CNS). More than 2.8 million people are living with MS worldwide, notably in North America, Australia, Canada, and northern Europe (Walton, King et al. 2020). The diagnosis of MS is based on the McDonald criteria according to the evaluation of symptoms and laboratory findings (McGinley, Goldschmidt et al. 2021). The age of the patients at the time point of diagnosis ranges from 20 to 50 and the incidence in women is nearly three times than in men (McGinley, Goldschmidt et al. 2021). The patients present physical and cognitive disabilities, such as weakness, blurred vision, fatigue, and tingling sensations. Four different courses of MS have been identified (Fig. 1a) (Hurwitz 2009). The most common one is relapsing-remitting (RR) MS, which affects approximately 80 % of the patients, marked by phases of progression and remission but with overall increasing disability over time. Most patients living with RRMS eventually turn into secondary progressive (SP) MS (Fig. 1b). In this stage, the disease progresses gradually without remission. Another 10-15 % of MS patients shows disease progression from the onset of the disease, defined as primary progressive (PP) MS (Fig. 1c). Last, clinically isolated syndrome (CIS) is termed as one single episode of neurologic symptoms, which lasts more than 24 hours (Fig. 1d). Currently, MS cannot be cured, but the treatment of RRMS with disease-modifying therapies and lifestyle modifications are successfully applied to improve the life quality via slowing down the disease progression, reducing the severity of attacks and frequency of relapses (McGinley, Goldschmidt et al. 2021). The etiology of MS is still unknown, but the interplay of environmental and genetic factors is believed to contribute to MS development and influence its outcome. The environmental risk factors identified include Epstein–Barr virus infection, smoking, and childhood obesity (McGinley, Goldschmidt et al. 2021). Many genetic risk factors are associated with an increased susceptibility to MS (Patsopoulos 2018), the major histocompatibility complex (MHC) being one of the strongest factors. For example, people with the human leukocyte antigen (HLA)-DR1*15:01 allele have a high risk of MS (Patsopoulos, Barcellos et al. 2013), indicating that T cells, which recognize and are activated by MHC/antigen complex contribute to the disease.

Experimental autoimmune encephalomyelitis (EAE) is a widely used animal model for MS to study MS pathogenesis and to explore possible treatment options. EAE can be induced by active immunization with myelin antigens, such as myelin oligodendrocyte glycoprotein (MOG), proteolipid protein (PLP), and myelin basic protein (MBP). A classic course of EAE is observed in MOG_{35-55} immunized C57BL/6 mice (Mendel, Kerlero de Rosbo et al. 1995). The stages consist of pre-onset, onset, peak, and remission (Fig. 1e). Alternatively, EAE can be induced by adoptive transfer of autoreactive $CD4^+$ T cells, which are primed by myelin antigens to induce a profound T-cell mediated CNS disease (Constantinescu, Farooqi et al. 2011). $CD4^+$ T cells are crucial for the induction of EAE and also contribute to MS. Among the $CD4^+$ T cells, interferon (IFN)-γ producing Th1 cells, interleukin (IL)-17 producing Th17 cells, and granulocyte-macrophage colony-stimulating factor (GM-CSF) producing T cells are the principal effector cells, which can induce EAE independently by passive transfer (Domingues, Mues et al. 2010, Codarri, Gyulveszi et al. 2011). EAE shares numerous clinical, immunological, and pathological features with MS, including neuroinflammation, glial cell activation, axon loss, and overt demyelinated lesions (Constantinescu, Farooqi et al. 2011). The lesions, termed as an area of damage caused by inflammation, can be classified into 1. active inflammatory lesions with numerous T cells and macrophages, and 2. chronic lesions with fewer leukocytes, but profound tissue damage and glial scars. There are also some differences in the pathology of human MS and murine EAE. The differences between MS and EAE include 1. the lesions in EAE are mainly discovered in the spinal cord, whereas, the lesions are located in the brains of MS patients (Simmons, Pierson et al. 2013), 2. $CD8^+$ T cells are the predominant lymphocytes in MS lesions and are involved in the pathogenesis of MS (Salou, Nicol et al. 2015), whereas, $CD4^+$ T cells are the dominant cell type in the lesions of mice with EAE. In addition, successful treatment of murine EAE with immune modulators could fail to show effectivity in MS. Therefore, care should be taken while extrapolating findings from EAE to MS.

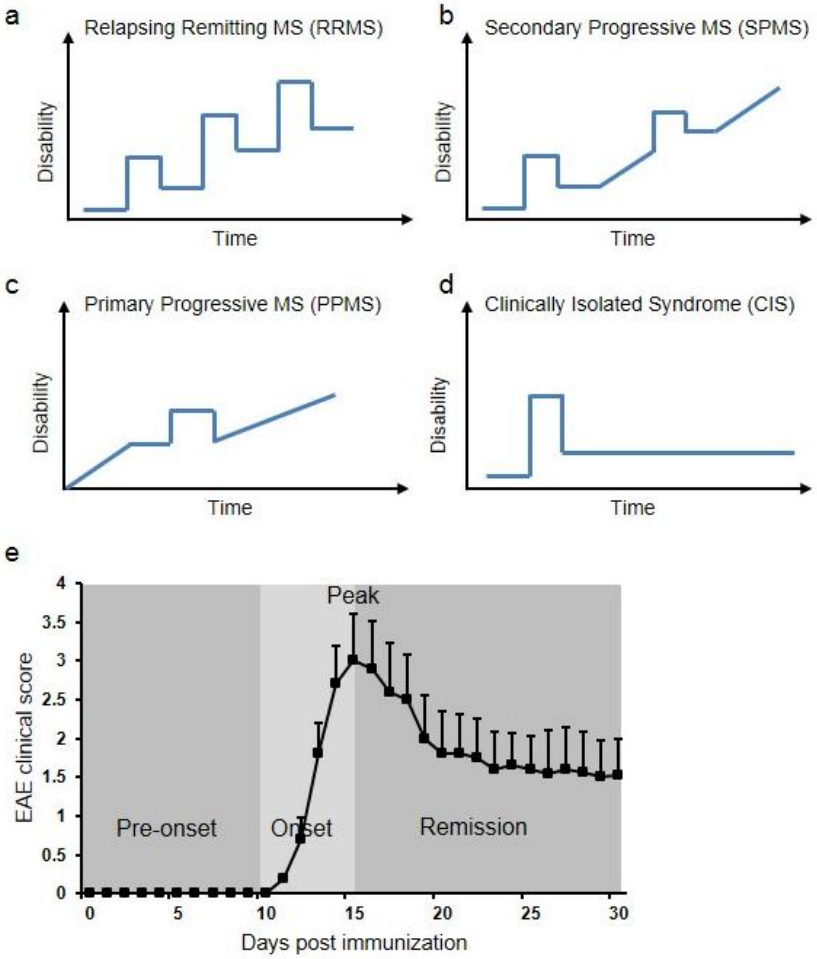

Figure 1. Clinical courses of MS and EAE

The clinical courses of MS include relapsing remitting (RR) MS (a), secondary progressive (SP) MS (b), primary progressive (PP) MS (c), clinically isolated syndrome (CIS) (d). In RRMS, patients experience several episodes of attacks after remission. In SPMS, the disease course progresses gradually. In PPMS, the disease progresses continuously after onset without remission. CIS is described as a single episode of symptoms. e. The classic course of EAE consists of pre-onset, onset, peak, and remission. EAE is induced by immunization with MOG_{35-55} in complete Freund's adjuvant and C57BL/6 mice develop a single attack followed by recovery after the peak of disease.

1.2 Astrocytes

1.2.1 Astrocytes

Astrocytes represent the most abundant glial cell population in CNS and play diverse roles in the development and homeostasis of the CNS. The end-feet of astrocytes form glia limitans to ensheath the blood vessels, supporting the integrity of the blood-brain barrier (BBB) and creating a crucial barrier selectively allowing the transmission of small molecules into CNS. Astrocytes regulate neuronal activity by maintaining extracellular ions and energy metabolism, glutamate uptake, and promoting synapse formation and remodeling (Walz 2000, Brown and Ransom 2007, Chung, Allen et al. 2015). Lipids, the substrates for myelin synthesis and membrane homeostasis in oligodendrocytes, are synthesized by astrocytes (Camargo, Goudriaan et al. 2017). In addition, astrocytes establish heterotypic coupling with oligodendrocytes via gap junctions to facilitate metabolic transportation and myelin function. Recently, Sanmarco et al. found that astrocytes limit the spread of inflammation via acquiring the signal from IFN-γ^+ NK cells and upregulating TNF-related apoptosis-inducing ligand (TRAIL), which induces the apoptosis of effector T cells (Sanmarco, Wheeler et al. 2021).

Astrocytes are distributed in the whole CNS and can be divided into two groups according to their location and morphology: fibrous astrocytes in white matter, which contact axons at the node of Ranvier, and protoplasmic astrocytes in grey matter, which enwrap blood vessels with their end-feet. The functions performed by the two groups are different: fibrous astrocytes are involved in metabolic support, while protoplasmic astrocytes participate in the synaptic processes (Gonzalez-Giraldo, Forero et al. 2021). Recently, investigators have identified more regional and functional-specific diversity of astrocytes (John Lin, Yu et al. 2017, Borggrewe, Grit et al. 2021). For example, subcortical astrocytes promote neurite growth and synaptic activity of neurons, whereas astrocytes from the spinal cord and forebrain highly express genes related to myelination and cholesterol synthesis.

In CNS diseases, astrocytes respond to various factors, such as pathogens, cytokines, growth factors, environmental toxins, and undergo morphological and functional changes. In particular, astrogliosis is a common pathological hallmark characterized by the upregulation of the intermediate filament glial fibrillary acidic protein (GFAP) in the activated astrocytes. In reverse, reactive astrocytes are vital regulators of pathological diseases, including MS,

Alzheimer's disease (AD), and Parkinson's disease (PD) (Li, Li et al. 2019). Further studies identified two distinct phenotypes of astrocytes, A1 and A2 (Liddelow, Guttenplan et al. 2017). A1 astrocytes, induced by microglia-derived IL-1α, tumor necrosis factor (TNF), and complement component 1q (C1q), are characterized by the expression of the complement component 3 (C3) and are the dominant phenotype in neurodegenerative diseases. A1 astrocytes partially lose the capacities of synapse formation and myelin debris clearance, instead, produce neurotoxic factors triggering the rapid death of neurons and oligodendrocytes. In contrast, neuroprotective A2 astrocytes upregulate the production of neurotrophic factors, including brain-derived neurotrophic factor (BDNF), vascular endothelial growth factor (VEGF), and basic fibroblast growth factor (bFG). Considering the distinct roles of A1 and A2 astrocytes, the reversion of A1 to A2 astrocytes may be a promising therapeutic approach for the treatment of neurodegenerative diseases.

1.2.2 Astrocytes in EAE and MS

The mechanism underlying the neuroinflammatory process in EAE, can be described as a two-wave phenomenon (Wang, Deckert et al. 2013). Autoantigen-specific T cells are activated in the periphery and migrate to subarachnoid/perivascular space (wave I), where they are reactivated by local antigen presenting cells (APCs) and initiate the inflammatory cascades. In response to inflammatory stimuli produced by autoantigen-specific T cells, such as TNF, IL-17, and GM-CSF, adjacent CNS-resident cells release chemoattractant chemokines and cytokines, leading to the second round of recruitment of immune cells into the CNS, including monocytes and macrophages which attack myelin sheath and lead to neuronal loss (wave II). Glial cells, including astrocytes and microglia, are essential players in the transition from wave I to wave II and regulate neuroinflammation. Notably, the importance of astrocytes in initiating and maintaining MS has been pointed out by Wheeler and Rothhammer et al., who showed that environmental exposure to commensal bacterial metabolites and the herbicide linuron promotes pathogenic activities of astrocytes (Rothhammer, Borucki et al. 2018, Wheeler, Jaronen et al. 2019). Additionally, the presence of reactive astrocytes from the pre-lesion stage to the late chronic stage of disease indicates a fundamentally important role of astrocytes in MS (Ludwin, Rao et al. 2016). Further research confirmed that the dominant phenotype of astrocytes in demyelinating lesions is A1 (Liddelow, Guttenplan et al. 2017), which indicates the detrimental role of astrocytes in MS. Similarly, astrocytes acquire an immune-activated phenotype in EAE, which contribute to

neuroinflammation by producing chemokines (e.g., C-C motif chemokine ligand (CCL) 2, CCL20, C-X-C motif ligand 1 (CXCL1), CXCL10) and cytokines (e.g., TNF, IL-1, IL-6), to recruit and activate lymphocytes and microglia (Fig. 2). For example, CCL2 is primarily expressed by astrocytes and has a profound impact on the outcome of EAE. Astrocyte-specific CCL2-deficient mice had an improved course of the disease and flow cytometric analysis of the brain and spinal cord showed a reduced number of M1 macrophages and Th17 cells (Moreno, Bannerman et al. 2014). Importantly, CCL2 regulates the BBB integrity by reducing the surface levels of tight junction proteins on endothelial cells, thereby increasing the permeability of the endothelial barrier (Stamatovic, Keep et al. 2009). Furthermore, CCL2 expressed by perivascular astrocytes is involved in T cell extravasation as confocal microscopy analysis showed highly immunoreactive CCL2-expressing astrocytes in the areas with T cell infiltration (Carrillo-de Sauvage, Gomez et al. 2012). Other chemokines released by astrocytes are known for the recruitment of various types of immune cells, such as, CCL20 for $CCR6^+$ immune cells (Reboldi, Coisne et al. 2009), CXCL1 for neutrophils (Michael, Bricio-Moreno et al. 2020), and CXCL10 for $CXCR3^+$ T cells (Sorensen, Trebst et al. 2002). Astrocytes are the principal cells in the antioxidative stress response to sustain CNS homeostasis. However, during EAE, astrocytes produce increased inducible nitric oxide synthase (iNOS) which generates nitric oxide (NO) (Liu, Zhao et al. 2001). Oligodendrocytes and oligodendrocyte progenitor cells (OPCs) are vulnerable to free radicals and tend to undergo cell death. In all, reactive astrocytes together with leukocytes and microglia create a microenvironment rich in pro-inflammatory factors and oxidative stress. In contrast, neuroprotective roles are impaired in astrocytes, as reflected by the diminished production of neurotrophic factors and impaired glutamate buffering (Hardin-Pouzet, Krakowski et al. 1997, Liddelow, Guttenplan et al. 2017).

The role of astrocytes in MS pathogeneses is complex, as depletion of reactive astrocytes at early stages leads to a worse disease outcome (Toft-Hansen, Fuchtbauer et al. 2011), indicating the overall protective role of astrocytes in MS (Fig. 2). The protective roles of astrocytes include scar formation, induction of T cell apoptosis, and myelin repair to promote the remission (Yi, Schluter et al. 2019). Reactive astrocytes play a crucial role in the formation of glial scars, a physical barrier which prevents the spread of inflammation. In addition, they eliminate T cells by inducing apoptosis and are thereby fostering the recovery process. Astrocytes constitutively express Fas ligand (FasL) and the levels are increased in

astrocytes in chronic MS lesions. The importance of FasL in astrocytes has been illustrated by GFAP-Cre $FasL^{fl/fl}$ mice, with a specific deletion of FasL in astrocytes. GFAP-Cre $FasL^{fl/fl}$ mice fail to eliminate infiltrating Fas^{+} $CD4^{+}$ T cells, are unable to recover after the disease peak upon EAE induction, and suffer persisting paralysis (Wang, Haroon et al. 2013). TRAIL expressed on astrocytic end-feet induces the apoptosis of effector T cells in perivascular space (Sanmarco, Wheeler et al. 2021). In addition, astrocytes facilitate the regeneration by recruiting microglia to clear myelin debris, and promoting survival, proliferation, and differentiation of OPCs (Skripuletz, Hackstette et al. 2013, Lohrberg, Winkler et al. 2020).

Considering the importance of protective astrocytes in CNS diseases and the presence of apoptotic astrocytes in MS lesions (Dowling, Husar et al. 1997, Palma, Yauch et al. 1999), it is worth exploring the mechanism behind astrocyte activation and apoptosis. Our previous study identified that the receptor gp130 is associated with astrocytic survival via activating Ras/extracellular-signal-regulated kinase (ERK) pathway. Compared to GFAP-Cre $gp130^{fl/fl}$ mice, $gp130^{fl/fl}$ mice had an attenuated autoimmune T cell response and myelin damage (Haroon, Drogemuller et al. 2011, Toft-Hansen, Fuchtbauer et al. 2011). Previous studies have identified Fas (CD95) as a cell death inducer of astrocytes, which is widely expressed in reactive astrocytes in MS. Fas evokes caspase-dependent apoptosis when encountering FasL $(CD95L)^{+}$ $CD4^{+}$ T cells. Vice versa, $FasL^{+}$ astrocytes can induce the apoptosis of autoimmune $CD4^{+}$ T cells (Wang, Haroon et al. 2013). Nitric oxide (NO) acts in an autocrine way to trigger caspase-dependent apoptosis in astrocytes (Suk, Lee et al. 2001). Astrocytes are the major cell type to uptake glutamate, however, excessive glutamate can also induce apoptosis in an ERK1/2-dependent way (Szydlowska, Gozdz et al. 2010).

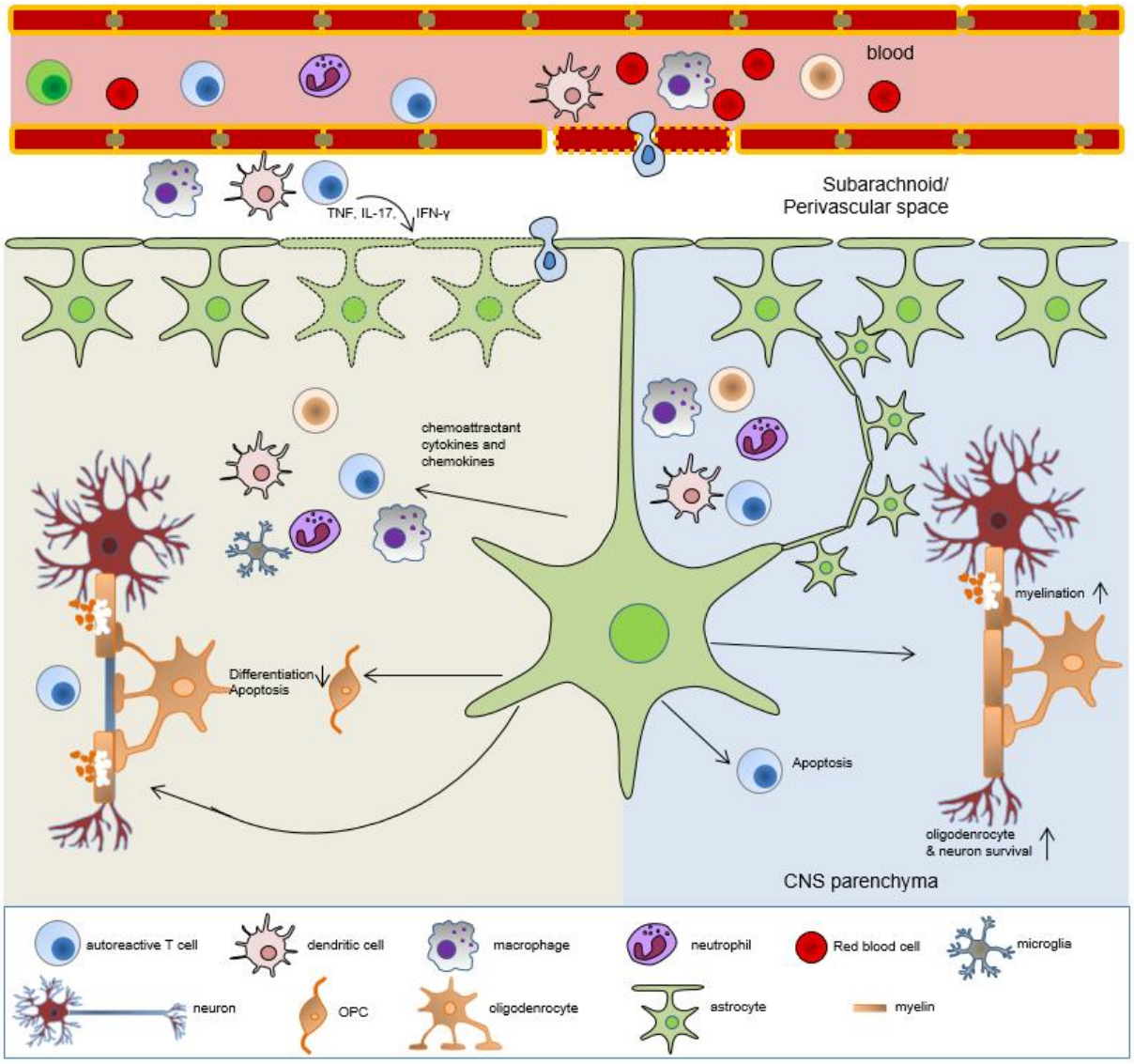

Figure 2. Schematic illustration of astrocyte functions in EAE and MS

In CNS autoimmunity, astrocytes are activated. These reactive astrocytes contribute to the inflammation by releasing cytokines and chemokines, which enhance the recruitment of immune cells to cause the damage of neurons and oligodendrocytes. On the other hand, reactive astrocytes form a glial scar to limit the spread of inflammation, trigger the apoptosis of T cells via death receptors, and promote regeneration (modified from (Yi, Schluter et al. 2019)).

1.2.3 Signaling in astrocytes during EAE

Astrocytes are crucial regulators of neuroinflammation. In response to various cytokines, including TNF, GM-CSF, IL-17 and IFN-γ, several signaling cascades are activated, such as

nuclear factor κB (NF-κB), mitogen-activated protein kinase (MAPK), and signal transducer and activator of transcription 1 (STAT1) (Fig. 3). The importance of the NF-κB pathway in pathogenic astrocytes in disease has been illustrated by the identification of genetic variant *rs7665090*^{G}, which is associated with the susceptibility to MS (Ponath, Lincoln et al. 2018). Astrocytes from MS patients harboring this risk variant show increased activation of NF-κB and expression of target gene products for lymphocyte recruitment and neurotoxicity, including A1 astrocyte marker C3, intercellular adhesion molecule 1 (ICAM1), CXCL10, and CCL5. Inhibition of the NF-κB pathway in astrocytes by silencing genes of the NF-κB cascade, such as IκB kinase (IKK) β, IκBα, or IKKγ, attenuates the course of EAE (van Loo, De Lorenzi et al. 2006, Brambilla, Persaud et al. 2009, Raasch, Zeller et al. 2011). The NF-κB pathway can be activated by multiple stimuli, such as GM-CSF, IL-17, TNF, and IL-1. Deletion of the GM-CSF receptor in astrocytes reduces the activation of the pro-inflammatory pathways and ameliorates EAE (Wheeler, Clark et al. 2020). IL-17, produced by Th17 cells, is increased in cerebrospinal fluid (CSF) and lesions in MS patients (Lock, Hermans et al. 2002, Kostic, Dzopalic et al. 2014). IL-17 deficient mice develop less severe EAE, with delayed disease onset, decreased clinical scores, and early remission (Komiyama, Nakae et al. 2006). The IL-17 signaling relies on the adaptor Act1. Deletion of astrocytic Act1 impairs IL-17-induced activation of NF-κB, inhibits the expression of inflammatory genes, and attenuates the ongoing clinical disease of EAE (Kang, Altuntas et al. 2010, Yan, Ding et al. 2012). In addition, increased levels of B4GALT6 and lactosylceramides (LacCer) have been found in astrocytes in MS lesions. Mechanistically, LacCer is synthesized by B4GALT6 and acts in an autocrine manner to activate NF-κB (Mayo, Trauger et al. 2014). Another key signaling pathway in astrocytes is induced by IFN-γ which triggers the JAK/STAT1 pathway. IFN-γ is a fingerprint cytokine mainly produced by Th1 cells and IFN-γ producing cells are found in the CNS before the onset of clinical symptoms (Olsson 1992), implicating the role of IFN-γ in disease initiation. Silencing the IFN-γ receptor in astrocytes suppresses chemokine expression, reduces the infiltration of inflammatory cells, and improves EAE outcomes (Ding, Yan et al. 2015). Furthermore, IFN-γ signaling increases the expression of C-X-C motif chemokine receptor (CXCR) 7, a receptor for CXCL12, specifically in spinal cord astrocytes, promoting the accumulation of Th1 cell in the spinal cord at the early stage of EAE (Williams, Manivasagam et al. 2020).

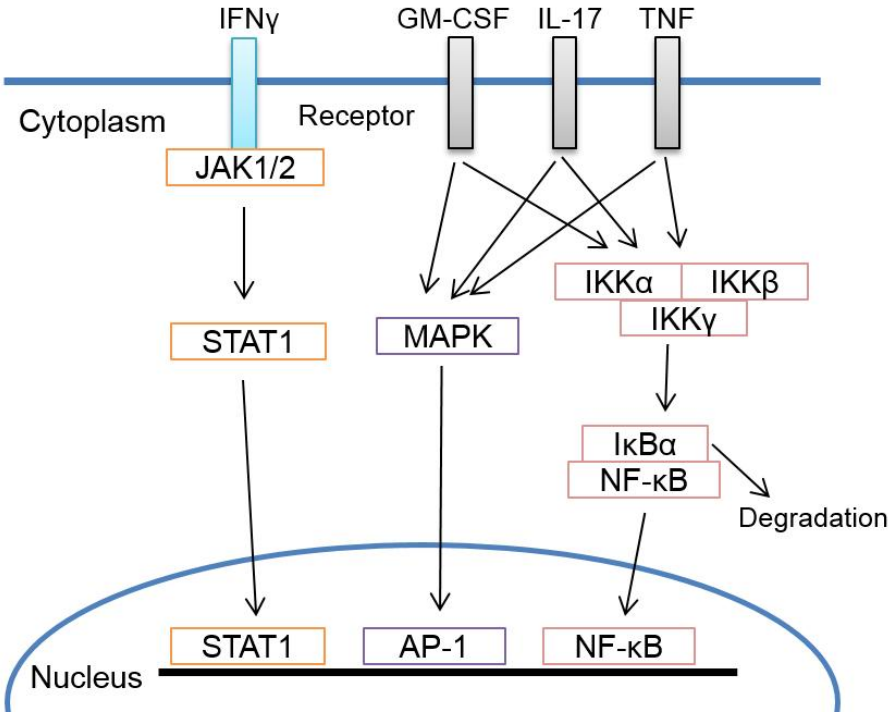

Figure 3. Signaling in astrocytes regulated by T cell-derived cytokines

Astrocytes respond to T cell-derived cytokines, such as IFN-γ, GM-CSF, TNF, and IL-17, and gain a pro-inflammatory phenotype by producing cytokines and chemokines. In general, the transcription factors of NF-κB, MAPK, and STAT1 are activated and promote the expression of target genes.

1.3 TNF signaling

TNF is expressed as a 26 kDa transmembrane protein (tmTNF) on the cell surface. tmTNF can be further cleaved into a 17 kDa soluble TNF (sTNF) by a metalloprotease, TNF-alpha converting enzyme (TACE). TNF is a pleiotropic cytokine that plays vital roles in cell homeostasis and disease pathogenesis, such as MS, rheumatoid arthritis, and inflammatory bowel disease (Holbrook, Lara-Reyna et al. 2019). In MS patients, TNF levels increase in CSF and lesions, which are mainly produced by immune cells and CNS-resident cells (Hofman, Hinton et al. 1989, Rossi, Motta et al. 2014, Fresegna, Bullitta et al. 2020). TNF binds to two distinct receptors: TNF receptor (TNFR) 1 and TNFR2. tmTNF has a high affinity to TNFR2, whereas sTNF mainly signals via TNFR1. TNFR2 is expressed on certain cell populations, such as endothelial cells, oligodendrocytes, and immune cells. The ligation of TNFR2 with tmTNF mediates anti-inflammatory response and can promote recovery in

EAE (Madsen, Motti et al. 2016, Raphael, Gomez-Rivera et al. 2019). TNFR1 is broadly expressed on many cell types and is associated with EAE severity (Eugster, Frei et al. 1999). It has been implicated that a single nucleotide polymorphism in *tnfrsf1a*, the TNFR1 encoding gene, increases the susceptibility to MS (De Jager, Jia et al. 2009), indicating the contribution of TNFR1 signaling in MS pathogenesis. The treatment with TNF antibodies shows promising outcomes in EAE. However, anti-TNF therapies in MS patients failed to ameliorate MS and instead, exacerbated clinical symptoms (van Oosten, Barkhof et al. 1996). The undesirable result partially relies on the genetic background. Gregory et al. discovered that anti-TNF therapies are effective in patients without *rs18000693*, the genetic variant which directs the expression of a soluble TNFR1 to neutralize the effect of TNF (Gregory, Dendrou et al. 2012). On the other hand, treatment with anti-TNF antibody and TNF inhibitors are nonselective that both TNFR1 and TNFR2 are blocked. Considering the protective role of TNFR2 signaling, specific blockage of TNFR1 or sTNF to ameliorate the disease (Fresegna, Bullitta et al. 2020), might be a promising therapy for MS.

TNF-induced NF-κB and MAPK

TNFR1 ligation triggers a series of events, including the activation of the MAPK and NF-κB pathways, ultimately, leading to the expression of pro-inflammatory and anti-apoptotic molecules (Fig. 4) (Gough and Myles 2020). The process is initiated by the reorganization of TNF receptor-associated death domain (TRADD) to TNFR1 upon TNF engagement (Hsu, Xiong et al. 1995). Subsequently, TNFR-associated factor 2 (TRAF2) and receptor-interacting protein kinase 1 (RIPK1) are rapidly recruited to TRADD to form complex I. The assembly of complex I further recruits the TGFβ-activated kinase 1 (TAK1) complex and IκB kinase (IKK) complex. The IKK complex is composed of two catalytic subunits IKKα/β and a regulatory subunit IKKγ, whereas, TAK1 complex consists of TAK1 and adaptor proteins MAPK-binding protein 2 and 3 (TAB2 and 3), which phosphorylate IKKβ to activate the IKK complex. NF-κB is kept in an inactive form in the cytoplasm by binding of the inhibitory protein IκBα. Upon stimulation, IκBα is phosphorylated by the activated IKK complex and undergoes degradation, thereby, allowing NF-κB to translocate into the nucleus and initiate the transcription of multiple pro-inflammatory and pro-survival genes. The TAK1 complex activates JNK and p38 MAPK via phosphorylation (Brenner, Blaser et al. 2015). In contrast, TNFR2 lacks the death domain enabling direct binding to TRAF2 and cellular inhibitor of

apoptosis protein (cIAP) 1/2 to regulate the cellular activities, including survival, proliferation, and migration (Yang, Islam et al. 2021).

TNF-induced apoptosis

TNF predominantly activates the NF-κB pathway and induces the expression of anti-apoptotic proteins to protect cells from death. However, under certain conditions, such as NF-κB blockage, cells are susceptible to TNF stimulation and undergo apoptosis (Wajant and Siegmund 2019). Apoptosis is a common biological process of cell death and can be identified by morphological changes. A characteristic feature is the collapse of subcellular components as a result of cleavage of cytoskeletal proteins in combination with cell shrinkage, nuclear fragmentation, formation of apoptotic bodies, and chromatin condensation (Belizario, Vieira-Cordeiro et al. 2015).

TNF triggers the formation of two sequential complexes (Schneider-Brachert, Tchikov et al. 2004). The initial assembly of complex I upon TNFR1 ligation takes place on the membrane within a few minutes of TNF stimulation and promotes cell survival and inflammation. Subsequently, TRADD, RIPK1, and TRAF2 undergo post-translational modifications and dissociate from TNFR1 to the cytosol. Apoptosis is induced by two distinct complexes: complex IIa and IIb, both triggering the activation of caspases. Complex IIa mediates RIPK1-independent apoptosis and complex IIb RIPK1-dependent apoptosis (Wang, Du et al. 2008). The assembly of complex IIa potentiates TNF-induced apoptosis in a RIPK1-independent way by promoting the degradation of anti-apoptotic protein cellular FADD-like IL-1β-converting enzyme-inhibitory protein (FLIP). In this process, RIPK1 is degraded in a proteasomal mediated way (Annibaldi, Wicky John et al. 2018), which allows the exposure of C-terminal death domain of TRADD to recruit FADD and caspase 8 (Hsu, Shu et al. 1996, Park, Jeong et al. 2014). RIPK1-dependent apoptosis occurs when TAK1 or the E3 ligases cIAP1/2 are absent, that RIPK1 assembles with FADD and pro-caspase 8 to form complex IIb. The assembly of complex II triggers autocatalytic cleavage and activation of procaspase 8. Caspase 8, processed from procaspase 8, cleaves procaspase 3 to generate effector caspase 3, which further targets multiple key cellular proteins to cause cell death. In addition, caspase 8 cleaves RIPK1 at D324 (Lin, Devin et al. 1999, Kim, Choi et al. 2000), to 1. prevent the interaction between RIPK1 and RIPK3 which triggers necroptosis, 2. terminate the activation of the NF-κB pathway, 3. promote apoptosis. The activity of caspase 8 is regulated by FLIP,

which forms a heteromer with caspase 8 and prevents the processing of caspase 8, thereby protecting cells from complex II-dependent apoptosis (Wang, Du et al. 2008). It is worth noting that TNFR2 has no death domain and does not cause cell death. However, TNFR2 is involved in TNFR1-induced apoptosis via promoting the proteasomal degradation of TRAF2 (Fotin-Mleczek, Henkler et al. 2002), thus, TRAF2 fails to perform as a pro-survival molecule by protecting cells from death via targeting caspase 8 for degradation and activating NF-κB pathway (Li, Yang et al. 2002, Gonzalvez, Lawrence et al. 2012).

TNF-induced necroptosis

In the absence of caspase-8, i.e when caspase 8 is inactive, or blocked, TNF mediates caspase-independent cell death, known as necroptosis. Necroptosis can also be initiated by other signals, such as death receptors and Toll-like receptors (TLRs) (Pasparakis and Vandenabeele 2015). The morphological characterization of necrotic cells includes: collapse of the cell membrane, swelling of organelle, release of cellular components, and perforation of the plasma membrane (Belizario, Vieira-Cordeiro et al. 2015). Necroptosis is always accompanied by inflammation, as necrotic cells release intracellular pro-inflammatory molecules to clear infected cells. Necroptosis requires the formation of the necrosome, a cytoplasm signaling complex formed by RIPK1 and RIPK3 (Li, McQuade et al. 2012). Initially, RIPK1 undergoes autophosphorylation at S166 when caspase 8 is blocked and subsequently, forms the necrosome via binding with RIPK3. Within the necrosome, RIPK3 becomes activated by autophosphorylation, which in turn, mediates the phosphorylation and activation of pseudokinase mixed lineage kinase domain-like (MLKL), thereby allowing the oligomerization of MLKL and translocation to the plasma membrane. Further, MLKL interacts with phosphatidylinositol phosphates and disrupts the integrity of cell membrane (Samson, Zhang et al. 2020). The kinase activities of RIPK1 and RIPK3 are essential in the execution of necroptosis, as treatment with necrostatins, inhibitors of RIPK1, blocks cell death.

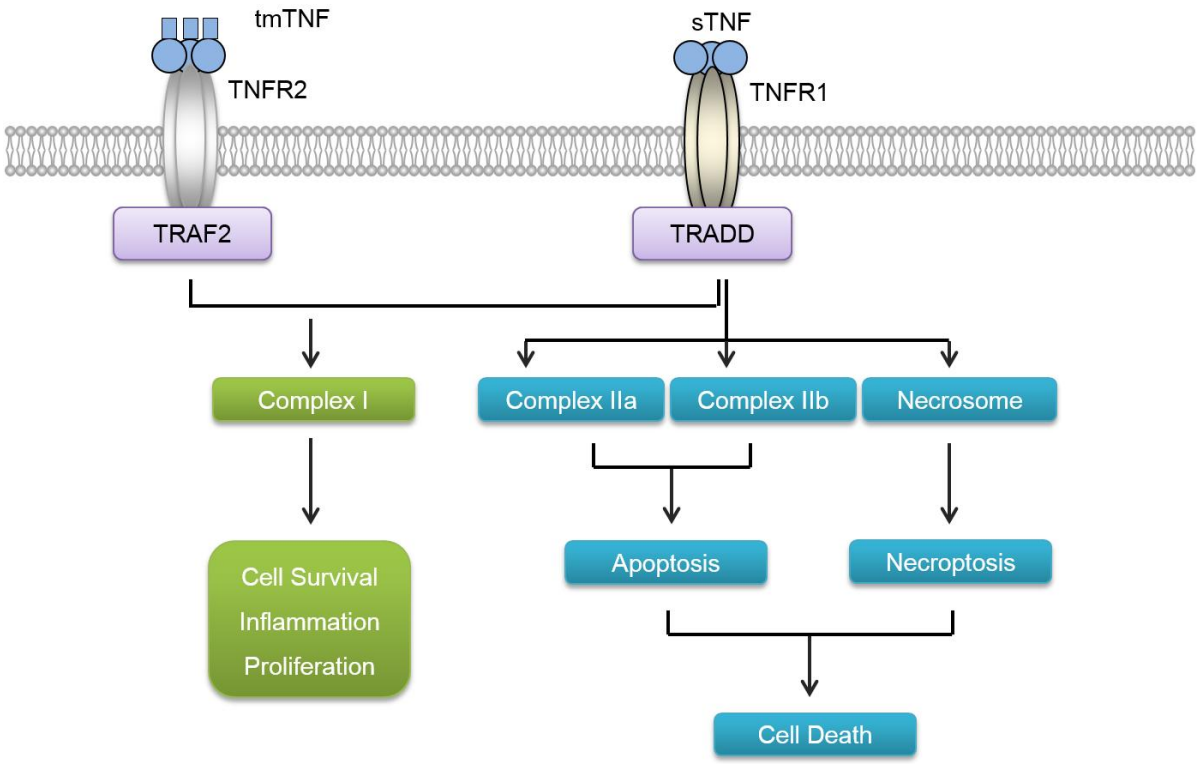

Figure 4. General information of TNF signaling

The death domain of TNFR1 recruits TRADD upon the ligation with sTNF. In contrast, TNFR2 has no death domain and can directly interact with TRAF2 to promote the assembly of complex I when it encounters tmTNF. The formation of complex I promotes cell survival and inflammation via the activation of the NF-κB and MAPK pathways. TNFR1 ligation also triggers cell death via forming complex II a/b and the necrosome (Modified from (Jang, Lee et al. 2021)).

1.4 Ubiquitination and deubiquitination

Ubiquitination is a post-translational modification that regulates localization, functions, and stability of proteins, thereby enabling rapid and dynamic regulation of various cellular processes, such as signaling transduction, protein degradation, DNA repair, and intracellular trafficking (Kliza and Husnjak 2020). Ubiquitination is an enzymatic process in which the lysine (K) residue of a substrate protein is tagged with ubiquitin (Ub), a highly conserved protein with 76 amino acids. The process is sequentially catalyzed by 3 different enzymes, namely, ubiquitin-activating enzymes (E1s), ubiquitin-conjugating enzymes (E2s), and ubiquitin ligases (E3s) (Fig. 5a) (Hershko and Ciechanover 1998). E1 activates Ub in an ATP-dependent process before conjugating to E2, which determines the type of ubiquitin linkage.

E3 mediates the transfer of ubiquitin from E2 to the substrate. E3s, the most abundant ubiquitin enzymes, determine the specificity of the substrate. The substrates can be modified by different types of ubiquitin chains, including monoubiquitination and polyubiquitination (Fig. 5b). Monoubiquitination is generated by conjugating a single ubiquitin to one or more sites of the substrate and is involved in DNA repair and gene expression (Passmore and Barford 2004). Polyubiquitination is the addition of the carboxyl-terminal glycine residue of ubiquitin to an internal lysine residue or the N-terminal (M1) of another ubiquitin. The type of polyubiquitination is determined by the type of the lysine linkage, which include K6, K11, K27, K29, K33, K48, and K63. Furthermore, the combinations of single or multiple linkage types increase the diversity of ubiquitination, such as homotypic chains and heterotypic chains (French, Koehler et al. 2021). Homotypic chains are built up by the same linkage, whereas heterotypic chains are formed by mixed linkages and can be further divided into mixed and branched chains. The fate of proteins is determined by the types of polyubiquitin linkages (Kliza and Husnjak 2020). For example, K11-, K48-linked ubiquitin chains and mixed K11/K48 chains generally target modified proteins for proteasome degradation; whereas, K63-linked, M1-, and branched chains function as a scaffold, facilitating signaling transduction, endocytosis, and DNA repair. The functions of other ubiquitin chains are still under investigation.

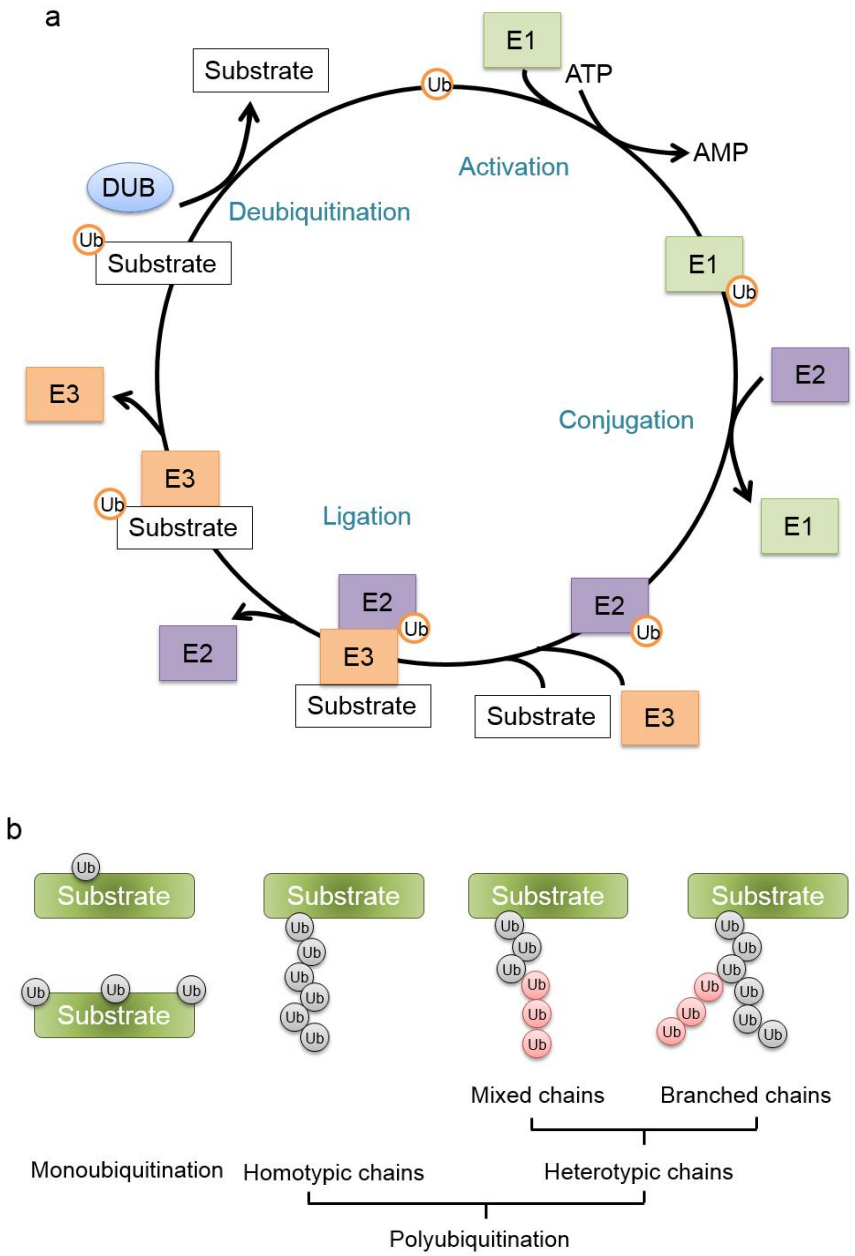

Figure 5. Ubiquitination

a. The process of ubiquitination and deubiquitination. The ubiquitination process is a sequential cascade catalyzed by E1s, E2s, and E3s. Ubiquitin is transferred to E1 in an ATP-dependent process for activation, then activated ubiquitin is conjugated to E2. Finally, ubiquitin is ligated to the target protein by E3. The ubiquitin chains can be dissembled by DUBs, which removes ubiquitin chains from the substrate (modified from (Woo and Kwon 2019)). b. Types of ubiquitin chains. Ubiquitin chains includes two types: monoubiquitin and polyubiquitination. Polyubiquitination can be further divided

into homotypic chains and heterotypic chains. Homotypic chains comprise of one type of linkage, including K6, K11, K27, K29, K33, K48, K63, and M1. Heterotypic chains contain multiple types of linkages and can be further classified into mixed chains and branched chains.

Ubiquitination is a reversible process and deubiquitinating enzymes (DUBs) can remove the ubiquitin chains by cleaving isopeptide or peptide bonds between ubiquitin chains and its substrate (Komander, Clague et al. 2009). Deubiquitination can prevent the degradation or alter the activation status of the substrate protein. Furthermore, DUBs recycle ubiquitin and modify the ubiquitin chain length by trimming. Until now, 102 DUBs have been identified in the human genome which can be classified into six families based on their structure (Harrigan, Jacq et al. 2018): ovarian tumour proteases (OTUs), ubiquitin-specific proteases (USPs), ubiquitin C-terminal hydrolases (UCHs), Machado-Josephin domain-containing proteases (MJDs), motif interacting with ubiquitin-containing novel DUB families (MINDYs), and JAB1/MPN/MOV34 metalloenzymes (JAMMs). DUBs show specificity for the types of ubiquitin chains and to a less extent to the substrates. For example, OTU deubiquitinase, ubiquitin aldehyde binding 1 (OTUB1) has a preference for K48-linked ubiquitination and targets multiple substrates, such as cIAP1 (Goncharov, Niessen et al. 2013), SOCS1 (Wang, Mulas et al. 2019), and Ubc13 (Mulas, Wang et al. 2020). Cylindromatosis (CYLD) mainly hydrolyzes K63-linked and M1-linked ubiquitination (Douanne, Andre-Gregoire et al. 2019). It is worth noting that many DUBs are associated with E3 ligases and the ubiquitination status of the substrate are finely regulated by the interaction between E3 and DUB (Sowa, Bennett et al. 2009). Accumulating evidence indicates that mutations or alterations of DUB functions are associated with multiple human diseases.

1.5 Ubiquitination and deubiquitination in TNF signaling

TNF signaling is regulated by E3 ligases and DUBs, which govern the formation of distinct signaling complexes and protein degradation (Fig. 6). cIAP1/2, an E3 ligase, promotes self-ubiquitination and ubiquitination of several components in complex I, notably RIPK1 with K11-, K48-, K63-linked chains. K11-linked ubiquitin chain on RIPK1 is involved in the activation of NF-κB via recruiting IKKγ (Dynek, Goncharov et al. 2010). K63-linked ubiquitin chains are conjugated at K377 of RIPK1 in humans (K376 in mice) (Ea, Deng et al. 2006), which works as a docking platform for downstream molecules, including TAB2 and IKKγ. TRAF2 undergoes K63-linked autoubiquitination within TNFR1 complex for the

recruitment of TAB2/3 and IKKα/β (Li, Wang et al. 2009). The NF-κB suppressor IκBα is subsequently attached with K48-linked ubiquitin chains after phosphorylation and undergoes proteasomal-mediated degradation, allowing nuclear translocation of NF-κB. Furthermore, the E3 ligase linear ubiquitin chain assembly complex (LUBAC) is recruited to K63-linked ubiquitin chains of cIAP1, which subsequently conjugates M1-ubiquitination on several substrates and stabilizes the signaling complexes, including RIPK1, IKKγ, TNFR1, and TRADD (Haas, Emmerich et al. 2009). The ubiquitination is fine-tuned by several DUBs, such as, A20, OTU deubiquitinase with linear linkage specificity (OTULIN), and CYLD. A20 is recruited to TNFR1 at later time points and terminates the activation of the NF-κB pathway by removing K63-linked ubiquitin chains from RIPK1 and meanwhile, adding K48-linked ubiquitin chains to RIPK1 (Wertz, O'Rourke et al. 2004). OTULIN specifically dissembles M1-linked chains on LUBAC to prevent its auto-M1-ubiquitination and inhibits the downstream events (Elliott, Nielsen et al. 2014). CYLD targets several components, including TRAF2, RIPK1, TAK1, and IKKγ, to regulate JNK and the NF-κB pathway (Blake and Toro 2009).

The ubiquitination status of TNF signaling molecules determines the switch from survival to death, notably, by RIPK1 ubiquitination. Upon TNF stimulation, RIPK1 is first modified with K63-linked ubiquitination, followed by cIAP1 mediated K48-linked ubiquitination for proteasome-mediated degradation (Annibaldi, Wicky John et al. 2018), which allows a switch from complex I to complex IIa. In addition, when cIAP1 is absent, non-ubiquitinated RIPK1 forms complex IIb with FADD and pro-caspase 8 to activate the caspase cascade. TRAF2 is reported to be an inhibitor for cell death. TRAF2 functions as E3 ligase by adding K48-linked ubiquitination on the p18 region of caspase 8 for proteasomal degradation (Gonzalvez, Lawrence et al. 2012). The apoptosis induced by TNFR1 requires the signals from TNFR2, which triggers K48-linked ubiquitination and proteasomal degradation of TRAF2 (Li, Yang et al. 2002). Necroptosis is regulated by ubiquitination as well. It is found that activated RIPK1 is linked with K63- and M1-linked ubiquitin chains for stabilization (de Almagro, Goncharov et al. 2015, Wang, Meng et al. 2017), thus, facilitating the accumulation of phosphorylated RIPK1 and RIPK3 in the necrosome (de Almagro, Goncharov et al. 2017). RIPK3 undergoes ubiquitination at multiple sites. For example, K63-linked ubiquitination at K5 of RIPK3 promotes the formation of complex RIPK1 and RIPK3, whereas A20 reduces the necroptosis via removing RIPK3 ubiquitination (Onizawa, Oshima et al. 2015).

At present, the complex processes of deubiquitination of TNF signaling molecules is only partially understood and it is likely that additional DUBs contribute to the regulation of TNF signaling. In this regard, Evans et. Al. suggested that OTU domain-containing 7B (OTUD7B), a 100 kDa DUB belonging to the OTU subfamily, is involved in TNF signaling (Evans, Taylor et al. 2001). However, the interaction partners of OTUD7B and its impact on the ubiquitination of TNF signaling molecules are still unknown.

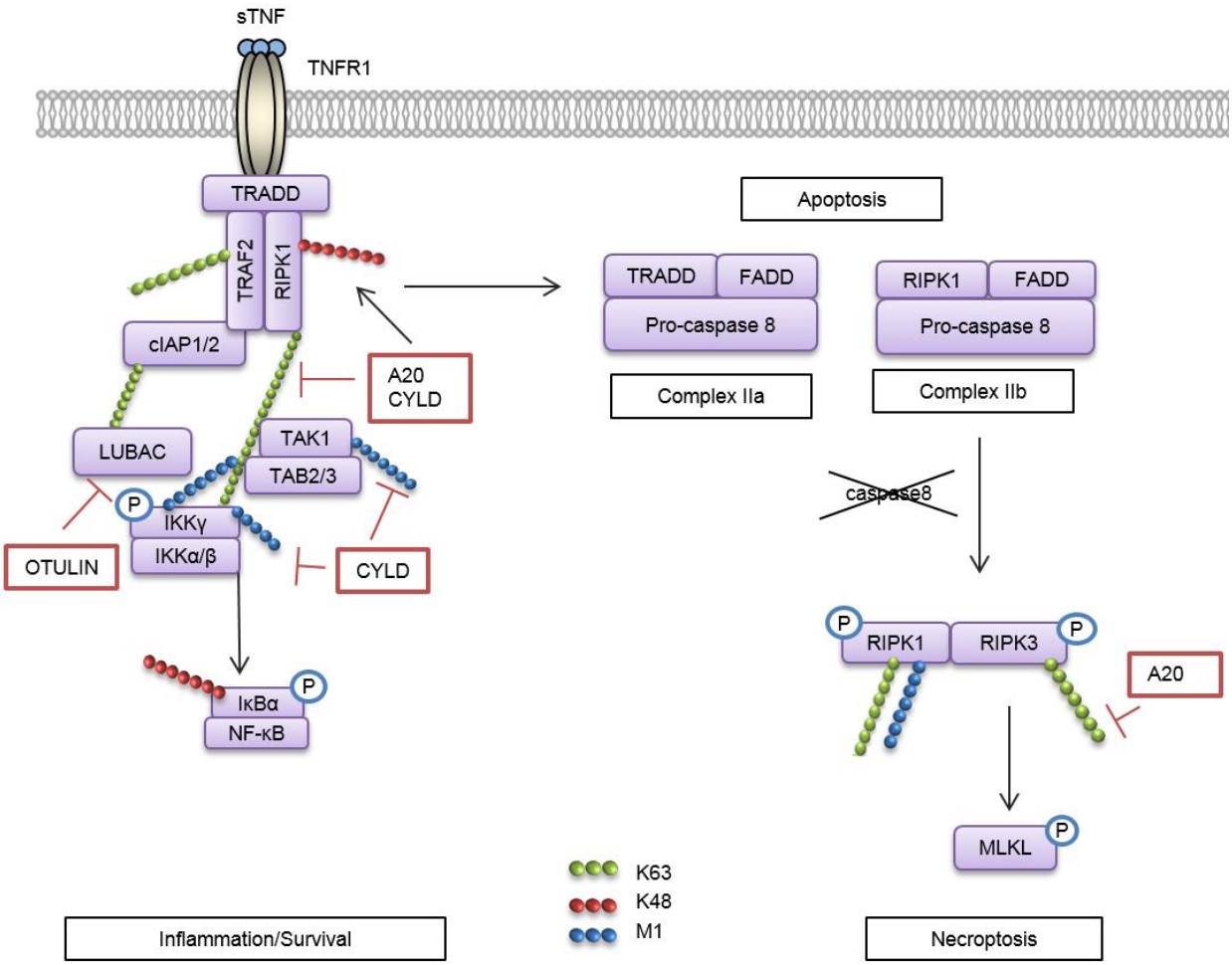

Figure 6. Ubiquitin system in TNF signaling

TNFR1 signaling is a fine-tuned network regulated by ubiquitination and deubiquitination. RIPK1 is ubiquitinated upon TNF treatment which is required for the activation of downstream events. A20 terminates signal transition by removing K63-linked ubiquitin chains from RIPK1 and works as an E3 ligase to add K48-linked ubiquitin chains on RIPK1. LUBAC binds to K63-linked ubiquitin chains of cIAP1 to stabilize the complex I by generating M1-linked chains and the process can be reversed by

OTULIN, a M1 specific DUB. Later, IκBα is attached with K48-linked ubiquitin chains for degradation. CYLD inhibits signal transduction by targeting various substrates, such as TRAF2, TAK1, and IKKγ. Subsequently, complex I undergoes internalization and interacts with procaspase 8 and FADD to initiate apoptosis. When caspase 8 is inactive, both activated RIPK1 and activated RIPK3 are modified with polyubiquitination for the formation of necrosome.

1.6 OTUD7B

OTUD7B, also known as cellular zinc finger anti-NF-κB (cezanne). The structure of OTUD7B is well studied (Fig. 7), which contains a ubiquitin-associated (UBA) domain, an A20-like Zinc Finger (ZnF) domain, a nuclear localization signal (NLS), and an OTU domain (Mader, Huber et al. 2020). Despite the presence of a NLS domain, OTUD7B is uniformly distributed in the cytoplasm (Evans, Taylor et al. 2001). The UBA domain recognizes ubiquitin chains and substrates via Leu9 and Ser10 sites (Ji, Cao et al. 2018). The OTU domain contains catalytic residues, C194, C209, and H358. ZnF is involved in substrate binding as well. Similar to TNFAIP3 (A20), OTUD7B harbors a TRAF binding (TRAFB) domain, which mediates its interaction with TRAF6 and TRAF3 (Evans, Taylor et al. 2001).

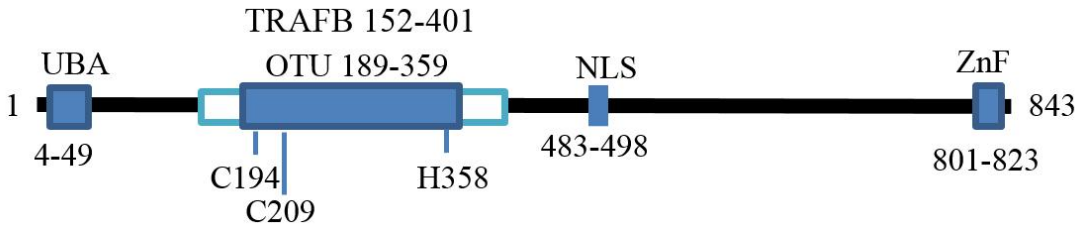

Figure 7. Structure of OTUD7B (human)

OTUD7B contains a UBA domain at the N-terminus, which is responsible for recognizing ubiquitin and substrates. The TRAFB domain is involved in binding of TRAFs. The OTU domain is important for the catalytic activity and the ZnF at the C-terminus is required for the interaction with substrates.

OTUD7B transcripts are found in multiple tissues and the expression is inducible, for example, by proinflammatory cytokines (Enesa, Zakkar et al. 2008), reactive oxygen species, non-canonical NF-κB (Hu, Brittain et al. 2013), and hypoxia (Luong le, Fragiadaki et al. 2013). OTUD7B functions by cleaving ubiquitin from linear or branched chains of

ubiquitinated substrates. OTUD7B-deficiency has no effect on the development and survival of mice (Hu, Brittain et al. 2013). However, by cleaving ubiquitin chains, such as K48-, K63-, K11-, and branched chains from target substrates, OTUD7B is involved in multiple cellular processes, such as cell cycle, differentiation, autophagy, mTORC2 signaling, and regulation of the NF-κB pathway.

OTUD7B in inflammation and immune response

OTUD7B was first identified in 2001 by Paul C. Evans as a DUB, which shares sequence and functional similarity to A20 (Evans, Taylor et al. 2001). In vitro studies showed that OTUD7B is a negative regulator of the NF-κB pathway and inhibits TNF-induced inflammatory responses in a negative feedback loop. Upon TNF stimulation, OTUD7B is recruited to TNFR1 complex and identifies K63-linked ubiquitin chains to remove ubiquitin chains from RIPK1 (Enesa, Zakkar et al. 2008, Ji, Cao et al. 2018). Mutation of Leu9 and Ser10 in the UBA domain impairs the recruitment of OTUD7B to the TNFR complex (Ji, Cao et al. 2018).

Hypoxia fosters inflammation via the activation of the NF-κB pathway. In this process, TRAF6 undergoes K63-linked ubiquitination. OTUD7B is induced in various cell types in the kidney during hypoxia and works in a negative feedback loop to suppress aberrant NF-κB activation via reducing K63-linked ubiquitination of TRAF6, thereby protecting mice from renal inflammation and injury upon ischemia/reperfusion injury (Luong le, Fragiadaki et al. 2013).

Hu et al. have shown that OTUD7B-deficient mice have an increase levels of fecal IgA and are more resistant to *Citrobacter rodentium* infection (Hu, Brittain et al. 2013), suggesting a role of OTUD7B in intestinal lymphoid homeostasis. Additionally, OTUD7B-deficient B cells and mouse embryonic fibroblasts exhibit hyper-activation of the non-canonical NF-κB pathway. OTUD7B-deficient cells have a notable increase of nuclear p52 and loss of cytoplasmic p100 compared to wild type cells in response to non-canonical NF-κB stimuli, which bind to the lymphotoxin-β receptor, cluster of differentiation 40 (CD40), and the B-cell activating factor (BAFF) receptor. TRAF3 is the target of OTUD7B for deubiquitination via the catalytical sites C194S/H358R, finally, OTUD7B stabilizes TRAF3 and inhibits NF-κB-inducing kinase (NIK) accumulation in non-canonical NF-κB signaling.

OTUD7B is also involved in T cell activation and differentiation via regulating T cell receptor (TCR) signaling (Hu, Wang et al. 2016). Upon TCR engagement, OTUD7B is rapidly recruited to Zap70 for deubiquitination, preventing its interaction with negative regulatory phosphatases Sts1 and Sts2, eventually, allowing phosphorylation and activation of Zap70 for signal transduction. Due to the dampened T cell responses, OTUD7B$^{-/-}$ mice are more resistant to EAE induction with a postponed onset and improved outcome, but susceptible to *Listeria monocytogenesis* infection with impaired pathogen control.

OTUD7B in cancer development and cellular processes

In addition to the immune system, OTUD7B is involved in the development and metastasis of various cancers, in particular by regulating EGFR signaling (Pareja, Ferraro et al. 2012), homeostasis of mechanistic target of rapamycin (mTOR) complex (Wang, Jie et al. 2017), and cell proliferation (Bonacci, Suzuki et al. 2018). OTUD7B is abundantly expressed in numerous cancers (Chen, Pang et al. 2020) and the OTUD7B levels predict the prognosis of patients in some types of cancer (Wang, Zhong et al. 2017, Lin, Shen et al. 2019).

With respect to cancer development, OTUD7B contributes to the DNA damage response and removes K11-linked ubiquitin chains from chromatin-bound proteins, thereby allowing the recruitment of DNA repair proteins (Wu, Liu et al. 2019). Other studies uncovered that the differentiation of neural progenitor cells is balanced by OTUD7B and E3 ligase complex CUL4A$^{DET1-COP1}$ (Cui, Zhang et al. 2018)

The importance of OTUD7B in cellular processes and diseases are gaining more attention. However, its functions in CNS homeostasis, especially under pathological conditions, are still unknown.

2. AIMS

Astrocytes are the most populated CNS resident cells and crucial for CNS homeostasis and neurological diseases. Astrocytes can be both neurotoxic and neuroprotective depending on the activated intracellular signaling pathways. OTUD7B has been reported to regulate multiple cellular events, notably, the NF-κB pathway to promote the expression of proinflammatory factors by targeting key molecules. However, the astrocyte-specific function of OTUD7B is unknown. Therefore, we aimed to get more insight into the role of OTUD7B as a regulator of astrocyte function in CNS autoimmunity. Specifically, we addressed the following open topics:

i. Evaluate the astrocyte specific function of OTUD7B in EAE.

ii. Define the in vivo role of OTUD7B in astrocytes during EAE.

iii. Identify the signaling pathways regulated by OTUD7B in astrocytes.

iv. Elucidate the mechanism by which OTUD7B influences these signaling pathways.

3. MATERIALS AND METHODS

3.1 Materials

3.1.1 Materials for animal experiments

MOG_{35-55} peptide	JPT, Berlin, Germany
Freund's adjuvant, Complete	Sigma-Aldrich, Steinheim, Germany
Mycobacterium tuberculosis H37Ra	BD Biosciences, Heidelberg, Germany
Pertussis toxin	Sigma-Aldrich, Steinheim, Germany
Isoflurane	CP-Pharma, Burgdorf, Germany
4% Paraformaldehyde (PFA)	Carl Roth, Karlsruhe, Germany
0.9 % NaCl	Fresenius Kabi, Bad Homburg, Germany
Percoll	GE Healthcare, Munich, Germany

3.1.2 Materials for cell culture

Astrocyte culture medium	DMEM (Gibco, Grand island, USA), 10% fetal calf serum (FCS) (Capricorn Scientific, Ebsdorfergrund, Germany), 1% 100U Penicillin/ Streptomycin (Gibco, Grand island, USA), 1% glutamate (Gibco, Grand island, USA)
Hank's balanced salt solution (HBSS)	Gibco, Grand island, USA
RPMI 1640 medium	Gibco, Grand island, USA
Non-essential amino acid (NEAA, 100 x)	Gibco, Grand island, USA
Dimethyl sulfoxide (DMSO)	Gibco, Grand island, USA
Ionomycin	Millipore, Darmstadt, Germany
GolgiPlug	BD Biosciences, Heidelberg, Germany
PBS	Thermo Fisher Scientific, Waltham, USA
Trypsin	Gibco, Grand island, USA
TNF	Peprotech, Hamburg, Germany
IL-17	Peprotech, Hamburg, Germany
IFN-γ	Peprotech, Hamburg, Germany
Necrostatin 1s (Nec 1s)	Biovision, Wehrheim, Germany

z-VAD-FMK	Enzo life science, Lörrach, Germany
Cycloheximide (CHX)	Sigma-Aldrich, Steinheim, Germany
MG132	Sigma-Aldrich, Steinheim, Germany
Trypan blue	Sigma-Aldrich, Steinheim, Germany

Cell culture was performed under laminar flow bench. The medium was pre-warmed in 37 °C water bath before use. Cells were kept in an incubator at 37 °C with 5 % CO_2 and 60 % of water vapor. Plastic materials for cell culture, including flasks, pipettes, and plates, were purchased from Greiner Bio-One (Frickenhausen, Germany) and Carl Roth (Karlsruhe, Germany).

3.1.3 Primers

Table 1. Primers for Genotyping

Primer	Primer sequence (5 '→ 3')	Amplicon size
GFAP Cre sense	GAC ACC AGA CCA ACT GGT AAT GGT AGC GAC	850bp
GFAP Cre anti-sense	GCA TCG AGC TGG GTA ATA AGC GTT GGC AAT	
OTUD7B flox sense	CAG AAT AAA GAG GTG GGT GAG C	
OTUD7B flox anti-sense	ACT CAC ATT GCA GTG ATC ATG C	
$OTUD7B^{wt/wt}$ amplicon size: 380 bp, $OTUD7B^{fl/fl}$ amplicon size: 347 bp		

All from Eurofins MWG Operon, Ebersberg, Germany

Table 2. Primers for real-time PCR

Primer	Assay ID
CXCL1	Mm04207460_m1
CXCL10	Mm00445235_m1
CXCL11	Mm00444662_m1
CCL2	Mm00441242_m1
CCL20	Mm01268754_m1

NOS2	Mm00440502_m1
IL-6	Mm00446190_m1
TNF	Mm00443258_m1
IFN-γ	Mm00801778_m1
IL-17	Mm00439619_m1
CSF2	Mm01290062_m1
OTUD7B	Mm01256852_m1
HPRT	Mm01545399_m1

All from Thermo Fisher Scientific, Waltham, USA

3.1.4 Materials for molecular biology

RNeasy Mini Kit	Qiagen, Hilden, Germany
Superscript II Reverse Transcriptase	Invitrogen, Karlsruhe, Germany
KAPA PROBE FAST Universal	Merck Millipore, Darmstadt, Germany
β-mercaptoethanol	Carl Roth, Karlsruhe, Germany
dNTPs	Invitrogen, Karlsruhe, Germany
Oligo dT	Invitrogen, Karlsruhe, Germany
Dithiothreitol (DTT)	Invitrogen, Karlsruhe, Germany
DNA-*free* kit	Invitrogen, Karlsruhe, Germany

3.1.5 Materials for proteomics

Filter paper	Bio-Rad, California, USA
Polyvinylidene fluoride (PVDF) membranes	Roche Diagnostics, Mannheim, Germany
Protein marker	Thermo Fisher Scientific, Waltham, USA
BCA protein assay kit	Thermo Fisher Scientific, Waltham, USA
Lane marker reducing sample buffer (5X)	Thermo Fisher Scientific, Waltham, USA
Bovine serum albumin (BSA)	Capricorn Scientific, Ebsdorfergrund, Germany

GammaBind G sepharose beads	GE Healthcare, Munich, Germany
Lysis buffer	RIPA buffer (10 x) (Cell Signaling Technology, Danvers, USA), phosSTOP (Roche Diagnostics, Mannheim, Germany), Protease Inhibitor Cocktail (Sigma-Aldrich, Steinheim, Germany), Phenylmethanesulfonylfluoride (PMSF) (Cell Signaling Technology, Danvers, USA)
Gel running buffer (pH 8.3)	25 mM Tris (Carl Roth, Karlsruhe, Germany), 0.1% sodium dodecyl sulfate (SDS) (Carl Roth, Karlsruhe, Germany), 250 mM glycine (Carl Roth, Karlsruhe, Germany)
Transfer buffer (pH 8.4)	25 mM Tris (Carl Roth, Karlsruhe, Germany), 0.1% sodium dodecyl sulphate (SDS) (Carl Roth, Karlsruhe, Germany), 500 mM glycine (Carl Roth, Karlsruhe, Germany), 20% methanol (J.T. Baker, Deventer, Netherlands)
TBS-Tween 20 (pH 7.4)	20 mM Tris (Carl Roth, Karlsruhe, Germany), 140 mM NaCl (PanReac AppliChem, Darmstadt, Germany), 0.1% (v/v) Tween 20 (PanReac AppliChem, Darmstadt, Germany)
SDS-PAGE separating gel	Distilled H_2O, 8% to 15% acrylamide 30% (Carl Roth, Karlsruhe, Germany), 0.4 M Tris (pH 8.8) (Carl Roth, Karlsruhe, Germany), 0.1% Sodium dodecyl sulfate (SDS) (Carl Roth, Karlsruhe, Germany), 0.1% ammonium persulfate (APS) (Carl Roth, Karlsruhe, Germany), 0.1% Tetramethylethylenediamine (TEMED) (PanReac AppliChem, Darmstadt, Germany)
SDS-PAGE stacking gel	Distilled H_2O, 5% acrylamide 30% (Carl Roth, Karlsruhe, Germany), 0.17 M Tris (pH 6.8) (Carl Roth, Karlsruhe, Germany), 0.1% Sodium

dodecyl sulfate (SDS) (Carl Roth, Karlsruhe, Germany), 0.1% ammonium persulfate (APS) (Carl Roth, Karlsruhe, Germany), 0.1% Tetramethylethylenediamine (TEMED) (PanReac AppliChem, Darmstadt, Germany)

3.1.6 Antibodies for western blot and immunoprecipitation

Table 3. Antibodies for western blot and immunoprecipitation

Antibody	Company	Catalog
OTUD7B	Proteintech group, Manchester, UK	16605-1-AP
Phospho-p38	Cell Signaling Technology, Danvers, USA	9215
P38	Cell Signaling Technology, Danvers, USA	9212
Phospho-JNK	Cell Signaling Technology, Danvers, USA	9251
JNK	Cell Signaling Technology, Danvers, USA	9252
Phospho-ERK	Cell Signaling Technology, Danvers, USA	9101
ERK	Cell Signaling Technology, Danvers, USA	9102
Phospho-IκBα	Cell Signaling Technology, Danvers, USA	2859
IκBα	Cell Signaling Technology, Danvers, USA	4812
TRAF2	Cell Signaling Technology, Danvers, USA	4724
Phospho-STAT1(701)	Cell Signaling Technology, Danvers, USA	9167
Phospho-STAT1(727)	Cell Signaling Technology, Danvers, USA	8826
STAT1	Cell Signaling Technology, Danvers, USA	9172
β-tubulin	Proteintech group, Manchester, UK	10068-1-AP
RIPK1	Cell Signaling Technology, Danvers, USA	3493
K63 ubiquitin	Merck Millipore, Darmstadt, Germany	05-1308
K48 ubiquitin	Cell Signaling Technology, Danvers, USA	4289
RIPK1	Cell Signaling Technology, Danvers, USA	3493

Caspase 3	Cell Signaling Technology, Danvers, USA	9662
Caspase 8	Cell Signaling Technology, Danvers, USA	4927
Cleaved caspase 8	Cell Signaling Technology, Danvers, USA	9429
FADD	Abcam, Cambrige, UK	ab124812
cIAP1	Abcam, Cambrige, UK	ab154525
TRADD	Cell Signaling Technology, Danvers, USA	3694
FLIP	Cell Signaling Technology, Danvers, USA	8510
GAPDH	Cell Signaling Technology, Danvers, USA	5174
Normal Rabbit IgG	Cell Signaling Technology, Danvers, USA	2729

Secondary antibodies for western blot

Polyclonal Rabbit Anti-Mouse Immunoglobulins/HRP (# P 0260) Dako, Glostrup, Denmark

Polyclonal Swine Anti-Rabbit Immunoglobulins/HRP (# P 0399) Dako, Glostrup, Denmark

IgG Fraction Monoclonal Mouse Anti-Rabbit IgG, light chain specific (#211-002-171) Jackson ImmunoResearch

3.1.7 Antibodies for flow cytometry

Table 4. Antibodies for flow cytometry

Name	Catalog	Color	Company
CD3e	12-0033-82	PE	eBioscience, San Diego, USA
CD3e	100222	APC-Cy7	BioLegend, San Diego, USA
CD4	100443	BV421	BioLegend, San Diego, USA
CD8	17-0081-82	APC	eBioscience, San Diego, USA
CD45	103130	PERCP	BioLegend, San Diego, USA
CD11b	101216	PE-Cy7	eBioscience, San Diego, USA
F4/80	123132	BV421	BioLegend, San Diego, USA
LY6C	17-5932-82	APC	eBioscience, San Diego, USA

LY6G	127608	PE	BioLegend, San Diego, USA
CD19	12-0193-82	PE	eBioscience, San Diego, USA
CD45R/B220	562922	BV421	BD Biosciences, Heidelberg, Germany
CD11c	12-0114-83	PE	eBioscience, San Diego, USA
ACSA-2	130-123-284	PE	Miltenyi Biotec, Bergisch Gladbach, Germany
CD16/CD32	14-0161-86		Invitrogen, Karlsruhe, Germany
Annexin V	640918	Pacific blue	BioLegend, San Diego, USA
7-AAD	00-6993-50		eBioscience, San Diego, USA
Fixable Viability	65-0866	eFluor 506	eBioscience, San Diego, USA

3.1.8 Kits

Anti-ACSA-2 MicroBead Kit, Mouse	Miltenyi Biotec, Bergisch Gladbach, Germany
NeuroCult™ Enzymatic Dissociation Kit	Stemcell Technologies, Cologne, Germany
Pierce ECL Plus Western Blotting Substrate	Thermo Fisher Scientific, Waltham, USA
Intracellular Fixation/Permeabilization Buffer Set	eBioscience, San Diego, USA
Annexin Binding Buffer	eBioscience, San Diego, USA
QIAshredder	Qiagen, Hilden, Germany
Pipettes	Eppendorf, Hamburg, Germany

3.1.9 Consumables

Glass Syringe	Carl Roth, Karlsruhe, Germany
Syringe	BD Biosciences, Heidelberg, Germany
Cell Strainer	Falcon, Durham, USA
Needles	B.Braun Melsungen AG, Melsungen, Germany
Cuvettes	Sarstedt AG & Co., Nümbrecht, Germany

5 ml Polystyrene Round-bottom Tube	Falcon, Durham, USA
LS Columns	Miltenyi Biotec, Bergisch Gladbach, Germany

3.1.10 Instruments

FACS Canto II Flow Cytometer	BD Biosciences, Heidelberg, Germany
Cytek Aurora	Cytek Biosciences, California, USA
Chemo Cam Luminescent Image Analysis System	INTAS, Göttingen, Germany
Semi Dry Blotter	Galileo Bioscience, Cambridge MA, USA
MACS Separators	Miltenyi Biotec, Bergisch Gladbach, Germany
LightCycler 480	Roche Diagnostics, Mannheim, Germany
Incubator	Heraeus, Hanau, Germany
Laminar Flow Bench	Heraeus, Hanau, Germany
Microscope Olympus-CX 41	Olympus, Hamburg, Germany
Naodrop ND-1000 spectrophotometer	Thermo Fisher Scientific, Waltham, USA
Thermomixer	Eppendorf, Hamburg, Germany
Pipette Boy	Eppendorf, Hamburg, Germany
Centrifuge Mikro 200R	Hettich, Tuttlingen, Germany
Centrifuge Rotanta 460R	Hettich, Tuttlingen, Germany
Mini-PROTEAN® Tetra Vertical Electrophoresis	Bio-Rad, California, USA
Water Bath	Thermo Fisher Scientific, Waltham, USA
Vortex Genius 3	IKA, Staufen, Germany
Hemocytometer	LO Laboroptik, Lancing, UK
Laboratory Balance	Sartorius, Goettingen, Germany
pH meter	SHOTT, Mainz, Germany

3.1.11 Software

FlowJo V10	Tree Star, Ashland, USA
GraphPad Prism 8	GraphPad Software, San Diego, USA
LabImage	INTAS, Göttingen, Germany

3.1.12 Animals

Glial fibrillary acidic protein (GFAP)-Cre OTUD7B$^{fl/fl}$ mice, which have a specific deletion of *otud7b* in astrocytes, were generated by crossing C57BL/6 OTUD7B$^{fl/fl}$ mice with C57BL/6 GFAP-Cre mice. C57BL/6 mice were obtained from Janvier (Le Genest-Saint Isle, France) and C57BL/6 OTUD7B$^{fl/fl}$ mice were generated by Ronald Naumann (Max Planck Institute of Molecular Cell Biology and Genetics, Transgenic Core Facility, Dresden, Germany). All animals were kept under specific pathogen-free (SPF) conditions in animal facilities. Animal care and experimental procedures were performed according to European animal protection law and approved by local authorities (Landesverwaltungsamt Halle, file number 42502-2-1260).

3.2 Methods

3.2.1 Genotyping of the mouse strains

Genotyping was carried out by cutting a tissue sample of the tail tip and the genomic DNA was isolated using KAPA Mouse Genotyping Kit according to the manufacturer's protocol. PCR was performed using primers against GFAP Cre and OTUD7B flox, as shown in Table 1 and the set of programs as shown in Table 5.

Table 5. PCR program

Steps	Temperature (°C)	Time	Cycles
Initial denaturation	95	3 min	
Denaturation	95	15 s	35 x
Annealing	60 / 64	15 s	
Extension	72	15 s	
Final extension	72	10 min	

The annealing temperature for GFAP Cre is 60 °C and the annealing temperature for OTUD7B flox is 64 °C.

3.2.2 EAE induction and assessment

MOG_{35-55} (MEVGWYRSPFSRVVHLYRNGK) peptide (4 mg) was dissolved in 2 ml cold PBS and 20 mg of killed Mycobacterium tuberculosis was dissolved in 2 ml complete Freund's adjuvant. Two components were emulsified with a glass tuberculin syringe. For active EAE induction, 8-12 weeks old mice were subcutaneous (s.c.) immunized with 200 µl emulsion. In addition, 200 ng pertussis toxin dissolved in 200 µl PBS was intraperitoneally (i.p.) injected at day 0 and 2 post immunization (p.i.).

Clinical symptoms of EAE and body weight were monitored daily in a double-blinded way and the score of EAE was recorded according to the severity which ranges from 0 to 5 (Table 6). Clinical scores and body weight were calculated as the average of all individuals in each group.

Table 6. EAE score

Score	Clinical sign
0	no sign
0.5	Partial tail weakness
1	Limp tail
1.5	Slowing of righting
2	Partial hind legs weakness
2.5	Dragging of hind legs
3	Complete paralysis of hind legs
3.5	Slight weakness of fore legs
4	Severe fore legs weakness
5	Death

3.2.3 Isolation of leukocytes

Mice were anesthetized with isoflurane and intracardially perfused with 0.9 % NaCl to remove intravascular leukocytes. The spinal cord was obtained, minced through 70 µm cell strainers, and the leukocytes were separated by Percoll gradient centrifugation. In short, the pellet was resuspended in 10 ml Percoll solution with a concentration of 1.098 g and 6 ml 1.22 g solution was added slowly to the bottom. Subsequently, a solution with a reduced density from 1.07 to 1.0 was added successively on top of 1.098 g solution. Single cells were harvested after centrifuge with a rapid start and a slow stop. The layers of density between 1.05 g, 1.07 g, and 1.098 g where the leukocytes accumulated were transferred to a new Falcon tube, followed by washing with cell culture medium (HBSS, 3 % FCS). Leukocytes from the spleen and lymph nodes were acquired by passing the organs through 70 µm cell strainers and erythrocytes were lysed by incubating in AKR lysis buffer (Table 7) for 10 mins on ice. The cells were resuspended in PBS and cell number was determined with a hemocytometer.

Table 7. Recipe for AKR lysis buffer

AKR lysis buffer (pH 7.2)	
NH_4Cl	155 mM
$KHCO_3$	10 mM
EDTA	0.1 mM

3.2.4 Flow cytometry

1 x 10^6 single-cell suspensions were transferred to FACS tubes and washed with cold PBS. For staining extracellular surface molecules, 1 µg anti-mouse CD16/CD32 antibody was added to tubes to block non-specific binding sites and incubated in the dark at 4 °C for 15 min. Subsequently, the cells were incubated with surface antibodies for 1h at 4 °C in the dark. Afterward, cells were washed with 2 ml cold PBS and resuspended in 200 µl cold PBS for FACS. For intracellular molecules, cells were treated with 500 ng/ml ionomycin and 50 ng/ml phorbol myristate acetate (PMA) in RPMI 1640 medium (10 % FCS, 1% NEAA, and 1 % L-glutamine) for 4 h at 37 °C to foster cytokine production. Then, 1 µl/ml GolgiPlug was added for another 12 h to block the transportation of intracellular proteins for concentration enrichment in Golgi complex. Cells were washed twice with cold PBS and incubated with CD16/CD32 followed by staining with extracellular antibodies. After washing, cells were fixed in 100 µl Fixation buffer for 1 h and washed with 1 x permeabilization buffer. Cells were then stained with intracellular antibodies diluted in permeabilization buffer for 1 h at 4 °C in the dark before washing with 1 x permeabilization buffer and resuspended in PBS. Samples were measured by FACS Canto II flow cytometer and the data were analyzed by FlowJo V10.

To detect the apoptosis, astrocytes were treated with TNF (0, 10, 40, 100 ng/ml) and/or CHX (10 µg/ml) for 24 h. Cells were harvested and washed with PBS before adding 1 x Annexin binding buffer. 5 µl pacific blue Annexin V was added to 100 µl resuspended cells and incubated for 15 min at room temperature before washing with 1 x Annexin binding buffer. Cells were resuspended in 200 µl 1x Annexin binding buffer and 5 µl 7-amino actinomycin D (7-AAD) was added for 10 min incubation before measuring with Cytek Aurora.

3.2.5 Magnetic-activated cell sorting (MACS) of astrocytes

The spinal cord was isolated from naïve and EAE mice at day 0 and 15 p.i. Single cell suspension was obtained from the spinal cord using NeuroCult™ Enzymatic Dissociation Kit according to the manufacturer's instruction. 1 x 10^7 Cells were resuspended in 80 µl MACS buffer (0.5 % BSA in PBS) and 10 µl anti-astrocyte cell surface antigen-2 (ACSA-2) Microbeads were added for 15 min incubation at 4 °C. Cells were washed with MACS buffer and centrifuged at 1200 rpm for 10 min. The pellet was resuspended in 500 µl MACS buffer and applied to the LS columns for separation. LS column placed in the magnetic field of MACS separator was rinsed with 3 ml MACS buffer for three times. Enriched astrocytes in the flow were flushed out through the columns and resuspended in PBS after centrifuge. Anti-ACSA-2-PE antibody was applied to measure the purity of astrocytes, which was more than 90 % measured by FACS Canto II.

3.2.6 Transcriptome

The spinal cord of naïve and EAE-induced OTUD7B$^{fl/fl}$ and GFAP-Cre OTUD7B$^{fl/fl}$ mice were isolated and used for astrocytes purification. RNA was isolated from purified astrocytes with RNeasy Mini Kit according to the manufactures' instruction and DNA was removed by DNA-free kit. Transcriptome data analysis was carried out in collaboration with Dr. Andreas Jeron (Institute of Medical Microbiology and Hospital Hygiene, Otto-von-Guericke University Magdeburg, Germany).

3.2.7 Primary astrocyte culture

1- to 2- day-old newborn mice were immersed in 70 % ethanol for sterilization and tails were cut for genotyping. Afterward, the brains were taken out from the heads and single cells were obtained in astrocyte culture medium by passing the brain through 70 µm cell strainers. Cells were cultured in an incubator at 37 °C, 5 % CO_2 for 10 days and the medium was renewed every three days. On day 10, cells were harvested by trypsin and subcultured in a new flask. To increase the purity of astrocytes in culture, adherent cells were subcultured more than twice to remove microglia and neurons before using for experiments.

3.2.8 Immunohistochemistry

Anesthetized mice were perfused first with 0.9 % NaCl followed by 4 % PFA in PBS. Brains and spinal cord were isolated and fixed in 4 % PFA at 4 °C for 24 h. Immunohistochemistry was performed by Prof. Dr. Martina Deckert (Department of Neuropathology, University Hospital Cologne, Germany). In short, tissues were stained for hemalum & eosin and cresyl violet-luxol fast blue (CV-LFB). For staining of macrophages and neurofilament, tissues were stained with LCA, CD3, and Mac3 according to an ABC protocol with 3,3' diaminobenzidine (Sigma) and H_2O_2 (Merck) as substrate. Astrocytes were stained with mouse anti-GFAP with M.O.M. Kit and streptavidin-FITC according to the manufacturer's instructions. Images were captured by a Zeiss Axiophot with Zeiss Axioplan objective lenses, a Zeiss Axicam camera, and Zeiss Axiovision software.

3.2.9 Astrocyte treatment

To analyze cytokine receptor-activated signaling pathways, astrocytes were stimulated with TNF (10 ng/ml), IL-17 (50 ng/ml), or IFN-γ (10 ng/ml), respectively, for the indicated time points. To detect cell death, astrocytes were treated with TNF (40 ng/ml) and CHX (10 µg/ml) for the indicated time points to induce apoptosis. In degradation assays, the proteasome inhibitor MG132 (10 µM) was added in combination with TNF and CHX, and cells were harvested and at 0, 1, 3, and 6 h post treatment.

3.2.10 Quantitative real time-PCR (RT-PCR)

The spinal cord or culture cells were harvested in RLT buffer and RNA was isolated by RNeasy Mini Kit according to the manufacturer's instruction. cDNA was generated with SuperScript reverse transcriptase kit. Quantitative RT-PCR was performed with Taqman gene expression primers against TNF, IFN-γ, IL-17, GM-CSF, OTUD7B, CXCL1, CXCL10, CCL2, CCL20, nitric oxide synthase 2 (NOS2), IL-6, and hypoxanthine guanine phosphoribosyl transferase (HPRT). Samples were amplified on LightCycler 480 system (Table 8). Data were normalized to the expression of the reference gene HPRT and the relative expression of respective genes was analyzed based on $\Delta\Delta C_t$ values.

Table 8. PCR program

Steps	Temperature (°C)	Time	Cycles
Activation	50	2 min	
Initial denaturation	95	10 min	1 x
Denaturation	95	15 s	50 x
Annealing/Extension	60	1 min	
Cooling	37	1 min	1 x

3.2.11 Immunoprecipitation

Astrocytes were harvested in RIPA lysis buffer and precleared by centrifugation. The protein concentration was determined by Bradford Assay and equal amounts of protein were used for immunoprecipitation. Cell lysate was precleared with IgG and 100 µl/ml GammaBind G Sepharose beads for 2 h at 4 °C on a rocker to remove the non-specific binding and the beads were removed by centrifugation at 12 000 rpm for 10 min. The lysates were incubated with primary antibodies against TRAF2, RIPK1 and OTUD7B, or rabbit IgG and incubated overnight at 4 °C. The immunocomplex was precipitated by incubating with GammaBind G Sepharose beads for another 2 h at 4 °C. The immunocomplex was washed 5 times with PBS by centrifugation at 12 000 rpm for 5 sec and denatured in 2 x lane marker reducing sample buffer at 99 °C for 5 min. The supernatant was harvested for western blot.

3.2.12 Western blot

Primary astrocytes and mouse tissues were lysed in cold lysis buffer on ice for 30 min. Lysates were precleared by centrifugation at 12 000 rpm for 10 min at 4 °C and the supernatant was transferred carefully to a new 1.5 ml tube. The concentration was determined by Bradford Assay following the instructions of the manufacturer. Proteins were denatured in 5 x lane marker reducing sample buffer at 99 °C for 5 min. Equal amounts of proteins were loaded to SDS-polyacrylamide gels for separation and subsequently transferred to polyvinylidene difluoride (PVDF) membranes followed by blocking in 5% BSA in TBS-Tween 20 for 1 h. Membranes were incubated with primary antibodies overnight at 4 °C and later, with secondary antibodies for 1 h. Membranes were immersed in ECL plus kit, images

were captured by Intas Chemo Cam Luminescent Image Analysis system, and analyzed by LabImage software.

3.2.13 Statistics

Statistical significance was determined by two-tailed Student's *t* test. P values <0.05 were considered significant and all experiments were performed at least twice.

4. RESULTS

4.1 Anti-inflammatory function of OTUD7B in astrocytes during EAE

4.1.1 OTUD7B expression is reduced in MS and increased in EAE

To determine the abundance of OTUD7B in different organs of mice, we evaluated the expression of OTUD7B in various tissues of C57BL/6 mice by western blot. As shown in Figure 8a, OTUD7B is widely expressed in multiple tissues, such as brain, heart, spleen, lymph node, and thymus, but not in liver and kidney. Notably, the amount of OTUD7B is much higher in brain as compared to other tissues, which indicates the potential role of OTUD7B in CNS.

We therefore studied the expression profile of OTUD7B in the human brain using the Gene Expression Omnibus database (GEO) (https://www.ncbi.nlm.nih.gov/geoprofiles/90447843). As shown in the database (accession number GSE38010), the basal mRNA expression of OTUD7B was higher in the brains of healthy subjects but much lower in MS brain lesions (Fig. 8b). These data illustrate that OTUD7B is expressed in the CNS of mice and humans and might play a protective role in CNS autoimmunity.

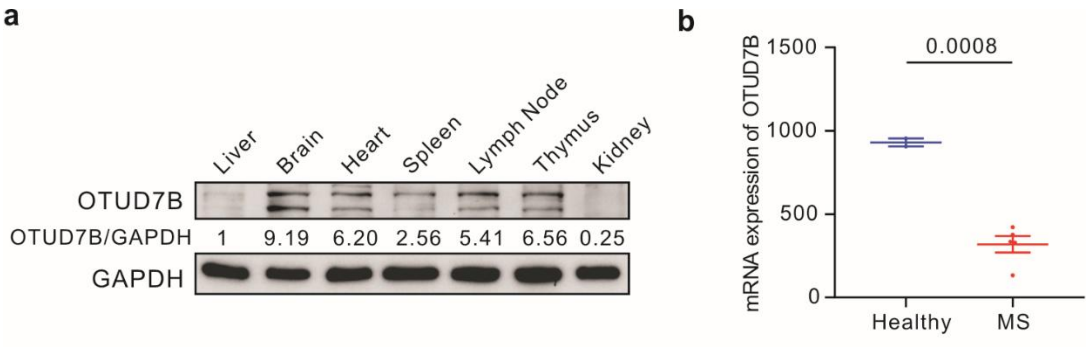

Figure 8. OTUD7B protein expression in mice and mRNA in MS brains

a. C57BL/6 mice were sacrificed and the tissues were harvested in RIPA lysis buffer. The expression of OTUD7B and GAPDH was determined by western blot. b. mRNA levels of OTUD7B from the brains of healthy subjects and MS patients were analyzed (GEO database, accession number GSE38010).

To further study the function of OTUD7B in CNS autoimmunity, we used EAE, a widely used animal model for MS. C57BL/6 mice were immunized with MOG_{35-55} peptide and pertussis toxin for EAE induction and the spinal cord were isolated at the peak (day 15) and during remission (day 22) of the disease. mRNA levels of OTUD7B were significantly upregulated at day 15 post-immunization (p.i.) compared to day 0, but were no longer increased at day 22 p.i. (Fig. 9a), indicating that OTUD7B levels were upregulated in the spinal cord of mice with full-blown EAE.

Since astrocytes are the most abundant cell population in the CNS, we evaluated OTUD7B levels in astrocytes. Astrocytes were isolated from the spinal cord of naïve and EAE mice (day 15 p.i.) using ACSA-2 MicroBeads by MACS and the purity was > 90 % as determined by FACS (Fig. 9b left). As shown in Figure 9b (right), mRNA levels of astrocytic OTUD7B were significantly increased in EAE mice compared to naïve mice.

The observation that in humans high levels of OTUD7B correspond to a healthy brain and astrocytes strongly upregulated OTUD7B during EAE raised the hypothesis that astrocytic OTUD7B might attenuate the course of EAE in mice.

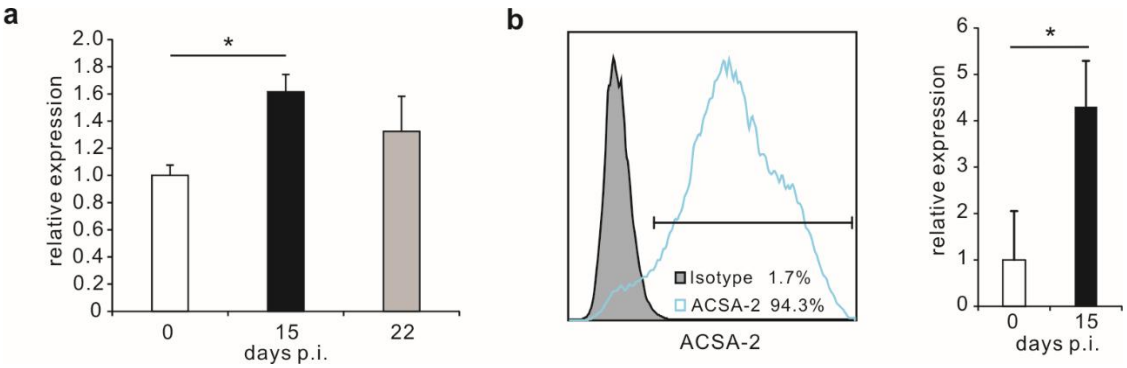

Figure 9. OTUD7B expression is increased in astrocytes during EAE

a. EAE was induced in C57BL/6 mice and the spinal cord were harvested in RLT buffer at indicated time points for RNA isolation. The expression of OTUD7B was measured by qRT-PCR and normalized to HPRT. b. Astrocytes were isolated by MACS with ACSA-2 MicroBeads from naïve and EAE mice, the purity of astrocytes was determined by flow cytometry by staining with ACSA-2 PE antibody. RNA was isolated from the purified astrocytes and OTUD7B level was determined by qRT-PCR.

4.1.2 Generation and characterization of mice with astrocytic deletion of OTUD7B

To explore the function of astrocytic OTUD7B in EAE, we used the Cre/loxP system to generate GFAP-Cre OTUD7B$^{fl/fl}$ mice which had a specific deletion of OTUD7B in astrocytes. To establish mice with astrocyte-specific deletion of OTUD7B, we used embryonic stem (ES) cells of The European Conditional Mouse Mutagenesis Program (EUCOMM; https://www.eummcr.org/search?q=otud7b&b=Go). These ES cells allow knock out first with conditional potential of the respective gene (https://www.eummcr.org/products/es-cells). The scheme of *otud7b* (exon 7) targeted ES cells is illustrated in Figure 10a. To obtain mice with a conditional deletion of *otud7b*, we collaborated with Ronald Naumann (Max Planck Institute, of Molecular Cell Biology and Genetics, Transgenic Core Facility, Dresden, Germany), who generated C57BL/6 OTUD7B$^{fl/wt\text{-}FRT/wt}$ mice by implantation of OTUD7B-targeted ES cells into albino C57BL/6 mice. C57BL/6-OTUD7B$^{fl/WT\text{-}FRT/wt}$ mice were crossed with B6.129S4-*Gt(ROSA)26Sor*$^{tm1(FLP1)Dym}$/RainJ mice (Jackson Laboratory, USA) which express the *Saccharomyces cerevisiae FLP1* recombinase gene driven by the *Gt(ROSA)26Sor* promoter., to delete the FRT sites. Deletion of the FRT sites was controlled by PCR and sequencing of the PCR products. In the Animal Facility of the University of Magdeburg, C57BL/6 OTUD7B$^{fl/wt}$ offsprings with deletion of the FRT sites were further crossed with C57BL/6 GFAP-Cre mice to obtain with GFAP-Cre OTUD7B$^{fl/fl}$ mice. WB analysis of astrocytes from GFAP-Cre OTUD7B$^{fl/fl}$ mice showed an efficient deletion of OTUD7B (Fig. 10b).

To determine whether OTUD7B deficiency in astrocytes affects the homeostasis of the immune system in lymphatic organs and the CNS, we analyzed the composition of immune cells, including CD4^{+} T cells, CD8^{+} T cells, B cells, CD11c^{+} cells, and monocyte/macrophage in spinal cord, spleen, and lymph node from OTUD7B$^{fl/fl}$ and GFAP-Cre OTUD7B$^{fl/fl}$ mice. In naïve mice, CD4^{+} and CD8^{+} T cells show similar and low frequency in spinal cord of both groups (Fig. 10c), the number of immune cells in spinal cord has no remarkable difference between two groups (Fig. 10d), indicating that OTUD7B deficiency does not cause spontaneous CNS inflammation. Similarly, OTUD7B deficiency in astrocytes did not affect the composition of immune cells in spleens (Fig. 10e) and lymph nodes (Fig. 10f).

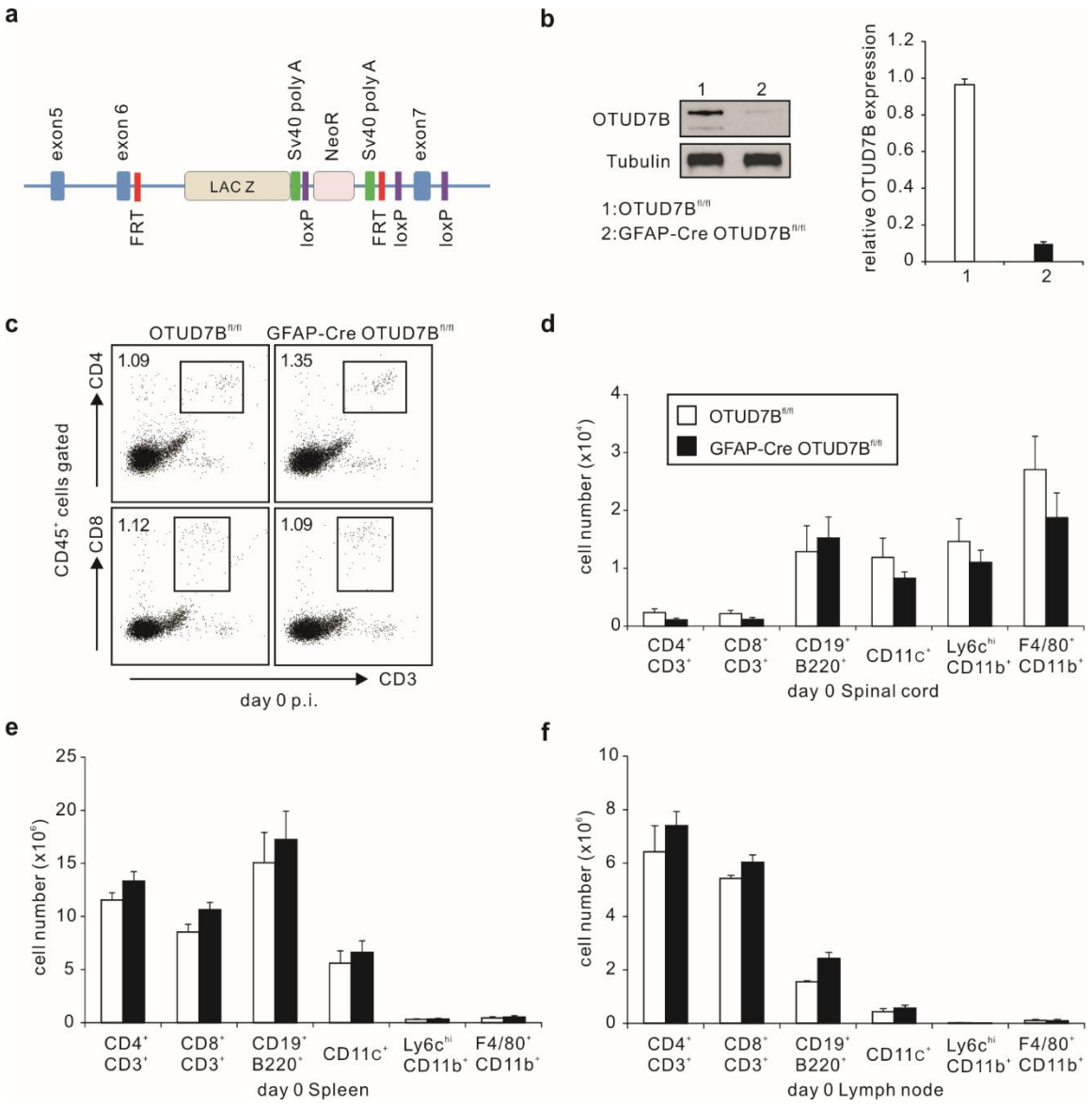

Figure 10. Characterization of GFAP-Cre OTUD7B$^{fl/fl}$ mice under homeostatic conditions

a. Schematic illustration of the ES cells with the targeted *otud7b* gene. b. Primary astrocytes were isolated from P0/1 pulps for culture and harvested in RIPA lysis buffer. OTUD7B levels were determined by western blot and relative expression was normalized to tubulin (n=3). c. The spinal cord of naïve OTUD7B$^{fl/fl}$ and GFAP-Cre OTUD7B$^{fl/fl}$ mice were isolated and stained for CD4^{+} T cells and CD8^{+} T cells. The cell number of leukocytes was calculated according to the percentage and total cell number in spinal cord (n=6) (d), spleen (n=7) (e), and lymph node (n=7) (f). Data show the mean with SEM.

4.2 Astrocytic OTUD7B ameliorates EAE

4.2.1 Aggravated EAE in GFAP-Cre OTUD7B$^{fl/fl}$ mice

To determine the function of astrocytic OTUD7B in CNS autoimmunity, EAE was induced in OTUD7B$^{fl/fl}$ (control mice with normal OTUD7B expression) and GFAP-Cre OTUD7B$^{fl/fl}$ mice by immunization with MOG_{35-55} and pertussis toxin. Clinical scores and body weight of each mouse were monitored daily. As illustrated in Table 9, both OTUD7B$^{fl/fl}$ and GFAP-Cre OTUD7B$^{fl/fl}$ had similar disease onset. However, GFAP-Cre OTUD7B$^{fl/fl}$ mice developed more severe symptoms and had higher disease incidence.

Table 9. OTUD7B deficiency in astrocytes reduces disease incidence and symptoms

Genotype	Disease incidence[a]	Day of onset[b]	Maximal score[c]
OTUD7B$^{fl/fl}$	20/25	13.0±0.7	1.8±0.3
GFAP-Cre OTUD7B$^{fl/fl}$	24/24	13.8±1.0	2.7±0.1
P Value		P=0.5	P<0.05

a: EAE was induced in OTUD7B$^{fl/fl}$ (n=25) and GFAP-Cre OTUD7B$^{fl/fl}$ (n=24) mice. The mice were monitored daily for clinical signs of EAE and mice with a score > 0.5 were recorded as diseased.
b: The day with first clinical score > 0.5 was recorded as the day of disease onset. Data show the mean ± SEM of all immunized mice per group.
c: Mice were monitored daily up to day 30 p.i. The highest clinical score was determined as the maximal score. Data show the mean ± SEM of all immunized mice per group.

Moreover, as shown in Figure 11a, GFAP-Cre OTUD7B$^{fl/fl}$ mice had more severe EAE course, concomitantly, body weight declined more dramatically in GFAP-Cre OTUD7B$^{fl/fl}$ as compared to OTUD7B$^{fl/fl}$ mice, indicating that astrocytic OTUD7B ameliorates EAE.

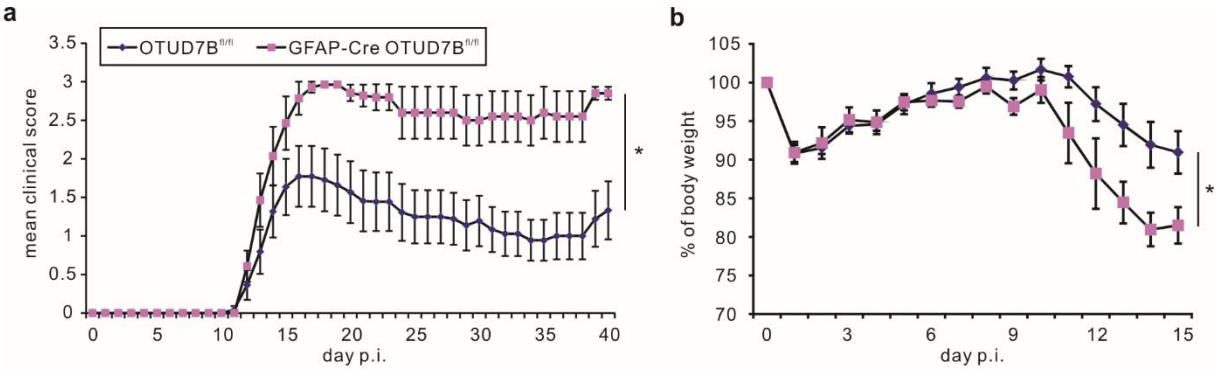

Figure 11. GFAP-Cre OTUD7B$^{fl/fl}$ mice developed more severe EAE

EAE was induced in OTUD7B$^{fl/fl}$ (n=11) and GFAP-Cre OTUD7B$^{fl/fl}$ (n=7) mice. The clinical scores (a) and body weight (b) were monitored daily after immunization. Data show mean clinal sore with SEM (* $p<0.05$).

4.2.2 Increased infiltration of immune cells in the spinal cord of GFAP-Cre OTUD7B$^{fl/fl}$ mice

EAE is mainly mediated by infiltrating leukocytes, especially CD4$^+$ T cells, which enter the CNS parenchyma and cause local inflammation and damage. We isolated leukocytes from the spinal cord of EAE mice of both groups at day 15 p.i. and analyzed the population of leukocytes by flow cytometry. As illustrated in Figure 12a, the frequency of CD4$^+$ T cells in the spinal cord from GFAP-Cre OTUD7B$^{fl/fl}$ mice was higher than in OTUD7B$^{fl/fl}$ mice at day 15 p.i. Moreover, due to the increased total leukocyte number, more infiltrating CD4$^+$ T cells, CD11c$^+$ cells, F4/80$^+$ CD11b$^+$ macrophages, and Ly6C^{hi} CD11b$^+$ inflammatory monocytes were detected in spinal cord of GFAP-Cre OTUD7B$^{fl/fl}$ mice (Fig. 12b).

Among the T cells, IFN-γ-producing, IL-17-producing, and GM-CSF-producing CD4$^+$ T cells are the major effectors in EAE and passive transfer of each subtype can induce EAE (Domingues, Mues et al. 2010, Codarri, Gyulveszi et al. 2011). Thus, we analyzed the subpopulations of CD4$^+$ T cells, and as shown in Figure 12c, the frequency of each subpopulation was similar at day 15 p.i., which indicates that OTUD7B does not influence the differentiation and composition of CD4$^+$ T cells. However, we observed that the total number of encephalitogenic IFN-γ$^+$, IL-17$^+$ and GM-CSF$^+$ CD4$^+$ T cells was increased in the spinal

cord of GFAP-Cre OTUD7B$^{fl/fl}$ mice compared to OTUD7B$^{fl/fl}$ mice at day 15 p.i. (Fig. 12d). Collectively, these data indicate that astrocytic OTUD7B ameliorates EAE by dampening the numbers of EAE-inducing encephalitogenic leukocytes in the spinal cord.

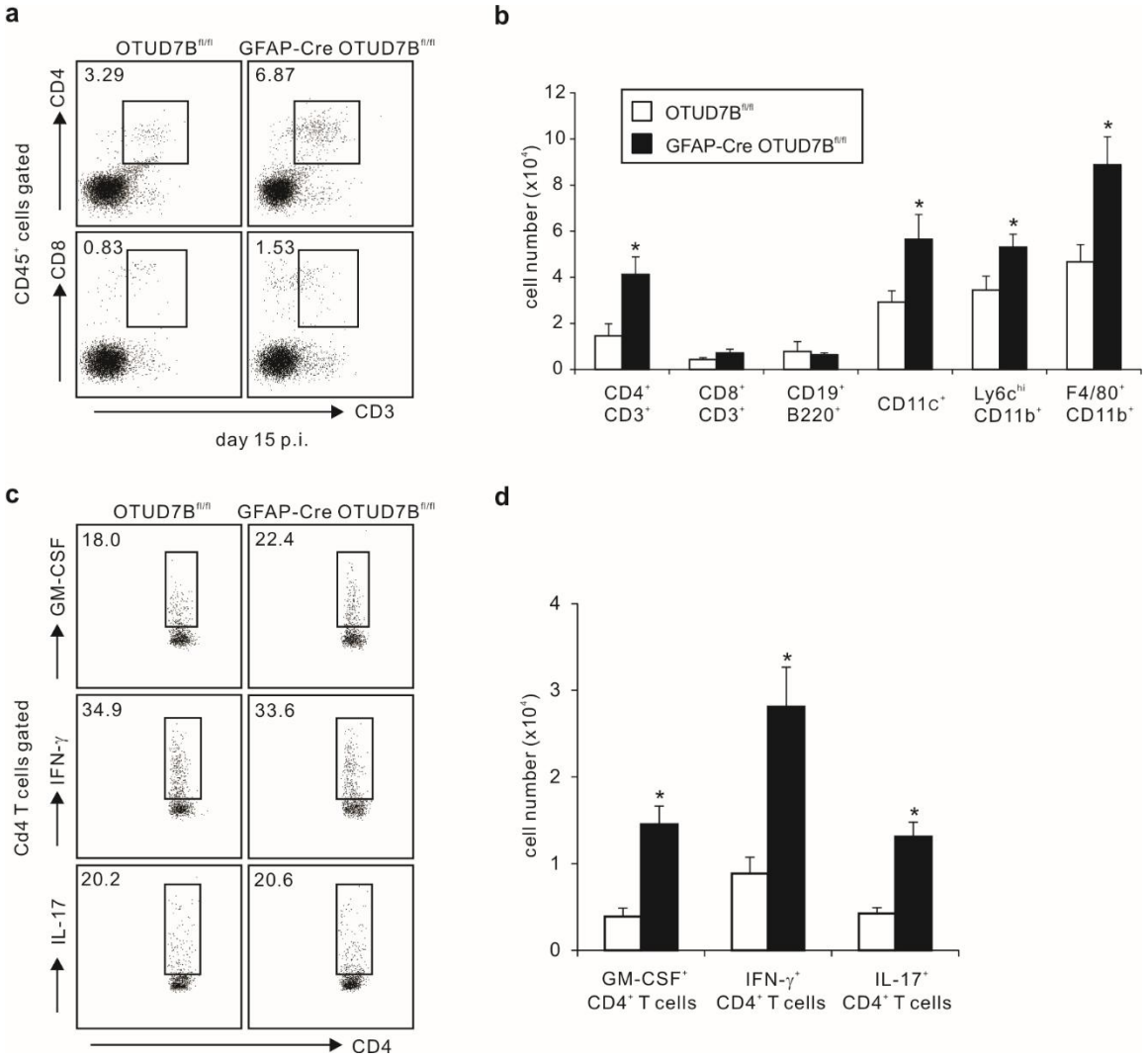

Figure 12. Increased infiltration of immune cells and encephalitogenic CD4$^+$ T cells in the spinal cord of GFAP-Cre OTUD7B$^{fl/fl}$ mice

The spinal cord from MOG$_{35-55}$ immunized OTUD7B$^{fl/fl}$ (n=9) and GFAP-Cre OTUD7B$^{fl/fl}$ (n=9) mice were isolated after 15 p.i. by Percoll gradient centrifugation for flow cytometry (mean±SEM, *p<0.05). a. The gating strategy of CD4$^+$ and CD8$^+$ CD3$^+$ T cells is shown. b. The absolute number of infiltrating leukocytes was calculated according to the total cell number and frequency. c. Subpopulations of CD4$^+$ T cells were gated by CD45$^+$ cells and the representative dot plots of IFN-γ$^+$, IL-17$^+$ and GM-CSF$^+$ CD4$^+$ T cells in the spinal cord of OTUD7B$^{fl/fl}$ and GFAP-Cre OTUD7B$^{fl/fl}$ mice are shown. d.

Absolute numbers of IFN-γ^+, IL-17^+ and GM-CSF^+ $CD4^+$ T cells were calculated according to the total cell number and frequency.

4.2.3 Increased transcription of proinflammatory factors in the spinal cord of GFAP-Cre OTUD7B$^{fl/fl}$ mice

Cytokines and chemokines released by immune cells and CNS resident cells, drive the neuroinflammation in EAE. Thus, we evaluated the mRNA levels of pro-inflammatory factors by quantitative RT-PCR in the spinal cord of mice with EAE. The mRNA levels of pro-inflammatory factors, including TNF, IL-17, IFN-γ, GM-CSF, NOS2, and CXCL10, were increased in the spinal cord of GFAP-cre OTUD7B$^{fl/fl}$ mice in comparison to OTUD7B$^{fl/fl}$ mice (Fig. 13a), suggesting astrocytic OTUD7B suppresses the neuroinflammation.

Astrocytes are one of the major cell types responding to CNS insults to produce pro-inflammatory factors. To evaluate the impact of OTUD7B on the mRNA levels of astrocytes in an unbiased manner, the transcriptome of astrocytes isolated from the spinal cord of OTUD7B$^{fl/fl}$ and GFAP-cre OTUD7B$^{fl/fl}$ mice was determined at day 0 and day 15 p.i. The transcriptome analysis detected major differences in the chemokine analysis of the different groups of mice. The basal levels of chemokines were low in astrocytes from naïve OTUD7B$^{fl/fl}$ and GFAP-Cre OTUD7B$^{fl/fl}$ mice. However, EAE induced an increased expression of chemokines at day 15 p.i. in astrocytes. Notably, the levels of chemokines, such as CXCL13, CCL7, CCL2, CXCL2, and CXCL10 were higher in astrocytes from GFAP-Cre OTUD7B$^{fl/fl}$ mice (Fig. 13b), indicating that OTUD7B suppresses the production of chemokines in astrocytes during EAE.

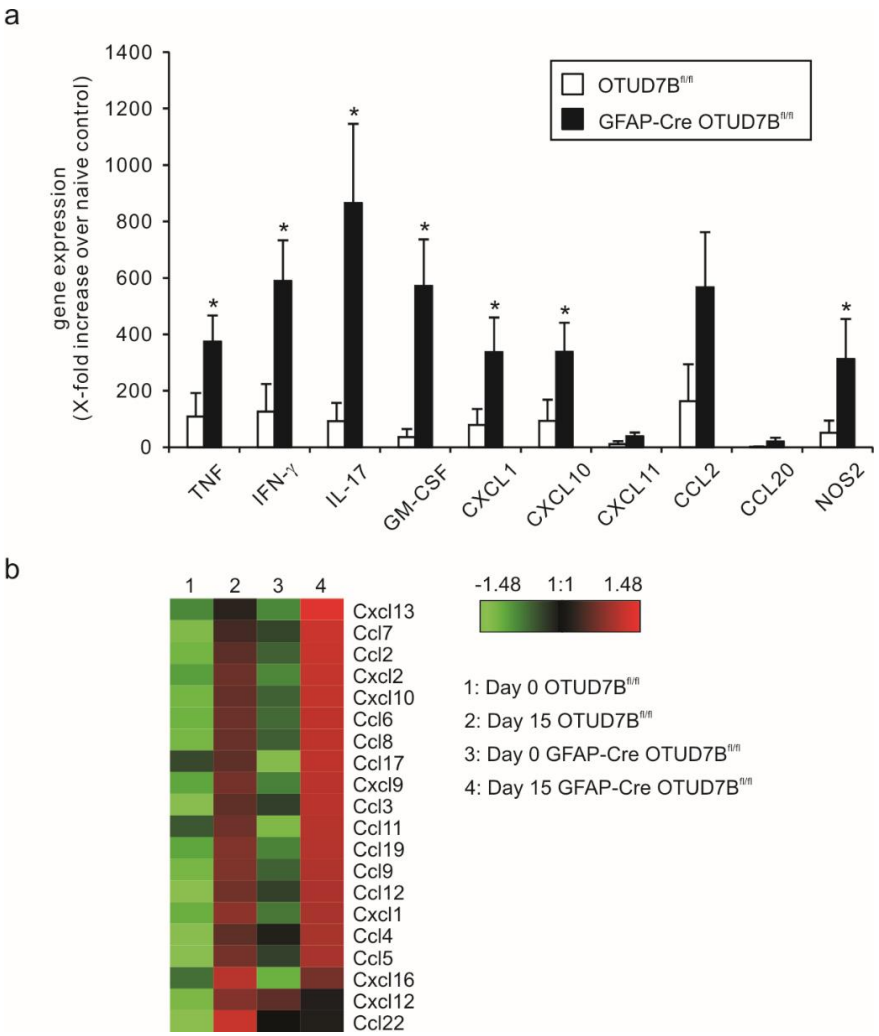

Figure 13. Increased cytokines and chemokines in spinal cord of GFAP-Cre OTUD7B$^{fl/fl}$ mice during EAE

a. RNA was isolated from the spinal cord of OTUD7B$^{fl/fl}$ and GFAP-Cre OTUD7B$^{fl/fl}$ mice from non-immunized and mice with EAE (day 15 p.i.) for quantitative RT-PCR analysis. Gene expression was normalized to HPRT and the fold-increased of immunized over non-immunized mice is shown (*$p<0.05$). b. Astrocytes were isolated from the spinal cord of OTUD7B$^{fl/fl}$ and GFAP-Cre OTUD7B$^{fl/fl}$ mice using anti-ACSA-2 MicroBeads and RNA was isolated followed by DNase treatment to reduce DNA contamination. Purified RNA was used for transcriptome analysis. Pooled RNA of 3-5 mice per group was analyzed.

4.2.4 OTUD7B suppressed TNF-induced expression of proinflammatory cytokines in astrocytes

Astrocytes are sensitive to CNS insult and are the major CNS resident cells producing pro-inflammatory factors. To further evaluate the influence of OTUD7B on pro-inflammatory responses in astrocytes, we performed an in vitro experiment and determined the mRNA levels of proinflammatory factors by RT-PCR in astrocytes. In these experiments, primary astrocytes were isolated from 1-2 day old newborn OTUD7B$^{fl/fl}$ and GFAP-Cre OTUD7B$^{fl/fl}$ mice, followed by stimulation with TNF, IFN-γ, and IL-17, which are fingerprint cytokines produced by encephalitogenic T cells. RNA was isolated after 16 h of incubation and RT-PCR was performed for the indicated factors. We observed a significant upregulation of chemokines and cytokines in OTUD7B-deficient astrocytes, including CXCL1, CXCL10, CXCL11, IL-6, CCL2, CCL20 and NOS2, upon TNF stimulation (Fig. 14). However, there was less difference between OTUD7B-sufficient and -deficient astrocytes upon IL-17 and IFN-γ stimulation. Only OTUD7B-deficient astrocytes expressed more CXCL1 in response to IL-17 and more IL-6 in response to IFN-γ. In summary, OTUD7B suppresses TNF-induced production of proinflammatory factors, but not IL-17 and IFN-γ induced in astrocytes, explaining the enhanced levels of chemokines in astrocytes from GFAP-Cre OTUD7B$^{fl/fl}$ mice which might be TNF-dependent.

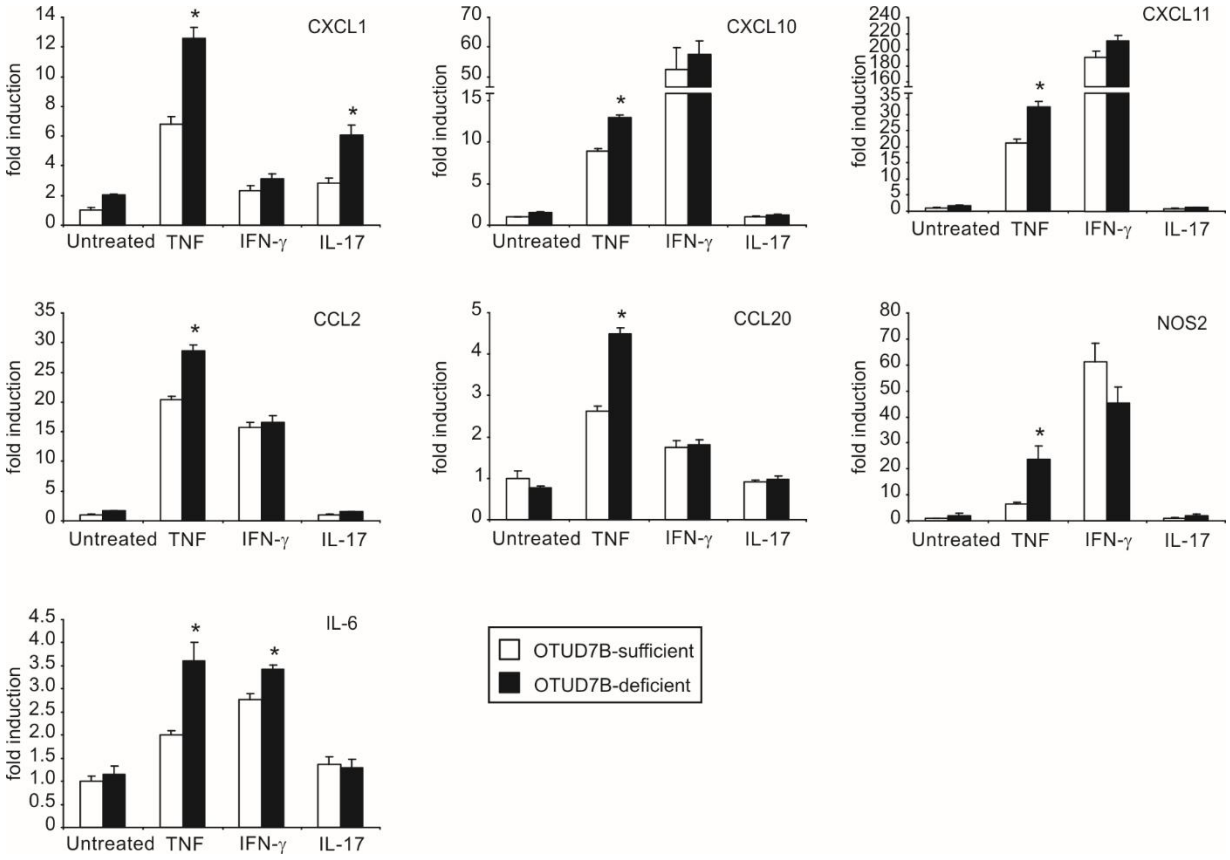

Figure 14. OTUD7B suppresses TNF-induced expression of pro-inflammatory factors

Primary astrocytes from OTUD7B$^{fl/fl}$ and GFAP-Cre OTUD7B$^{fl/fl}$ were left untreated or stimulated with 10 ng/ml TNF, 10 ng/ml IFN-γ, or 50 ng/ml IL-17 for 16 h as indicated. RNA was isolated for quantitative RT-PCR and gene expression was normalized to HPRT (mean±SEM, * $p < 0.05$).

4.2.5 OTUD7B impairs TNF-induced NF-κB and MAPK pathways

The engagement of TNF to TNFR1 activates both the NF-κB and MAPK pathways, including ERK1/2, JNK, and p38. To study the impact of OTUD7B on TNF signaling pathways, we stimulated cultured astrocytes from OTUD7B$^{fl/fl}$ and GFAP-Cre OTUD7B$^{fl/fl}$ mice with 10 ng/ml TNF for 0, 10, 30, and 60 min. In line with a previous study (Enesa, Zakkar et al. 2008), NF-κB was more activated in OTUD7B-deficient astrocytes as reflected by enhanced phosphorylation of p65 and IκBα in response to TNF (Fig. 15a). In addition, MAPK pathways, including p-JNK, p-ERK, p-p38, were also more activated in OTUD7B-deficient astrocytes upon TNF treatment, implying that OTUD7B is a crucial factor in controlling the proximal TNFR1 signaling to suppress the activation of the NF-κB and MAPK pathways. IFN-γ

activated signaling molecules, such as phosphorylated STAT1 at tyrosine 701 and 727, were slightly increased in OTUD7B-deficient astrocytes compared to OTUD7B-sufficient astrocytes (Fig. 15b). In addition, OTUD7B did not regulate the IL-17 signaling as indicated by similar activation of NF-κB and MAPK pathways (Fig. 15c). Thus, in good agreement with the RT-PCR, our data indicate that OTUD7B suppresses TNF-activated signaling including the MAPK and NF-κB pathways in astrocytes, but only has only a minor impact on IL-17 and IFN-γ signaling.

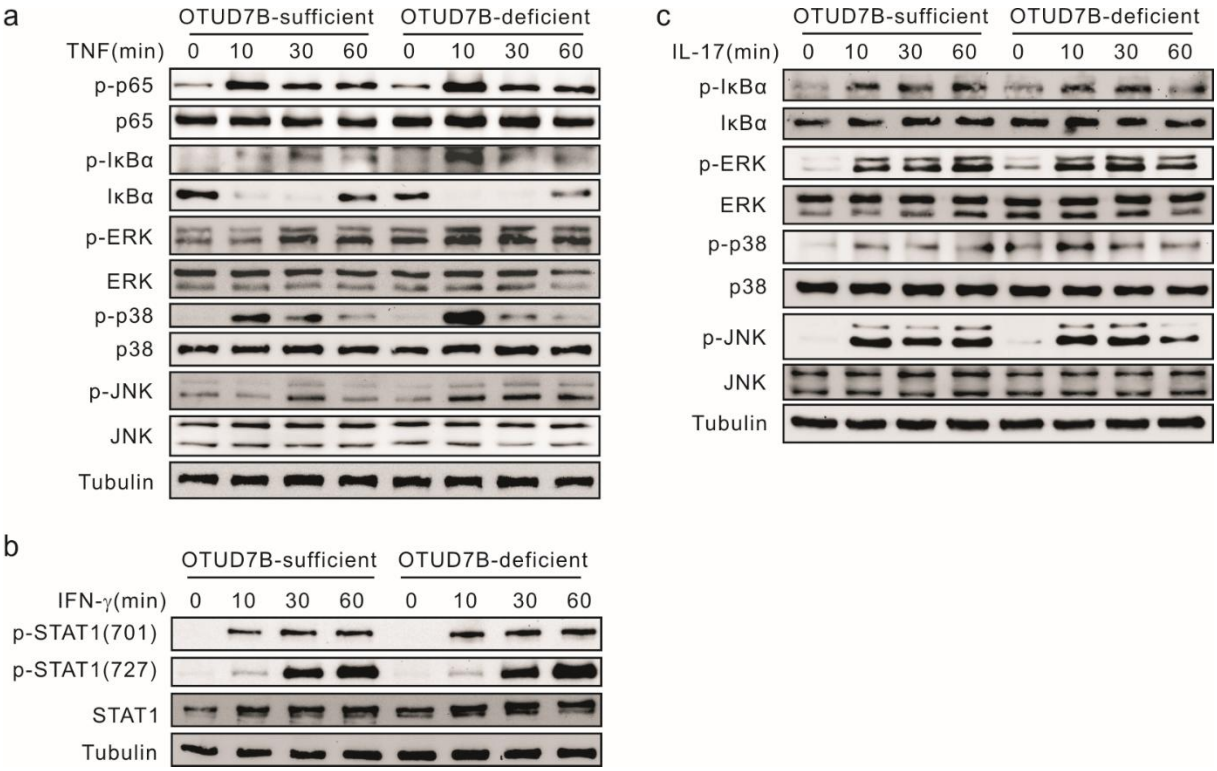

Figure 15. OTUD7B deficiency upregulates TNF signaling in astrocytes

Western blot of primary astrocytes from OTUD7B$^{fl/fl}$ and GFAP-Cre OTUD7B$^{fl/fl}$ which were stimulated with 10 ng/ml TNF (a), 10 ng/ml IFN-γ (b), or 50ng/ml IL-17 (c) for indicated time points.

4.2.6 OTUD7B deficiency leads to increased ubiquitination of RIPK1

TNF induced a stronger activation of the MAPK and NF-κB pathways in OTUD7B-deficient astrocytes, which implies that OTUD7B might directly regulate TNF signaling molecules. It

has been reported that OTUD7B can be recruited to the TNFR1 and regulate the ubiquitination of RIPK1 (Enesa, Zakkar et al. 2008). Here, a similar result was obtained for OTUD7B which reduced RIPK1 ubiquitination (Fig. 16a). However, we could not detect an interaction of OTUD7B with RIPK1.

We additionally screened the upstream molecules of TNF signaling which could interact with OTUD7B by immunoprecipitation. OTUD7B-sufficient astrocytes were stimulated with TNF (20 ng/ml) and immunoprecipitation was performed. We newly identified an interaction of OTUD7B with TRAF2 upon stimulation (Fig. 16b) and immunoprecipitation of TRAF2 also showed strong interaction with OTUD7B upon TNF stimulation (Fig. 16c), which indicates OTUD7B is recruited to TNFR1 complex upon TNF stimulation. Both TRAF2 and cIAP1 are E3 ligases, which mediate K63-linked ubiquitination of RIPK1 (Lee, Shank et al. 2004, Bertrand, Lippens et al. 2011). On the other hand, TRAF2 undergoes K63-linked ubiquitination which acts as a dock for IKK and TAK1 complex (Li, Wang et al. 2009). However, K63-linked ubiquitination of TRAF2 was not regulated by OTUD7B upon TNF stimulation (Fig. 16c).

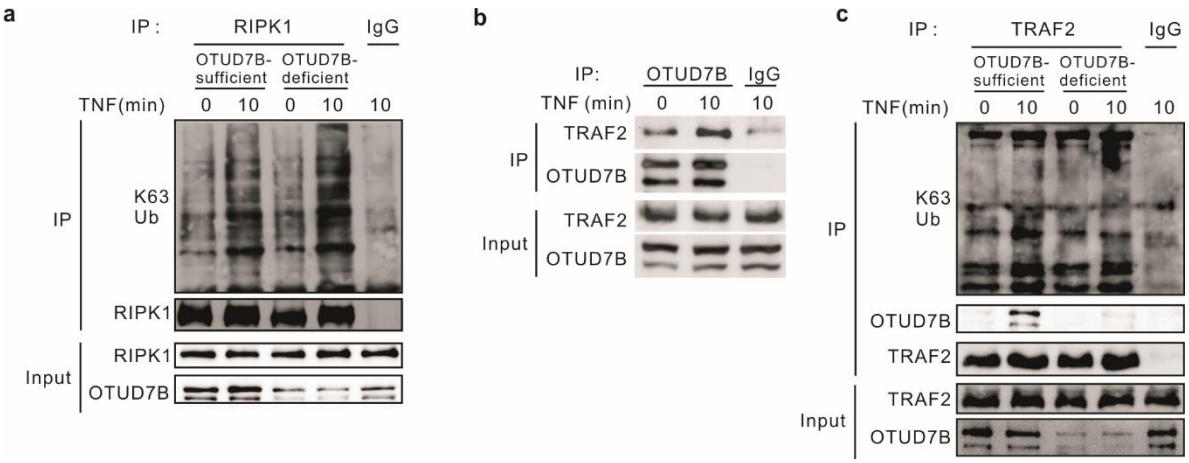

Figure 16. OTUD7B interacts with TRAF2 upon TNF stimulation

Astrocytes were stimulated with 20 ng/ml TNF for 10 min and cells were harvested for RIPK1 (a), OTUD7B (b), TRAF2 (c) immunoprecipitation. Western blots were performed to detect the indicated target proteins.

4.3 Pro-survival function of astrocytic OTUD7B in EAE

The loss of astrocyte in MS lesions has been reported (Dowling, Husar et al. 1997, Palma, Yauch et al. 1999). In good agreement with a protective function at a late stage of EAE, we have previously revealed that knockout of astrocytic glycoprotein 130, a receptor for cytokines of IL-6 family, caused the apoptosis of astrocytes in inflammatory lesions, leads to a chronic wide-spread infiltration of encephalitogenic T cells in the CNS and more severe EAE (Haroon, Drogemuller et al. 2011). Also, in EAE of GFAP-Cre OTUD7B$^{fl/fl}$ mice, hypertrophic and activated astrocytes with increased GFAP immunoreactivity were strongly reduced as compared to control mice (Fig. 17).

To explore the impact of OTUD7B on astrocyte morphology in EAE, the spinal cord of OTUD7B$^{fl/fl}$ and GFAP-Cre OTUD7B$^{fl/fl}$ mice were isolated and fixed for histological analysis. In control mice, astrocytes were strongly GFAP-positive and hypertrophic close to inflammatory lesions, whereas only few GFAP^{+} astrocytes were detectable close to inflammatory lesions in GFAP-Cre OTUD7B$^{fl/fl}$ mice (Fig.17). In non-immunize mice, astrocytes of both mouse strains were equally weak GFAP positive (data not shown). Thus, the more severe course of EAE in GFAP-Cre OTUD7B$^{fl/fl}$ mice correlates with a reduction of the number of hypertrophic astrocytes.

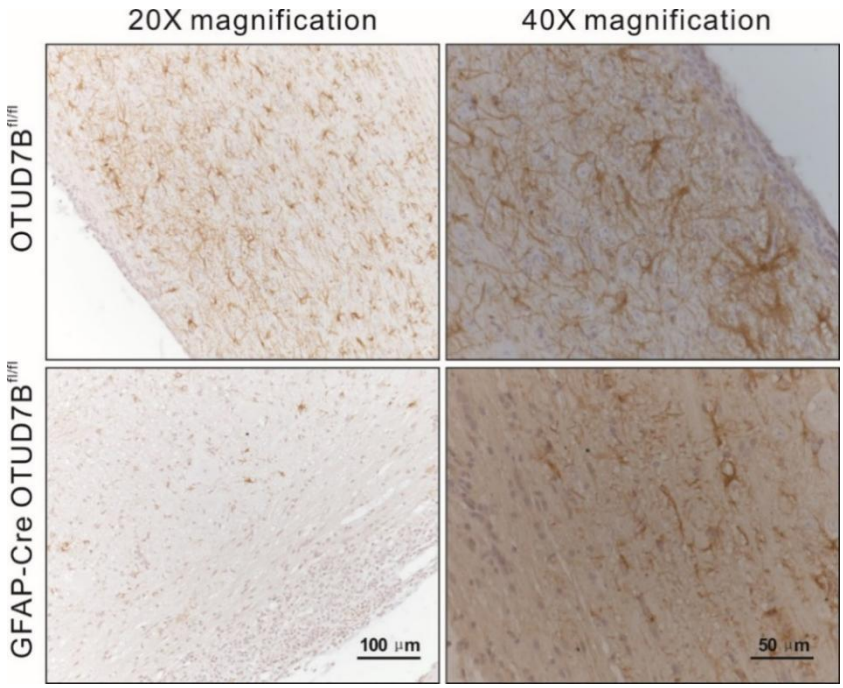

Figure 17. GFAP-Cre OTUD7B$^{fl/fl}$ mice have more astrocyte loss

OTUD7B$^{fl/fl}$ and GFAP-Cre OTUD7B$^{fl/fl}$ mice were immunized with MOG peptide for EAE induction. The spinal cord was harvested after 15 p.i. and immostained GFAP with slight hemalum counterstaining. Note the reduced numbers of hypertrophic GFAP^{+} astrocytes close to inflammatory lesions in GFAP-Cre OTUD7B$^{fl/fl}$ mice.

4.3.1 OTUD7B deficiency renders astrocytes susceptible to TNF and CHX induced cell death

Besides the pro-survival pathway, TNF can also induce cell death. Thus, to figure out if the reduction of astrocytes in inflammatory lesions of GFAP-Cre OTUD7B$^{fl/fl}$ mice was associated with TNF-induced cell death, we performed in vitro experiment by treating astrocytes with various concentrations of TNF for 24h and analyzed cell death by annexin V/7-AAD staining followed by flow cytometry. We detected that OTUD7B-sufficient astrocytes stimulated with increasing TNF were resistant to cell death (Fig. 18a). In contrast, OTUD7B-deficient astrocytes showed a slightly enhanced Annexin V staining with increasing TNF concentrations (Fig. 18a). Considering that TNF is a weak inducer of apoptosis, if the host cell protein synthesis is intact. Cycloheximide (CHX), a protein synthesis inhibitor, was added in our experiment. As shown in Figure 18b, OTUD7B-deficient astrocytes upon TNF plus CHX treatment, increased the number of Annexin V^{+} cells in both genotypes, but

significantly more in OTUD7B-deficient astrocytes indicating that OTUD7B protects cells from TNF-induced cell death.

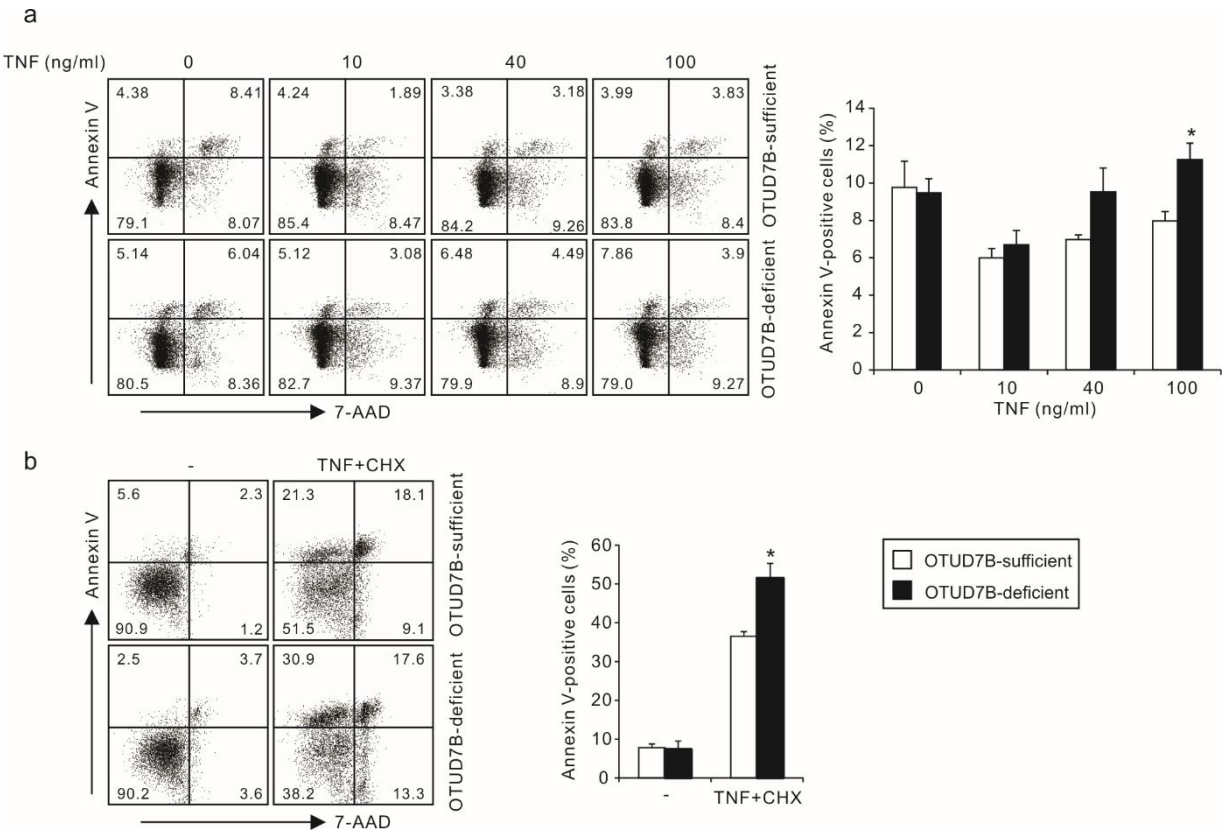

Figure 18. OTUD7B-deficient astrocytes undergo increased TNF-induced apoptosis

OTUD7B-suficient and -deficient astrocytes were stimulated with increased TNF (a) or TNF plus CHX (b) and cells were harvested after 24 h for Annexin V and 7-AAD staining (* $p<0.05$).

TNF-induced apoptosis depends on the cleavage of caspase-8, which subsequently cleaves downstream effector caspase-3. Thus, to investigate the mechanism by which OTUD7B regulates TNF-induced apoptosis, astrocytes were treated with TNF plus CHX for the indicated time periods. Cleaved active caspase-8 and caspase-3 were observed at 3h in both groups, however, OTUD7B-deficient astrocytes had more cleaved caspase-8 and cleaved caspase-3 upon TNF plus CHX co-treatment (Fig. 19a), indicating that OTUD7B protects astrocytes from TNF-induced apoptosis by suppressing the cleavage of caspase-8 and caspase-3. As the NF-κB and MAPK are implicated in the regulation of apoptotic cell death (Kaltschmidt, Kaltschmidt et al. 2000, Yue and Lopez 2020), we stimulated the astrocytes with TNF for longer time points to determine the activation of the MAPK and NF-κB

pathways. As shown in Figure 19b, there was no significant difference in the activation of the MAPK and NF-κB pathways at later time points upon TNF treatment. Only at early time points, NF-κB (p-p65, p-IkBa;10 min) and the MAPK (p-ERK, p-JNK and p-p38 10 min) were increased in TNF-stimulated OTUD7B-deficient astrocytes, indicating the enhanced apoptosis in OTUD7B-deficient astrocytes does not contribute to NF-κB and MAPK pathway. In summary, OTUD7B protects astrocytes from TNF-induced apoptosis which is independent of the activation of canonical NF-κB and MAPK pathways.

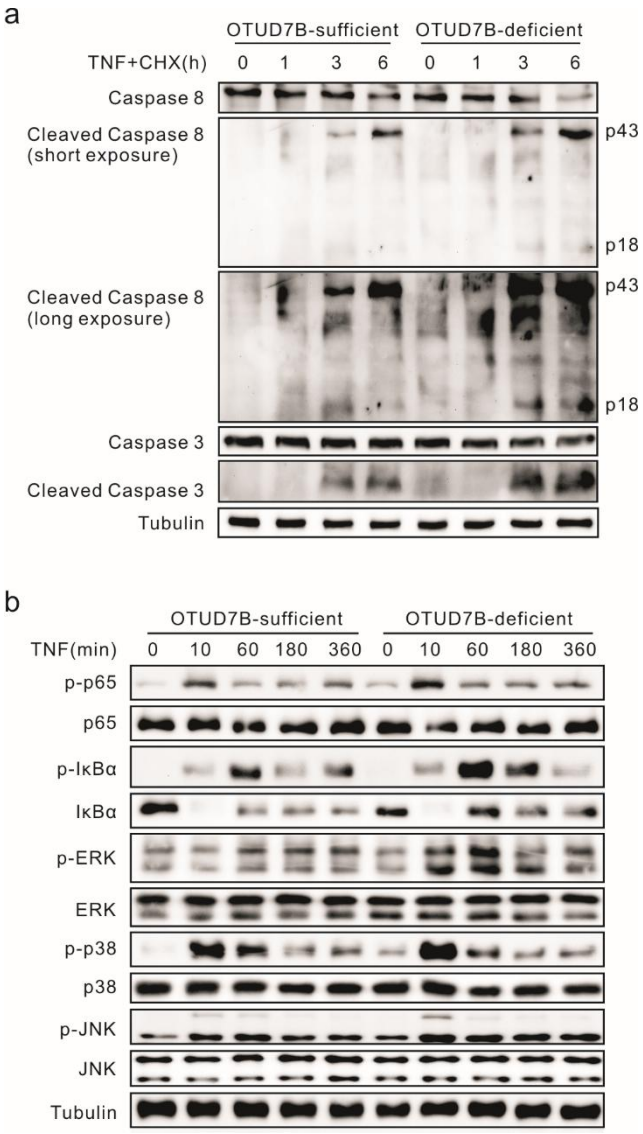

Figure 19. OTUD7B protects astrocytes from TNF-induced apoptosis

a. OTUD7B-suficient and -deficient astrocytes were treated with 40 ng/ml TNF plus 10 μg/ml CHX for the indicated time points and western blot was performed to detect cleavage of caspase-3 and

caspase-8. b. OTUD7B-suficient and -deficient astrocytes were treated with TNF for the indicated time points. Cells were harvested for western blot and the activation of NF-κB and MAPK pathways was determined.

4.3.2 OTUD7B protects RIPK1 and TRAF2 from degradation

To identify the key molecules regulated by OTUD7B in TNF signaling, we checked the levels of several molecules in TNF-induced apoptotic pathway in OTUD7B-sufficient and -deficient astrocytes. Here, we found that the levels of RIPK1 and TRAF2 were reduced at 3h after stimulation with TNF plus CHX, however, the reduction was more pronounced in OTUD7B-deficient astrocytes (Fig. 20a, 20b). It is known that CHX sensitizes cells to TNF-induced apoptosis by preventing the translation of pro-survival proteins such as FLIP. However, FLIP decreased equally in both groups. Moreover, the levels of cIAP1, FADD and TRADD had no difference between two groups (Fig. 20a). Though, some reports indicated that loss of RIPK1 leads to the degradation of cIAP1 (Gentle, Wong et al. 2011), cIAP1 levels did not reduce in both groups upon co-treatment with TNF and CHX (Fig. 20a). To clarify the mechanism of RIPK1 and TRAF2 reduction, cells were treated with proteasome inhibitor MG132. The degradation was rescued by MG132 in OTUD7B-deficient astrocytes (Fig. 20c), which indicates that both RIPK1 and TRAF2 undergo proteasomal degradation. In addition, treatment with the RIPK1 kinase inhibitor Nec1s or/and caspase inhibitor zVAD strongly suppressed the cleavage of caspase-3 in OTUD7B-deficient astrocytes (Fig. 20d), indicating OTUD7B might protect cells from caspase-dependent apoptosis via regulating the kinase activity of RIPK1.

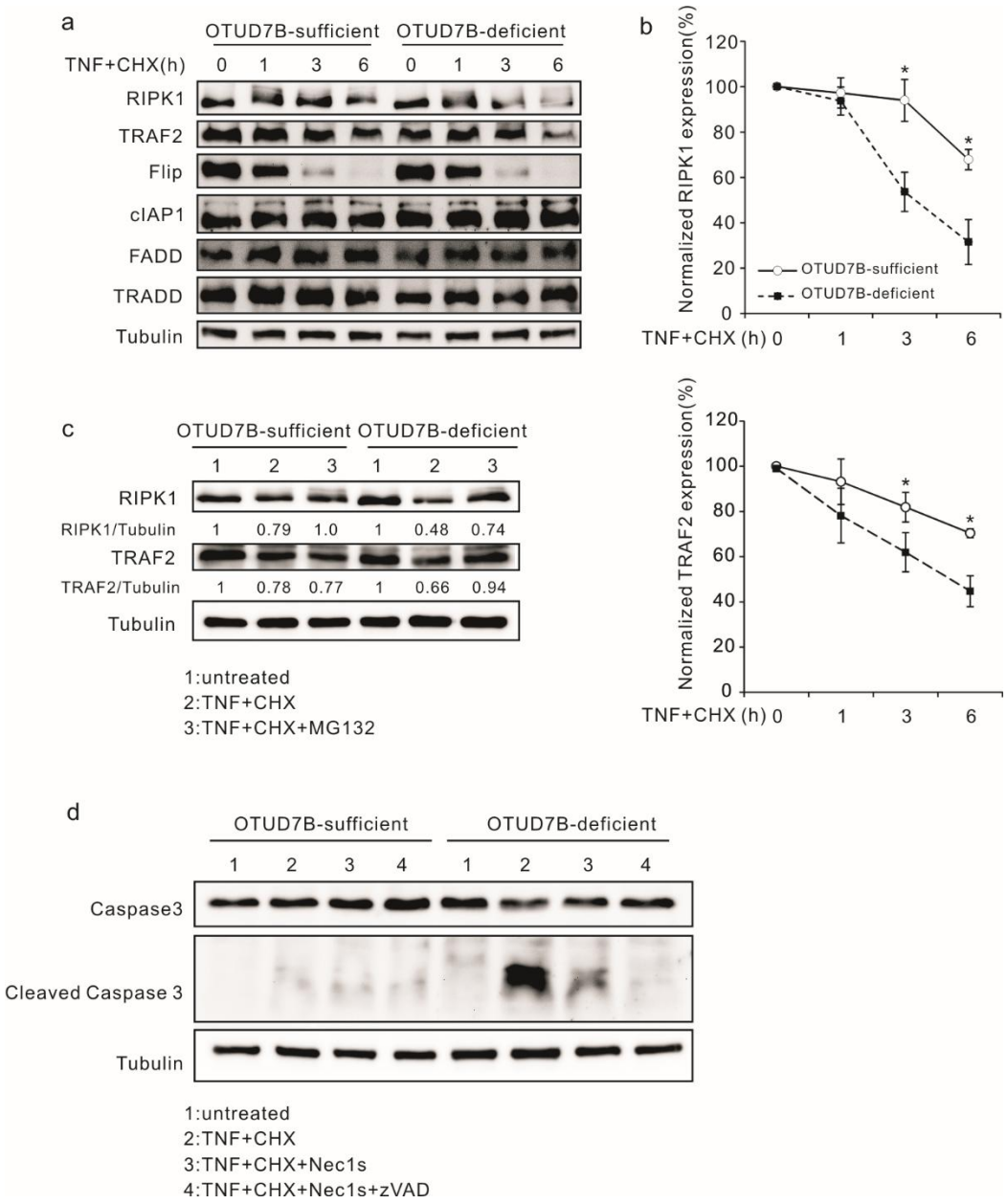

Figure 20. OTUD7B deficiency destabilizes RIPK1 and TRAF2

a. OTUD7B-suficient and -deficient astrocytes were stimulated with TNF plus CHX for the indicated time points and the expression of proteins was evaluated by western blot. b. Quantification of TRAF2 and RIPK1 expression (mean±SEM, *p<0.05). c. OTUD7B-suficient and -deficient astrocytes were treated with TNF, CHX, and MG132 for 6h before harvest for western blot analysis. d. OTUD7B-suficient and -deficient astrocytes were treated with TNF, CHX, and Nec1s/zVAD for 6h before harvest for caspase 3 analysis.

4.3.3 OTUD7B stabilizes TRAF2 and RIPK1 via removing K48-linked ubiquitin chains

Upon TNF stimulation, the TNFR complex undergoes internalization to terminate the activation of the NF-κB pathway and to favor cell death. RIPK1 is attached with K48-linked ubiquitin chains for degradation (Annibaldi, Wicky John et al. 2018), which further mediates the proteasomal degradation of TRAF2 and facilitates the recruitment of caspase-8 and FADD to form complex II. As TNF induces the assembly of K48-linked ubiquitin chains on RIPK1 and TRAF2 for degradation, we investigated whether OTUD7B regulated the proteasomal degradation of RIPK1 and TRAF2 via K48-linked ubiquitination. To this end, we incubated the cells with MG132 to block the degradation of ubiquitinated proteins and we found that OTUD7B reduced TNF-induced reduced K48 poly-ubiquitination of RIPK1 and TRAF2 in OTUD7B-deficient astrocytes compared to OTUD7B-sufficient astrocytes (Fig. 21a, 21b), indicating that OTUD7B protects TRAF2 and RIPK1 from degradation by removing K48-linked ubiquitin chains.

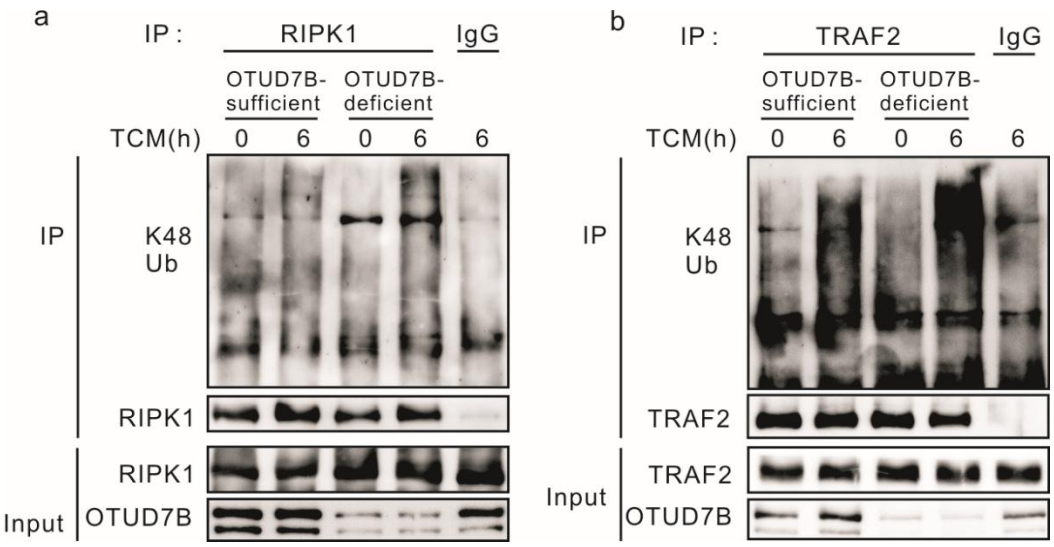

Figure 21. OTUD7B removes K48-linked ubiquitin chains from RIIPK1 and TRAF2

OTUD7B-sufficient and -deficient astrocytes were treated with TNF plus CHX in the presence of MG132. Cells were harvested after 6 h for RIPK1 (1) and TRAF2 (b) immunoprecipitation to determine the statues of K48-linked ubiquitination.

4.3.4 OTUD7B interacts with TRAF2 and RIPK1 in a time-dependent manner

We found that OTUD7B is involved in both pro-inflammatory and cell death signaling triggered by TNF. To investigate how OTUD7B regulates proinflammatory pathways and apoptosis, we immunoprecipitated OTUD7B after different time points of TNF treatment. Here, we found that TRAF2 was associated with OTUD7B under static conditions and the interaction was enhanced after 10 min but dropped after 360 min (Fig. 22). In contrast, RIPK1 bound to OTUD7B only at 360 min post stimulation and the interaction was missing at early time points. These data indicate a dual role of OTUD7B in TNF signaling: (i) OTUD7B suppresses TNF-induced activation of the NF-κB and MAPK by interaction with TRAF2 and reduction of K63-linked ubiquitin chains from RIPK1 at early time points, and (ii) OTUD7B suppresses TNF-induced apoptosis by removing K48-linked ubiquitin chains from RIPK1 leading to stabilization of RIPK1 at later time points.

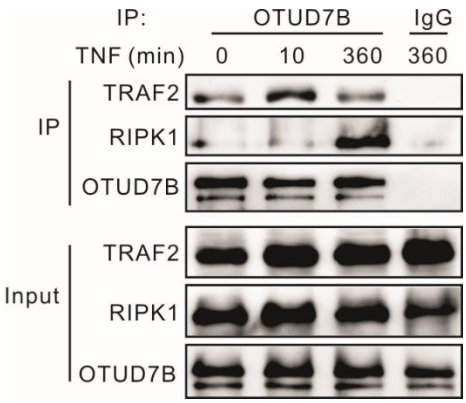

Figure 22. OTUD7B removes K48-linked ubiquitin chains from RIPK1 and TRAF2

Astrocytes were treated with 20 ng/ml TNF for the indicated time point before proteins were harvested for OTUD7B immunoprecipitation. Western blot was performed to determine the interaction of RIPK1 and TRAF2 with OTUD7B.

5. DISCUSSION

Our study identified OTUD7B as a crucial suppressor of astrocyte activation and as an anti-apoptotic molecule in EAE.

Astrocytic OTUD7B ameliorates EAE

We identified that OTUD7B was expressed in multiple tissues and most prominently in the brain of C57BL/6 mice. Also in humans, OTUD7B mRNA is strongly expressed in the brain (Evans, Taylor et al. 2001), implying a more general function of OTUD7B in the CNS of mammals. In the course of EAE, OTUD7B was upregulated in the spinal cord of mice at the peak of disease and declined slightly during remission, which can be reasoned by the finding from Enesa et al. that pro-inflammatory factors upregulate the expression of OTUD7B (Enesa, Zakkar et al. 2008). In this regard, OTUD7B might act as a negative-feedback inhibitor of pro-inflammatory signaling and contribute to the remission of EAE. Likewise, our GEO database analyses indicate that OTUD7B levels were low in MS lesions compared to healthy controls further indicating that a reduction of OTUD7B expression was associates with a failure to terminate an autoimmune response in the CNS. Since OTUD7B was upregulated in astrocytes of wildtype mice with EAE and astrocyte-specific deletion of OTUD7B exacerbated EAE, our data further substantiate the protective function of astrocytic OTUD7B in EAE and extent our understanding of the molecular functions of astrocytes in CNS autoimmunity.

GFAP-Cre OTUD7B$^{fl/fl}$ mice were more susceptible to EAE compared to OTUD7B$^{fl/fl}$ mice, with higher clinical scores and an increased disease incidence. A previous study by Hu et al. showed that conventional OTUD7B knockout mice, which lack OTUD7B in all cells are resistant to EAE due to impaired induction of autoimmune T cells (Hu, Wang et al. 2016). Mechanistically, OTU7B is important for proximal T cell receptor signaling by deubiquitination of tyrosine kinase ZAP70. The study of Hu et al. and our data imply a cell type-dependent function of OTUD7B in CNS diseases. To decipher these cell type-specific functions, we established a conditional OTUD7B mouse strain and focused on the role of OTUD7B in astrocytes. GFAP-Cre OTUD7B$^{fl/fl}$ mice had more severe CNS damage with increased demyelination and inflammation. Correspondingly, we observed more infiltration of CD4^{+} T cells, DCs, and monocytes/macrophages in the spinal cord of GFAP-Cre OTUD7B$^{fl/fl}$

mice, which are the major contributors to the neuroinflammation and demyelination. $CD4^+$ T cells are the primary effectors that initiate the disease and passive transfer of encephalitogenic $CD4^+$ T cells, including GM-CSF^+, IFN-γ^+, and IL-17^+ $CD4^+$ T cells is able to induce EAE (Domingues, Mues et al. 2010, Codarri, Gyulveszi et al. 2011). We detected increased numbers of these encephalitogenic $CD4^+$ T cells in the spinal cord of GFAP-Cre OTUD7B$^{fl/fl}$ mice, which explains the profound CNS damage. In addition, the levels of pro-inflammatory factors were increased in the spinal cord of GFAP-Cre OTUD7B$^{fl/fl}$ mice, which also contribute to neuroinflammation. Our ex vivo transcriptome analysis of astrocytes and the in vitro stimulation of astrocytes uncovered that OTUD7B-deficient astrocytes produced more chemokines, indicating that in astrocytes OTUD7B is an important factor limiting the recruitment of inflammatory leukocytes to the CNS. Collectively, our results identify that OTUD7B is an important factor limiting the pro-inflammatory and disease-promoting activity of astrocytes in EAE.

OTUD7B suppresses TNF-induced proinflammatory response in astrocytes

In EAE, the activation of astrocytes is largely mediated by the cytokines TNF, IFN-γ, and IL-17 produced by autoimmune $CD4^+$ T cells in CNS autoimmunity. The detrimental aspect of EAE is the induction of proinflammatory cytokines, which activate astrocytes via their cognate receptors. Here, we found that OTUD7B-deficient astrocytes showed only a slight difference in cytokine expression upon stimulation with IL-17 and IFN-γ, respectively, whereas activation with TNF induced strongly increased cytokine and chemokine production in OTUD7B-deficient astrocytes. In good agreement, TNF-induced signaling pathways including the NF-κB and MAPK were more activated in OTUD7B-deficient astrocytes, as shown by the enhanced phosphorylation of p65, p38 MAPK and ERK. On the contrary, IL-17 and IFN-γ activated pathways had no significant difference between OTUD7B-sufficient and -deficient astrocytes further suggesting that TNF signaling is the crucial pathway regulated by OTUD7B and the astrocyte-specific protective functions of OTUD7B in EAE rely on the regulation of TNF signaling in astrocytes. This is consistent with previous studies that OTUD7B suppresses TNF and IL-1 signaling (Enesa, Zakkar et al. 2008). However, it is worth noting that the regulation of the NF-κB pathway by OTUD7B is cell type-dependent, in contrast to astrocytes, OTUD7B does not regulate canonical NF-κB signaling in primary mouse embryonic fibroblasts, bone-marrow-derived macrophages, and splenic B cells (Hu, Brittain et al. 2013). The reasons for these cell tape-specific differences are at present unclear,

but may at least partially rely on differences in the amount of expressed cytokine receptors and signal strengths.

TNF is a proinflammatory cytokine and the levels are increased in the CSF and lesions of MS patients (Lock, Hermans et al. 2002, Kostic, Dzopalic et al. 2014). The importance of TNF in MS pathology has been illustrated by the protective effect of TNFR1 blockage in the animal model. Intraperitoneal administration of the TNFR1 inhibitor TROS to transgenic mice expressing human TNFR1 effectively delayed disease onset and improved the disease outcome (Steeland, Van Ryckeghem et al. 2017). Soluble TNF functions through TNFR1, which triggers the activation of the NF-κB and MAPK pathways. The rapid ubiquitination of RIPK1 is crucial in promoting the production of proinflammatory cytokines and chemokines, and RIPK1 K63-polyubiquitin chains works as a docking platform for downstream molecules. OTUD7B has been reported as a negative regulator of TNF signaling (Enesa, Zakkar et al. 2008), it is recruited to TNFR1 complex via UBA domain and removes ubiquitin chains from RIPK1 to terminate the downstream events (Enesa, Zakkar et al. 2008). In good agreement, in our study, RIPK1 K63-linked ubiquitination was enhanced in OTUD7B-deficient astrocytes upon TNF stimulation. However, we could not detect a direct interaction between OTUD7B and RIPK1, indicating that RIPK1 might not be the direct target of OTUD7B. Upon TNF stimulation, TRADD is recruited to TNFR1 and works as a dock for TRAF2 and RIPK1. TRAF2 further recruits the E3 ligase cIAP1/2, which ubiquitinates multiple substrates, including K63-linked ubiquitination of RIPK1 (Bertrand, Milutinovic et al. 2008). The association of TRAF2 with DUBs has been reported that CYLD interacts with TRAF2 to disassembly its K63-linked ubiquitin chains, thereby, suppressing the NF-κB pathway (Kovalenko, Chable-Bessia et al. 2003). OTUD7B contains TRAF binding domain, allowing its interaction with TRAF3 and TRAF6 for deubiquitination (Evans, Taylor et al. 2001, Hu, Brittain et al. 2013). Here, we found that OTUD7B was rapidly recruited to TRAF2 upon TNF stimulation. TRAF2 is reported to undergo K63-linked ubiquitination which is sufficient for the recruitment of downstream molecules (Li, Wang et al. 2009). However, K63-linked ubiquitination of TRAF2 was unchanged in OTUD7B-deficient astrocytes in comparison to OTUD7B-sufficient astrocytes. Of note, complex formation of the DUBs and E3 ligase is widely existing (Komander, Clague et al. 2009), to allow the rapid regulation of ubiquitination on target substrates. In this regard, the complex formation of TRAF2 and OTUD7B has been illustrated by Wang et al, that OTUD7B and TRAF2 oppositely regulate

the ubiquitination of the same substrate GβL in mTOR signaling (Wang, Jie et al. 2017). With respect to TNF stimulated astrocytes, TRAF2 might function as a scaffold for OTUD7B which allows its recognition and cleavage of K63-linked ubiquitin chains on RIPK1. Alternatively, the interaction between TRAF2 and OTUD7B might be required to block the transfer of K63-linked ubiquitination to RIPK1 or OTUD7B might antagonize the E3 ligase activity of TRAF2 to reduce K63 ubiquitination of RIPK1.

OTUD7B protects astrocytes from TNF-induced cell death

Previously, our group has shown that astrocytes contribute to the termination of the intracerebral autoimmune response by the induction of FasL-dependent apoptosis of activated $CD4^+$ T cells (Wang, Haroon et al. 2013). Thus, in addition to pro-inflammatory functions at early stages of EAE, astrocytes play an important role in resolving EAE at later stages of the disease. Further, our group demonstrated that astrocyte gp130-dependent survival of astrocytes contributes to the remission of EAE as mice with astrocytic gp130 deficiency failed to recover from EAE. Mechanistically, cytokines of the IL-6 cytokine family activated gp130 signaling in astrocytes, which prevented astrocytic apoptosis in inflammatory lesions of mice with EAE (Haroon, Drogemuller et al. 2011). In the present study, active EAE lesions were also largely devoid of activated astrocytes in GFAP-Cre $OTUD7B^{fl/fl}$ mice, whereas lesions of control animals showed numerous hypertrophic astrocytes. These histological data indicate that OTUD7B might regulate astrocyte survival in EAE and the aggravated EAE in GFAP-Cre $OTUD7B^{fl/fl}$ mice may also be caused by the loss of astrocytes.

Previous studies have shown that astrocytes in the grey matter of secondary progressive MS patients were cleaved caspase-3 positive (Picon, Jayaraman et al. 2021), indicating that astrocytes undergo apoptosis in MS. However, the reasons for astrocyte death are still unclear. Here, we found that TNF plus CHX treatment triggers in vitro apoptosis of astrocytes. Of note, OTUD7B deficiency leads to enhanced cleavage of caspase 3 upon TNF and CHX treatment, implicating that OTUD7B deficiency sensitizes astrocytes to TNF-induced apoptosis. These results emphasize the importance of OTUD7B in TNF-induced inflammation and apoptosis and indicate the importance of astrocytic OTUD7B in attenuating EAE course and CNS damage.

TNF can induce cell death via the activation of caspases. Here, we found that OTUD7B-deficient astrocytes were more prone to apoptosis upon TNF plus CHX treatment. The apoptosis in OTUD7B-deficient astrocytes was independent of the NF-κB and MAPK activation which is in line with previous reports on apoptosis, RIPK1 and NF-κB activation (Filliol, Piquet-Pellorce et al. 2016). RIPK1 is activated in astrocytes and microglia of MS patients and augments pro-inflammatory signaling (Zelic, Pontarelli et al. 2021). In addition, we identified that RIPK1 can also contribute to astrocyte apoptosis, since RIPK1 inhibition with Nec1s was sufficient to protect OTUD7B-deficient cells from death.

TNF stimulation results in the internalization of TNFR1, which in turn triggers the addition of K48-linked ubiquitin chains on RIPK1 by cIAP1 for proteasomal degradation (Annibaldi, Wicky John et al. 2018). In our study, we observed that the levels of RIPK1 and TRAF2 decreased stronger in OTUD7B-deficient astrocytes upon TNF and CHX treatment. This reduction can be suppressed by the proteasome inhibitor MG132, indicating that OTUD7B protects RIPK1 and TRAF2 from proteasome-mediated degradation. The degradation of RIPK1 is reported to be mediated by E3 ligase cIAP1/2, which conjugate K48-linked ubiquitin chains to RIPK1 (Annibaldi, Wicky John et al. 2018). TRAF2 promotes the survival by adding K48-linked ubiquitin chains on caspase 8 for proteasomal degradation to terminate caspase 8 processing (Gonzalvez, Lawrence et al. 2012). Considering RIPK1 and TRAF2 exert pro-survival and anti-apoptotic roles in TNF signaling (Filliol, Piquet-Pellorce et al. 2016), the reduced levels of TRAF2 and RIPK1 explain the increased apoptosis in OTUD7B-deficient astrocytes. Here, FLIP, TRADD, FADD, and cIAP1 are not regulated by OTUD7B, as the levels were similar in OTUD7B-sufficient and -deficient astrocytes. Previous studies reported that loss of RIPK1 lead to the degradation of cIAP1 (Gentle, Wong et al. 2011), however, we did not observe a reduced level of cIAP1. Moreover, we identified RIPK1 as a target of OTUD7B which removes K48-linked ubiquitination and promotes the formation of complex IIa. The mechanism of TRAF2 degradation is still unclear, it might be 1. RIPK1-dependent, as RIPK1 deficiency in liver parenchymal cells, leads to the reduction of TRAF2 which leads to TNF-induced apoptosis (Filliol, Piquet-Pellorce et al. 2016, Schneider, Gautheron et al. 2017), 2. TNFR2-dependent, though TNFR1 is dominantly expressed on astrocytes than TNFR2, it has been found that TNFR2^{+} astrocytes are present at the border of chronic active lesions (Veroni, Serafini et al. 2020), while engagement with TNFR2 induces TRAF2 degradation and potentiates TNFR1 associated apoptosis (Fotin-Mleczek, Henkler et

al. 2002). Collectively, these findings demonstrated that OTUD7B suppresses apoptosis by stabilizing RIPK1. Of note, necroptosis is not considered as an important cell death pathway in astrocytes. In our study, MLKL levels were low in astrocytes and a previous study by Matija Zelic et.al illustrated that astrocytes are resistant to RIPK1-kinase-mediated necroptosis induced by TNF plus 5Z-7-oxozeaenol, a TAK1 kinase inhibitor or TNF plus Smac mimetic and zVAD (Zelic, Pontarelli et al. 2021).

We identified that OTUD7B regulates early TNF-mediated astrocyte activation and chemokine production and later time points to TNF-dependent apoptosis. The mechanisms on how TNF triggers these distinct cellular outcomes in astrocytes are still unclear. It might depend on the amount of TNF with higher TNF concentration favoring cell death. Additionally, astrocytes are highly heterogeneous and TNF might trigger distinct consequences in different subpopulations of astrocytes. However, our study newly indicates the dynamic interaction of OTUD7B with TRAF2 and RIPK1 is another potential regulator of TNF the diverse functions of TNF in astrocytes.

Conclusion

Our combined in vivo and in vitro studies indicate a dual disease stage-specific and TNF-regulated function of astrocytic OTUD7B in EAE. Early after in vitro stimulation with TNF and upon induction of EAE, OTUD7B suppresses chemokine production of astrocytes and diminishes the recruitment of T cells to the CNS (Fig. 23). Mechanically, OTUD7B is recruited to TRAF2 upon TNF engagement and removes K63-linked ubiquitin chains from RIPK1 to terminate the activation of the NF-κB and MAPK pathways, thereby, suppressing the inflammatory response in astrocytes. At late stage of disease and in vitro, OTUD7B prevents astrocyte apoptosis in TNF-rich environment (Fig. 23), which facilitates the termination of the autoimmune responses and recovery from EAE. In astrocytes, OTUD7B directly interacts with RIPK1 and removes K48-linked ubiquitin chains. In all, our findings emphasized the redundant protective role of OTUD7B in EAE and characterized anti-inflammatory and anti-apoptotic role of OTUD7B in astrocytes upon TNF challenge, therefore providing a promising target for MS treatment.

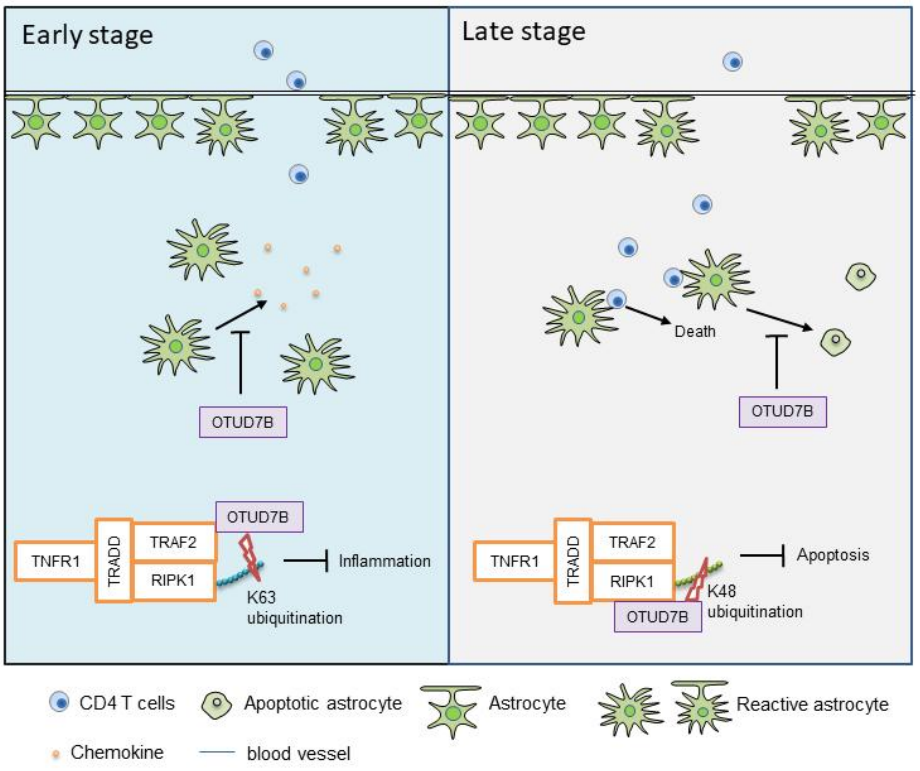

Figure 23. Summary of the study

In our study, we explored the function of OTUD7B in astrocytes during EAE. Astrocytes contribute to the neuroinflammation in EAE by producing chemokines via activating the NF-κB and MAPK pathways, which are suppressed by OTUD7B. Furthermore, OTUD7B protects astrocytes from apoptosis, therefore, restraining the spread of damage.

REFERENCES

Annibaldi, A., S. Wicky John, T. Vanden Berghe, K. N. Swatek, J. Ruan, G. Liccardi, K. Bianchi, P. R. Elliott, S. M. Choi, S. Van Coillie, J. Bertin, H. Wu, D. Komander, P. Vandenabeele, J. Silke and P. Meier (2018). "Ubiquitin-Mediated Regulation of RIPK1 Kinase Activity Independent of IKK and MK2." Mol Cell **69**(4): 566-580 e565.

Belizario, J., L. Vieira-Cordeiro and S. Enns (2015). "Necroptotic Cell Death Signaling and Execution Pathway: Lessons from Knockout Mice." Mediators Inflamm **2015**: 128076.

Bertrand, M. J., S. Lippens, A. Staes, B. Gilbert, R. Roelandt, J. De Medts, K. Gevaert, W. Declercq and P. Vandenabeele (2011). "cIAP1/2 are direct E3 ligases conjugating diverse types of ubiquitin chains to receptor interacting proteins kinases 1 to 4 (RIP1-4)." PLoS One **6**(9): e22356.

Bertrand, M. J., S. Milutinovic, K. M. Dickson, W. C. Ho, A. Boudreault, J. Durkin, J. W. Gillard, J. B. Jaquith, S. J. Morris and P. A. Barker (2008). "cIAP1 and cIAP2 facilitate cancer cell survival by functioning as E3 ligases that promote RIP1 ubiquitination." Mol Cell **30**(6): 689-700.

Blake, P. W. and J. R. Toro (2009). "Update of cylindromatosis gene (CYLD) mutations in Brooke-Spiegler syndrome: novel insights into the role of deubiquitination in cell signaling." Hum Mutat **30**(7): 1025-1036.

Bonacci, T., A. Suzuki, G. D. Grant, N. Stanley, J. G. Cook, N. G. Brown and M. J. Emanuele (2018). "Cezanne/OTUD7B is a cell cycle-regulated deubiquitinase that antagonizes the degradation of APC/C substrates." EMBO J **37**(16).

Borggrewe, M., C. Grit, I. D. Vainchtein, N. Brouwer, E. M. Wesseling, J. D. Laman, B. J. L. Eggen, S. M. Kooistra and E. Boddeke (2021). "Regionally diverse astrocyte subtypes and their heterogeneous response to EAE." Glia **69**(5): 1140-1154.

Brambilla, R., T. Persaud, X. Hu, S. Karmally, V. I. Shestopalov, G. Dvoriantchikova, D. Ivanov, L. Nathanson, S. R. Barnum and J. R. Bethea (2009). "Transgenic inhibition of astroglial NF-kappa B improves functional outcome in experimental autoimmune encephalomyelitis by suppressing chronic central nervous system inflammation." J Immunol **182**(5): 2628-2640.

Brenner, D., H. Blaser and T. W. Mak (2015). "Regulation of tumour necrosis factor signalling: live or let die." Nat Rev Immunol **15**(6): 362-374.

Brown, A. M. and B. R. Ransom (2007). "Astrocyte glycogen and brain energy metabolism." Glia **55**(12): 1263-1271.

Camargo, N., A. Goudriaan, A. F. van Deijk, W. M. Otte, J. F. Brouwers, H. Lodder, D. H. Gutmann, K. A. Nave, R. M. Dijkhuizen, H. D. Mansvelder, R. Chrast, A. B. Smit and M. H. G. Verheijen (2017). "Oligodendroglial myelination requires astrocyte-derived lipids." PLoS Biol **15**(5): e1002605.

Carrillo-de Sauvage, M. A., A. Gomez, C. M. Ros, F. Ros-Bernal, E. D. Martin, A. Perez-Valles, J. M. Gallego-Sanchez, E. Fernandez-Villalba, C. Barcia, Sr., C. Barcia, Jr. and M. T. Herrero (2012). "CCL2-expressing astrocytes mediate the extravasation of T lymphocytes in the brain. Evidence from patients with glioma and experimental models in vivo." PLoS One **7**(2): e30762.

Chen, X., Z. Pang, Y. Wang, L. Zhu, J. Liu and J. Du (2020). "Cezanne contributes to cancer progression by playing a key role in the deubiquitination of IGF-1R." Am J Cancer Res **10**(12): 4342-4356.

Chung, W. S., N. J. Allen and C. Eroglu (2015). "Astrocytes Control Synapse Formation, Function, and Elimination." Cold Spring Harb Perspect Biol **7**(9): a020370.

Codarri, L., G. Gyulveszi, V. Tosevski, L. Hesske, A. Fontana, L. Magnenat, T. Suter and B. Becher (2011). "RORgammat drives production of the cytokine GM-CSF in helper T cells, which is essential for the effector phase of autoimmune neuroinflammation." Nat Immunol **12**(6): 560-567.

Constantinescu, C. S., N. Farooqi, K. O'Brien and B. Gran (2011). "Experimental autoimmune encephalomyelitis (EAE) as a model for multiple sclerosis (MS)." Br J Pharmacol **164**(4): 1079-1106.

Cui, C. P., Y. Zhang, C. Wang, F. Yuan, H. Li, Y. Yao, Y. Chen, C. Li, W. Wei, C. H. Liu, F. He, Y. Liu and L. Zhang (2018). "Dynamic ubiquitylation of Sox2 regulates proteostasis and governs neural progenitor cell differentiation." Nat Commun **9**(1): 4648.

de Almagro, M. C., T. Goncharov, A. Izrael-Tomasevic, S. Duttler, M. Kist, E. Varfolomeev, X. Wu, W. P. Lee, J. Murray, J. D. Webster, K. Yu, D. S. Kirkpatrick, K. Newton and D.

Vucic (2017). "Coordinated ubiquitination and phosphorylation of RIP1 regulates necroptotic cell death." Cell Death Differ **24**(1): 26-37.

de Almagro, M. C., T. Goncharov, K. Newton and D. Vucic (2015). "Cellular IAP proteins and LUBAC differentially regulate necrosome-associated RIP1 ubiquitination." Cell Death Dis **6**: e1800.

De Jager, P. L., X. Jia, J. Wang, P. I. de Bakker, L. Ottoboni, N. T. Aggarwal, L. Piccio, S. Raychaudhuri, D. Tran, C. Aubin, R. Briskin, S. Romano, M. S. G. C. International, S. E. Baranzini, J. L. McCauley, M. A. Pericak-Vance, J. L. Haines, R. A. Gibson, Y. Naeglin, B. Uitdehaag, P. M. Matthews, L. Kappos, C. Polman, W. L. McArdle, D. P. Strachan, D. Evans, A. H. Cross, M. J. Daly, A. Compston, S. J. Sawcer, H. L. Weiner, S. L. Hauser, D. A. Hafler and J. R. Oksenberg (2009). "Meta-analysis of genome scans and replication identify CD6, IRF8 and TNFRSF1A as new multiple sclerosis susceptibility loci." Nat Genet **41**(7): 776-782.

Ding, X., Y. Yan, X. Li, K. Li, B. Ciric, J. Yang, Y. Zhang, S. Wu, H. Xu, W. Chen, A. E. Lovett-Racke, G. X. Zhang and A. Rostami (2015). "Silencing IFN-gamma binding/signaling in astrocytes versus microglia leads to opposite effects on central nervous system autoimmunity." J Immunol **194**(9): 4251-4264.

Domingues, H. S., M. Mues, H. Lassmann, H. Wekerle and G. Krishnamoorthy (2010). "Functional and pathogenic differences of Th1 and Th17 cells in experimental autoimmune encephalomyelitis." PLoS One **5**(11): e15531.

Douanne, T., G. Andre-Gregoire, A. Thys, K. Trillet, J. Gavard and N. Bidere (2019). "CYLD Regulates Centriolar Satellites Proteostasis by Counteracting the E3 Ligase MIB1." Cell Rep **27**(6): 1657-1665 e1654.

Dowling, P., W. Husar, J. Menonna, H. Donnenfeld, S. Cook and M. Sidhu (1997). "Cell death and birth in multiple sclerosis brain." J Neurol Sci **149**(1): 1-11.

Dynek, J. N., T. Goncharov, E. C. Dueber, A. V. Fedorova, A. Izrael-Tomasevic, L. Phu, E. Helgason, W. J. Fairbrother, K. Deshayes, D. S. Kirkpatrick and D. Vucic (2010). "c-IAP1 and UbcH5 promote K11-linked polyubiquitination of RIP1 in TNF signalling." EMBO J **29**(24): 4198-4209.

Ea, C. K., L. Deng, Z. P. Xia, G. Pineda and Z. J. Chen (2006). "Activation of IKK by TNFalpha requires site-specific ubiquitination of RIP1 and polyubiquitin binding by NEMO." Mol Cell **22**(2): 245-257.

Elliott, P. R., S. V. Nielsen, P. Marco-Casanova, B. K. Fiil, K. Keusekotten, N. Mailand, S. M. Freund, M. Gyrd-Hansen and D. Komander (2014). "Molecular basis and regulation of OTULIN-LUBAC interaction." Mol Cell **54**(3): 335-348.

Enesa, K., M. Zakkar, H. Chaudhury, A. Luong le, L. Rawlinson, J. C. Mason, D. O. Haskard, J. L. Dean and P. C. Evans (2008). "NF-kappaB suppression by the deubiquitinating enzyme Cezanne: a novel negative feedback loop in pro-inflammatory signaling." J Biol Chem **283**(11): 7036-7045.

Eugster, H. P., K. Frei, R. Bachmann, H. Bluethmann, H. Lassmann and A. Fontana (1999). "Severity of symptoms and demyelination in MOG-induced EAE depends on TNFR1." Eur J Immunol **29**(2): 626-632.

Evans, P. C., E. R. Taylor, J. Coadwell, K. Heyninck, R. Beyaert and P. J. Kilshaw (2001). "Isolation and characterization of two novel A20-like proteins." Biochem J **357**(Pt 3): 617-623.

Filliol, A., C. Piquet-Pellorce, J. Le Seyec, M. Farooq, V. Genet, C. Lucas-Clerc, J. Bertin, P. J. Gough, M. T. Dimanche-Boitrel, P. Vandenabeele, M. J. Bertrand and M. Samson (2016). "RIPK1 protects from TNF-alpha-mediated liver damage during hepatitis." Cell Death Dis **7**(11): e2462.

Fotin-Mleczek, M., F. Henkler, D. Samel, M. Reichwein, A. Hausser, I. Parmryd, P. Scheurich, J. A. Schmid and H. Wajant (2002). "Apoptotic crosstalk of TNF receptors: TNF-R2-induces depletion of TRAF2 and IAP proteins and accelerates TNF-R1-dependent activation of caspase-8." J Cell Sci **115**(Pt 13): 2757-2770.

French, M. E., C. F. Koehler and T. Hunter (2021). "Emerging functions of branched ubiquitin chains." Cell Discov **7**(1): 6.

Fresegna, D., S. Bullitta, A. Musella, F. R. Rizzo, F. De Vito, L. Guadalupi, S. Caioli, S. Balletta, K. Sanna, E. Dolcetti, V. Vanni, A. Bruno, F. Buttari, M. Stampanoni Bassi, G. Mandolesi, D. Centonze and A. Gentile (2020). "Re-Examining the Role of TNF in MS Pathogenesis and Therapy." Cells **9**(10).

Gentle, I. E., W. W. Wong, J. M. Evans, A. Bankovacki, W. D. Cook, N. R. Khan, U. Nachbur, J. Rickard, H. Anderton, M. Moulin, J. M. Lluis, D. M. Moujalled, J. Silke and D. L. Vaux (2011). "In TNF-stimulated cells, RIPK1 promotes cell survival by stabilizing TRAF2

and cIAP1, which limits induction of non-canonical NF-kappaB and activation of caspase-8." J Biol Chem **286**(15): 13282-13291.

Goncharov, T., K. Niessen, M. C. de Almagro, A. Izrael-Tomasevic, A. V. Fedorova, E. Varfolomeev, D. Arnott, K. Deshayes, D. S. Kirkpatrick and D. Vucic (2013). "OTUB1 modulates c-IAP1 stability to regulate signalling pathways." EMBO J **32**(8): 1103-1114.

Gonzalez-Giraldo, Y., D. A. Forero, G. E. Barreto and A. Aristizabal-Pachon (2021). "Common genes and pathways involved in the response to stressful stimuli by astrocytes: A meta-analysis of genome-wide expression studies." Genomics **113**(2): 669-680.

Gonzalvez, F., D. Lawrence, B. Yang, S. Yee, R. Pitti, S. Marsters, V. C. Pham, J. P. Stephan, J. Lill and A. Ashkenazi (2012). "TRAF2 Sets a threshold for extrinsic apoptosis by tagging caspase-8 with a ubiquitin shutoff timer." Mol Cell **48**(6): 888-899.

Gough, P. and I. A. Myles (2020). "Tumor Necrosis Factor Receptors: Pleiotropic Signaling Complexes and Their Differential Effects." Front Immunol **11**: 585880.

Gregory, A. P., C. A. Dendrou, K. E. Attfield, A. Haghikia, D. K. Xifara, F. Butter, G. Poschmann, G. Kaur, L. Lambert, O. A. Leach, S. Promel, D. Punwani, J. H. Felce, S. J. Davis, R. Gold, F. C. Nielsen, R. M. Siegel, M. Mann, J. I. Bell, G. McVean and L. Fugger (2012). "TNF receptor 1 genetic risk mirrors outcome of anti-TNF therapy in multiple sclerosis." Nature **488**(7412): 508-511.

Haas, T. L., C. H. Emmerich, B. Gerlach, A. C. Schmukle, S. M. Cordier, E. Rieser, R. Feltham, J. Vince, U. Warnken, T. Wenger, R. Koschny, D. Komander, J. Silke and H. Walczak (2009). "Recruitment of the linear ubiquitin chain assembly complex stabilizes the TNF-R1 signaling complex and is required for TNF-mediated gene induction." Mol Cell **36**(5): 831-844.

Hardin-Pouzet, H., M. Krakowski, L. Bourbonniere, M. Didier-Bazes, E. Tran and T. Owens (1997). "Glutamate metabolism is down-regulated in astrocytes during experimental allergic encephalomyelitis." Glia **20**(1): 79-85.

Haroon, F., K. Drogemuller, U. Handel, A. Brunn, D. Reinhold, G. Nishanth, W. Mueller, C. Trautwein, M. Ernst, M. Deckert and D. Schluter (2011). "Gp130-dependent astrocytic survival is critical for the control of autoimmune central nervous system inflammation." J Immunol **186**(11): 6521-6531.

Harrigan, J. A., X. Jacq, N. M. Martin and S. P. Jackson (2018). "Deubiquitylating enzymes and drug discovery: emerging opportunities." Nat Rev Drug Discov **17**(1): 57-78.

Hershko, A. and A. Ciechanover (1998). "The ubiquitin system." Annu Rev Biochem **67**: 425-479.

Hofman, F. M., D. R. Hinton, K. Johnson and J. E. Merrill (1989). "Tumor necrosis factor identified in multiple sclerosis brain." J Exp Med **170**(2): 607-612.

Holbrook, J., S. Lara-Reyna, H. Jarosz-Griffiths and M. McDermott (2019). "Tumour necrosis factor signalling in health and disease." F1000Res **8**.

Hsu, H., H. B. Shu, M. G. Pan and D. V. Goeddel (1996). "TRADD-TRAF2 and TRADD-FADD interactions define two distinct TNF receptor 1 signal transduction pathways." Cell **84**(2): 299-308.

Hsu, H., J. Xiong and D. V. Goeddel (1995). "The TNF receptor 1-associated protein TRADD signals cell death and NF-kappa B activation." Cell **81**(4): 495-504.

Hu, H., G. C. Brittain, J. H. Chang, N. Puebla-Osorio, J. Jin, A. Zal, Y. Xiao, X. Cheng, M. Chang, Y. X. Fu, T. Zal, C. Zhu and S. C. Sun (2013). "OTUD7B controls non-canonical NF-kappaB activation through deubiquitination of TRAF3." Nature **494**(7437): 371-374.

Hu, H., H. Wang, Y. Xiao, J. Jin, J. H. Chang, Q. Zou, X. Xie, X. Cheng and S. C. Sun (2016). "Otud7b facilitates T cell activation and inflammatory responses by regulating Zap70 ubiquitination." J Exp Med **213**(3): 399-414.

Hurwitz, B. J. (2009). "The diagnosis of multiple sclerosis and the clinical subtypes." Ann Indian Acad Neurol **12**(4): 226-230.

Jang, D. I., A. H. Lee, H. Y. Shin, H. R. Song, J. H. Park, T. B. Kang, S. R. Lee and S. H. Yang (2021). "The Role of Tumor Necrosis Factor Alpha (TNF-alpha) in Autoimmune Disease and Current TNF-alpha Inhibitors in Therapeutics." Int J Mol Sci **22**(5).

Ji, Y., L. Cao, L. Zeng, Z. Zhang, Q. Xiao, P. Guan, S. Chen, Y. Chen, M. Wang and D. Guo (2018). "The N-terminal ubiquitin-associated domain of Cezanne is crucial for its function to suppress NF-kappaB pathway." J Cell Biochem **119**(2): 1979-1991.

John Lin, C. C., K. Yu, A. Hatcher, T. W. Huang, H. K. Lee, J. Carlson, M. C. Weston, F. Chen, Y. Zhang, W. Zhu, C. A. Mohila, N. Ahmed, A. J. Patel, B. R. Arenkiel, J. L. Noebels,

C. J. Creighton and B. Deneen (2017). "Identification of diverse astrocyte populations and their malignant analogs." Nat Neurosci **20**(3): 396-405.

Kaltschmidt, B., C. Kaltschmidt, T. G. Hofmann, S. P. Hehner, W. Droge and M. L. Schmitz (2000). "The pro- or anti-apoptotic function of NF-kappaB is determined by the nature of the apoptotic stimulus." Eur J Biochem **267**(12): 3828-3835.

Kang, Z., C. Z. Altuntas, M. F. Gulen, C. Liu, N. Giltiay, H. Qin, L. Liu, W. Qian, R. M. Ransohoff, C. Bergmann, S. Stohlman, V. K. Tuohy and X. Li (2010). "Astrocyte-restricted ablation of interleukin-17-induced Act1-mediated signaling ameliorates autoimmune encephalomyelitis." Immunity **32**(3): 414-425.

Kim, J. W., E. J. Choi and C. O. Joe (2000). "Activation of death-inducing signaling complex (DISC) by pro-apoptotic C-terminal fragment of RIP." Oncogene **19**(39): 4491-4499.

Kliza, K. and K. Husnjak (2020). "Resolving the Complexity of Ubiquitin Networks." Front Mol Biosci **7**: 21.

Komander, D., M. J. Clague and S. Urbe (2009). "Breaking the chains: structure and function of the deubiquitinases." Nat Rev Mol Cell Biol **10**(8): 550-563.

Komiyama, Y., S. Nakae, T. Matsuki, A. Nambu, H. Ishigame, S. Kakuta, K. Sudo and Y. Iwakura (2006). "IL-17 plays an important role in the development of experimental autoimmune encephalomyelitis." J Immunol **177**(1): 566-573.

Kostic, M., T. Dzopalic, S. Zivanovic, N. Zivkovic, A. Cvetanovic, I. Stojanovic, S. Vojinovic, G. Marjanovic, V. Savic and M. Colic (2014). "IL-17 and glutamate excitotoxicity in the pathogenesis of multiple sclerosis." Scand J Immunol **79**(3): 181-186.

Kovalenko, A., C. Chable-Bessia, G. Cantarella, A. Israel, D. Wallach and G. Courtois (2003). "The tumour suppressor CYLD negatively regulates NF-kappaB signalling by deubiquitination." Nature **424**(6950): 801-805.

Lee, T. H., J. Shank, N. Cusson and M. A. Kelliher (2004). "The kinase activity of Rip1 is not required for tumor necrosis factor-alpha-induced IkappaB kinase or p38 MAP kinase activation or for the ubiquitination of Rip1 by Traf2." J Biol Chem **279**(32): 33185-33191.

Li, J., T. McQuade, A. B. Siemer, J. Napetschnig, K. Moriwaki, Y. S. Hsiao, E. Damko, D. Moquin, T. Walz, A. McDermott, F. K. Chan and H. Wu (2012). "The RIP1/RIP3 necrosome forms a functional amyloid signaling complex required for programmed necrosis." Cell **150**(2): 339-350.

Li, K., J. Li, J. Zheng and S. Qin (2019). "Reactive Astrocytes in Neurodegenerative Diseases." Aging Dis **10**(3): 664-675.

Li, S., L. Wang and M. E. Dorf (2009). "PKC phosphorylation of TRAF2 mediates IKKalpha/beta recruitment and K63-linked polyubiquitination." Mol Cell **33**(1): 30-42.

Li, X., Y. Yang and J. D. Ashwell (2002). "TNF-RII and c-IAP1 mediate ubiquitination and degradation of TRAF2." Nature **416**(6878): 345-347.

Liddelow, S. A., K. A. Guttenplan, L. E. Clarke, F. C. Bennett, C. J. Bohlen, L. Schirmer, M. L. Bennett, A. E. Munch, W. S. Chung, T. C. Peterson, D. K. Wilton, A. Frouin, B. A. Napier, N. Panicker, M. Kumar, M. S. Buckwalter, D. H. Rowitch, V. L. Dawson, T. M. Dawson, B. Stevens and B. A. Barres (2017). "Neurotoxic reactive astrocytes are induced by activated microglia." Nature **541**(7638): 481-487.

Lin, D. D., Y. Shen, S. Qiao, W. W. Liu, L. Zheng, Y. N. Wang, N. Cui, Y. F. Wang, S. Zhao and J. H. Shi (2019). "Upregulation of OTUD7B (Cezanne) Promotes Tumor Progression via AKT/VEGF Pathway in Lung Squamous Carcinoma and Adenocarcinoma." Front Oncol **9**: 862.

Lin, Y., A. Devin, Y. Rodriguez and Z. G. Liu (1999). "Cleavage of the death domain kinase RIP by caspase-8 prompts TNF-induced apoptosis." Genes Dev **13**(19): 2514-2526.

Liu, J. S., M. L. Zhao, C. F. Brosnan and S. C. Lee (2001). "Expression of inducible nitric oxide synthase and nitrotyrosine in multiple sclerosis lesions." Am J Pathol **158**(6): 2057-2066.

Lock, C., G. Hermans, R. Pedotti, A. Brendolan, E. Schadt, H. Garren, A. Langer-Gould, S. Strober, B. Cannella, J. Allard, P. Klonowski, A. Austin, N. Lad, N. Kaminski, S. J. Galli, J. R. Oksenberg, C. S. Raine, R. Heller and L. Steinman (2002). "Gene-microarray analysis of multiple sclerosis lesions yields new targets validated in autoimmune encephalomyelitis." Nat Med **8**(5): 500-508.

Lohrberg, M., A. Winkler, J. Franz, F. van der Meer, T. Ruhwedel, N. Sirmpilatze, R. Dadarwal, R. Handwerker, D. Esser, K. Wiegand, C. Hagel, A. Gocht, F. B. Konig, S. Boretius, W. Mobius, C. Stadelmann and A. Barrantes-Freer (2020). "Lack of astrocytes hinders parenchymal oligodendrocyte precursor cells from reaching a myelinating state in osmolyte-induced demyelination." Acta Neuropathol Commun **8**(1): 224.

Ludwin, S. K., V. Rao, C. S. Moore and J. P. Antel (2016). "Astrocytes in multiple sclerosis." Mult Scler **22**(9): 1114-1124.

Luong le, A., M. Fragiadaki, J. Smith, J. Boyle, J. Lutz, J. L. Dean, S. Harten, M. Ashcroft, S. R. Walmsley, D. O. Haskard, P. H. Maxwell, H. Walczak, C. Pusey and P. C. Evans (2013). "Cezanne regulates inflammatory responses to hypoxia in endothelial cells by targeting TRAF6 for deubiquitination." Circ Res **112**(12): 1583-1591.

Mader, J., J. Huber, F. Bonn, V. Dotsch, V. V. Rogov and A. Bremm (2020). "Oxygen-dependent asparagine hydroxylation of the ubiquitin-associated (UBA) domain in Cezanne regulates ubiquitin binding." J Biol Chem **295**(8): 2160-2174.

Madsen, P. M., D. Motti, S. Karmally, D. E. Szymkowski, K. L. Lambertsen, J. R. Bethea and R. Brambilla (2016). "Oligodendroglial TNFR2 Mediates Membrane TNF-Dependent Repair in Experimental Autoimmune Encephalomyelitis by Promoting Oligodendrocyte Differentiation and Remyelination." J Neurosci **36**(18): 5128-5143.

Mayo, L., S. A. Trauger, M. Blain, M. Nadeau, B. Patel, J. I. Alvarez, I. D. Mascanfroni, A. Yeste, P. Kivisakk, K. Kallas, B. Ellezam, R. Bakshi, A. Prat, J. P. Antel, H. L. Weiner and F. J. Quintana (2014). "Regulation of astrocyte activation by glycolipids drives chronic CNS inflammation." Nat Med **20**(10): 1147-1156.

McGinley, M. P., C. H. Goldschmidt and A. D. Rae-Grant (2021). "Diagnosis and Treatment of Multiple Sclerosis: A Review." JAMA **325**(8): 765-779.

Mendel, I., N. Kerlero de Rosbo and A. Ben-Nun (1995). "A myelin oligodendrocyte glycoprotein peptide induces typical chronic experimental autoimmune encephalomyelitis in H-2b mice: fine specificity and T cell receptor V beta expression of encephalitogenic T cells." Eur J Immunol **25**(7): 1951-1959.

Michael, B. D., L. Bricio-Moreno, E. W. Sorensen, Y. Miyabe, J. Lian, T. Solomon, E. A. Kurt-Jones and A. D. Luster (2020). "Astrocyte- and Neuron-Derived CXCL1 Drives Neutrophil Transmigration and Blood-Brain Barrier Permeability in Viral Encephalitis." Cell Rep **32**(11): 108150.

Moreno, M., P. Bannerman, J. Ma, F. Guo, L. Miers, A. M. Soulika and D. Pleasure (2014). "Conditional ablation of astroglial CCL2 suppresses CNS accumulation of M1 macrophages and preserves axons in mice with MOG peptide EAE." J Neurosci **34**(24): 8175-8185.

Mulas, F., X. Wang, S. Song, G. Nishanth, W. Yi, A. Brunn, P. K. Larsen, B. Isermann, U. Kalinke, A. Barragan, M. Naumann, M. Deckert and D. Schluter (2020). "The deubiquitinase OTUB1 augments NF-kappaB-dependent immune responses in dendritic cells in infection and inflammation by stabilizing UBC13." Cell Mol Immunol.

Olsson, T. (1992). "Cytokines in neuroinflammatory disease: role of myelin autoreactive T cell production of interferon-gamma." J Neuroimmunol **40**(2-3): 211-218.

Onizawa, M., S. Oshima, U. Schulze-Topphoff, J. A. Oses-Prieto, T. Lu, R. Tavares, T. Prodhomme, B. Duong, M. I. Whang, R. Advincula, A. Agelidis, J. Barrera, H. Wu, A. Burlingame, B. A. Malynn, S. S. Zamvil and A. Ma (2015). "The ubiquitin-modifying enzyme A20 restricts ubiquitination of the kinase RIPK3 and protects cells from necroptosis." Nat Immunol **16**(6): 618-627.

Palma, J. P., R. L. Yauch, S. Lang and B. S. Kim (1999). "Potential role of CD4+ T cell-mediated apoptosis of activated astrocytes in Theiler's virus-induced demyelination." J Immunol **162**(11): 6543-6551.

Pareja, F., D. A. Ferraro, C. Rubin, H. Cohen-Dvashi, F. Zhang, S. Aulmann, N. Ben-Chetrit, G. Pines, R. Navon, N. Crosetto, W. Kostler, S. Carvalho, S. Lavi, F. Schmitt, I. Dikic, Z. Yakhini, P. Sinn, G. B. Mills and Y. Yarden (2012). "Deubiquitination of EGFR by Cezanne-1 contributes to cancer progression." Oncogene **31**(43): 4599-4608.

Park, Y. H., M. S. Jeong and S. B. Jang (2014). "Death domain complex of the TNFR-1, TRADD, and RIP1 proteins for death-inducing signaling." Biochem Biophys Res Commun **443**(4): 1155-1161.

Pasparakis, M. and P. Vandenabeele (2015). "Necroptosis and its role in inflammation." Nature **517**(7534): 311-320.

Passmore, L. A. and D. Barford (2004). "Getting into position: the catalytic mechanisms of protein ubiquitylation." Biochem J **379**(Pt 3): 513-525.

Patsopoulos, N. A. (2018). "Genetics of Multiple Sclerosis: An Overview and New Directions." Cold Spring Harb Perspect Med **8**(7).

Patsopoulos, N. A., L. F. Barcellos, R. Q. Hintzen, C. Schaefer, C. M. van Duijn, J. A. Noble, T. Raj, Imsgc, Anzgene, P. A. Gourraud, B. E. Stranger, J. Oksenberg, T. Olsson, B. V. Taylor, S. Sawcer, D. A. Hafler, M. Carrington, P. L. De Jager and P. I. de Bakker (2013).

"Fine-mapping the genetic association of the major histocompatibility complex in multiple sclerosis: HLA and non-HLA effects." PLoS Genet **9**(11): e1003926.

Picon, C., A. Jayaraman, R. James, C. Beck, P. Gallego, M. E. Witte, J. van Horssen, N. D. Mazarakis and R. Reynolds (2021). "Neuron-specific activation of necroptosis signaling in multiple sclerosis cortical grey matter." Acta Neuropathol **141**(4): 585-604.

Ponath, G., M. R. Lincoln, M. Levine-Ritterman, C. Park, S. Dahlawi, M. Mubarak, T. Sumida, L. Airas, S. Zhang, C. Isitan, T. D. Nguyen, C. S. Raine, D. A. Hafler and D. Pitt (2018). "Enhanced astrocyte responses are driven by a genetic risk allele associated with multiple sclerosis." Nat Commun **9**(1): 5337.

Raasch, J., N. Zeller, G. van Loo, D. Merkler, A. Mildner, D. Erny, K. P. Knobeloch, J. R. Bethea, A. Waisman, M. Knust, D. Del Turco, T. Deller, T. Blank, J. Priller, W. Bruck, M. Pasparakis and M. Prinz (2011). "IkappaB kinase 2 determines oligodendrocyte loss by non-cell-autonomous activation of NF-kappaB in the central nervous system." Brain **134**(Pt 4): 1184-1198.

Raphael, I., F. Gomez-Rivera, R. A. Raphael, R. R. Robinson, S. Nalawade and T. G. Forsthuber (2019). "TNFR2 limits proinflammatory astrocyte functions during EAE induced by pathogenic DR2b-restricted T cells." JCI Insight **4**(24).

Reboldi, A., C. Coisne, D. Baumjohann, F. Benvenuto, D. Bottinelli, S. Lira, A. Uccelli, A. Lanzavecchia, B. Engelhardt and F. Sallusto (2009). "C-C chemokine receptor 6-regulated entry of TH-17 cells into the CNS through the choroid plexus is required for the initiation of EAE." Nat Immunol **10**(5): 514-523.

Rossi, S., C. Motta, V. Studer, F. Barbieri, F. Buttari, A. Bergami, G. Sancesario, S. Bernardini, G. De Angelis, G. Martino, R. Furlan and D. Centonze (2014). "Tumor necrosis factor is elevated in progressive multiple sclerosis and causes excitotoxic neurodegeneration." Mult Scler **20**(3): 304-312.

Rothhammer, V., D. M. Borucki, E. C. Tjon, M. C. Takenaka, C. C. Chao, A. Ardura-Fabregat, K. A. de Lima, C. Gutierrez-Vazquez, P. Hewson, O. Staszewski, M. Blain, L. Healy, T. Neziraj, M. Borio, M. Wheeler, L. L. Dragin, D. A. Laplaud, J. Antel, J. I. Alvarez, M. Prinz and F. J. Quintana (2018). "Microglial control of astrocytes in response to microbial metabolites." Nature.

Salou, M., B. Nicol, A. Garcia and D. A. Laplaud (2015). "Involvement of CD8(+) T Cells in Multiple Sclerosis." Front Immunol **6**: 604.

Samson, A. L., Y. Zhang, N. D. Geoghegan, X. J. Gavin, K. A. Davies, M. J. Mlodzianoski, L. W. Whitehead, D. Frank, S. E. Garnish, C. Fitzgibbon, A. Hempel, S. N. Young, A. V. Jacobsen, W. Cawthorne, E. J. Petrie, M. C. Faux, K. Shield-Artin, N. Lalaoui, J. M. Hildebrand, J. Silke, K. L. Rogers, G. Lessene, E. D. Hawkins and J. M. Murphy (2020). "MLKL trafficking and accumulation at the plasma membrane control the kinetics and threshold for necroptosis." Nat Commun **11**(1): 3151.

Sanmarco, L. M., M. A. Wheeler, C. Gutierrez-Vazquez, C. M. Polonio, M. Linnerbauer, F. A. Pinho-Ribeiro, Z. Li, F. Giovannoni, K. V. Batterman, G. Scalisi, S. E. J. Zandee, E. S. Heck, M. Alsuwailm, D. L. Rosene, B. Becher, I. M. Chiu, A. Prat and F. J. Quintana (2021). "Gut-licensed IFNgamma(+) NK cells drive LAMP1(+)TRAIL(+) anti-inflammatory astrocytes." Nature **590**(7846): 473-479.

Schneider-Brachert, W., V. Tchikov, J. Neumeyer, M. Jakob, S. Winoto-Morbach, J. Held-Feindt, M. Heinrich, O. Merkel, M. Ehrenschwender, D. Adam, R. Mentlein, D. Kabelitz and S. Schutze (2004). "Compartmentalization of TNF receptor 1 signaling: internalized TNF receptosomes as death signaling vesicles." Immunity **21**(3): 415-428.

Schneider, A. T., J. Gautheron, M. Feoktistova, C. Roderburg, S. H. Loosen, S. Roy, F. Benz, P. Schemmer, M. W. Buchler, U. Nachbur, U. P. Neumann, R. Tolba, M. Luedde, J. Zucman-Rossi, D. Panayotova-Dimitrova, M. Leverkus, C. Preisinger, F. Tacke, C. Trautwein, T. Longerich, M. Vucur and T. Luedde (2017). "RIPK1 Suppresses a TRAF2-Dependent Pathway to Liver Cancer." Cancer Cell **31**(1): 94-109.

Simmons, S. B., E. R. Pierson, S. Y. Lee and J. M. Goverman (2013). "Modeling the heterogeneity of multiple sclerosis in animals." Trends Immunol **34**(8): 410-422.

Skripuletz, T., D. Hackstette, K. Bauer, V. Gudi, R. Pul, E. Voss, K. Berger, M. Kipp, W. Baumgartner and M. Stangel (2013). "Astrocytes regulate myelin clearance through recruitment of microglia during cuprizone-induced demyelination." Brain **136**(Pt 1): 147-167.

Sorensen, T. L., C. Trebst, P. Kivisakk, K. L. Klaege, A. Majmudar, R. Ravid, H. Lassmann, D. B. Olsen, R. M. Strieter, R. M. Ransohoff and F. Sellebjerg (2002). "Multiple sclerosis: a study of CXCL10 and CXCR3 co-localization in the inflamed central nervous system." J Neuroimmunol **127**(1-2): 59-68.

Sowa, M. E., E. J. Bennett, S. P. Gygi and J. W. Harper (2009). "Defining the human deubiquitinating enzyme interaction landscape." Cell **138**(2): 389-403.

Stamatovic, S. M., R. F. Keep, M. M. Wang, I. Jankovic and A. V. Andjelkovic (2009). "Caveolae-mediated internalization of occludin and claudin-5 during CCL2-induced tight junction remodeling in brain endothelial cells." J Biol Chem **284**(28): 19053-19066.

Steeland, S., S. Van Ryckeghem, G. Van Imschoot, R. De Rycke, W. Toussaint, L. Vanhoutte, C. Vanhove, F. De Vos, R. E. Vandenbroucke and C. Libert (2017). "TNFR1 inhibition with a Nanobody protects against EAE development in mice." Sci Rep **7**(1): 13646.

Suk, K., J. Lee, J. Hur, Y. S. Kim, M. Lee, S. Cha, S. Yeou Kim and H. Kim (2001). "Activation-induced cell death of rat astrocytes." Brain Res **900**(2): 342-347.

Szydlowska, K., A. Gozdz, M. Dabrowski, M. Zawadzka and B. Kaminska (2010). "Prolonged activation of ERK triggers glutamate-induced apoptosis of astrocytes: neuroprotective effect of FK506." J Neurochem **113**(4): 904-918.

Toft-Hansen, H., L. Fuchtbauer and T. Owens (2011). "Inhibition of reactive astrocytosis in established experimental autoimmune encephalomyelitis favors infiltration by myeloid cells over T cells and enhances severity of disease." Glia **59**(1): 166-176.

van Loo, G., R. De Lorenzi, H. Schmidt, M. Huth, A. Mildner, M. Schmidt-Supprian, H. Lassmann, M. R. Prinz and M. Pasparakis (2006). "Inhibition of transcription factor NF-kappaB in the central nervous system ameliorates autoimmune encephalomyelitis in mice." Nat Immunol **7**(9): 954-961.

van Oosten, B. W., F. Barkhof, L. Truyen, J. B. Boringa, F. W. Bertelsmann, B. M. von Blomberg, J. N. Woody, H. P. Hartung and C. H. Polman (1996). "Increased MRI activity and immune activation in two multiple sclerosis patients treated with the monoclonal anti-tumor necrosis factor antibody cA2." Neurology **47**(6): 1531-1534.

Veroni, C., B. Serafini, B. Rosicarelli, C. Fagnani, F. Aloisi and C. Agresti (2020). "Connecting Immune Cell Infiltration to the Multitasking Microglia Response and TNF Receptor 2 Induction in the Multiple Sclerosis Brain." Front Cell Neurosci **14**: 190.

Wajant, H. and D. Siegmund (2019). "TNFR1 and TNFR2 in the Control of the Life and Death Balance of Macrophages." Front Cell Dev Biol **7**: 91.

Walton, C., R. King, L. Rechtman, W. Kaye, E. Leray, R. A. Marrie, N. Robertson, N. La Rocca, B. Uitdehaag, I. van der Mei, M. Wallin, A. Helme, C. Angood Napier, N. Rijke and P.

Baneke (2020). "Rising prevalence of multiple sclerosis worldwide: Insights from the Atlas of MS, third edition." Mult Scler **26**(14): 1816-1821.

Walz, W. (2000). "Role of astrocytes in the clearance of excess extracellular potassium." Neurochem Int **36**(4-5): 291-300.

Wang, B., Z. Jie, D. Joo, A. Ordureau, P. Liu, W. Gan, J. Guo, J. Zhang, B. J. North, X. Dai, X. Cheng, X. Bian, L. Zhang, J. W. Harper, S. C. Sun and W. Wei (2017). "TRAF2 and OTUD7B govern a ubiquitin-dependent switch that regulates mTORC2 signalling." Nature **545**(7654): 365-369.

Wang, H., H. Meng, X. Li, K. Zhu, K. Dong, A. K. Mookhtiar, H. Wei, Y. Li, S. C. Sun and J. Yuan (2017). "PELI1 functions as a dual modulator of necroptosis and apoptosis by regulating ubiquitination of RIPK1 and mRNA levels of c-FLIP." Proc Natl Acad Sci U S A **114**(45): 11944-11949.

Wang, J. H., X. P. Zhong, Y. F. Zhang, X. L. Wu, S. H. Li, P. E. Jian, Y. H. Ling, M. Shi, M. S. Chen, W. Wei and R. P. Guo (2017). "Cezanne predicts progression and adjuvant TACE response in hepatocellular carcinoma." Cell Death Dis **8**(9): e3043.

Wang, L., F. Du and X. Wang (2008). "TNF-alpha induces two distinct caspase-8 activation pathways." Cell **133**(4): 693-703.

Wang, X., M. Deckert, N. T. Xuan, G. Nishanth, S. Just, A. Waisman, M. Naumann and D. Schluter (2013). "Astrocytic A20 ameliorates experimental autoimmune encephalomyelitis by inhibiting NF-kappaB- and STAT1-dependent chemokine production in astrocytes." Acta Neuropathol **126**(5): 711-724.

Wang, X., F. Haroon, S. Karray, D. Martina and D. Schluter (2013). "Astrocytic Fas ligand expression is required to induce T-cell apoptosis and recovery from experimental autoimmune encephalomyelitis." Eur J Immunol **43**(1): 115-124.

Wang, X., F. Mulas, W. Yi, A. Brunn, G. Nishanth, S. Just, A. Waisman, W. Bruck, M. Deckert and D. Schluter (2019). "OTUB1 inhibits CNS autoimmunity by preventing IFN-gamma-induced hyperactivation of astrocytes." EMBO J.

Wertz, I. E., K. M. O'Rourke, H. Zhou, M. Eby, L. Aravind, S. Seshagiri, P. Wu, C. Wiesmann, R. Baker, D. L. Boone, A. Ma, E. V. Koonin and V. M. Dixit (2004). "De-ubiquitination and ubiquitin ligase domains of A20 downregulate NF-kappaB signalling." Nature **430**(7000): 694-699.

Wheeler, M. A., I. C. Clark, E. C. Tjon, Z. Li, S. E. J. Zandee, C. P. Couturier, B. R. Watson, G. Scalisi, S. Alkwai, V. Rothhammer, A. Rotem, J. A. Heyman, S. Thaploo, L. M. Sanmarco, J. Ragoussis, D. A. Weitz, K. Petrecca, J. R. Moffitt, B. Becher, J. P. Antel, A. Prat and F. J. Quintana (2020). "MAFG-driven astrocytes promote CNS inflammation." Nature **578**(7796): 593-599.

Wheeler, M. A., M. Jaronen, R. Covacu, S. E. J. Zandee, G. Scalisi, V. Rothhammer, E. C. Tjon, C. C. Chao, J. E. Kenison, M. Blain, V. T. S. Rao, P. Hewson, A. Barroso, C. Gutierrez-Vazquez, A. Prat, J. P. Antel, R. Hauser and F. J. Quintana (2019). "Environmental Control of Astrocyte Pathogenic Activities in CNS Inflammation." Cell **176**(3): 581-596 e518.

Williams, J. L., S. Manivasagam, B. C. Smith, J. Sim, L. L. Vollmer, B. P. Daniels, J. H. Russell and R. S. Klein (2020). "Astrocyte-T cell crosstalk regulates region-specific neuroinflammation." Glia **68**(7): 1361-1374.

Woo, S. M. and T. K. Kwon (2019). "E3 ubiquitin ligases and deubiquitinases as modulators of TRAIL-mediated extrinsic apoptotic signaling pathway." BMB Rep **52**(2): 119-126.

Wu, X., S. Liu, C. Sagum, J. Chen, R. Singh, A. Chaturvedi, J. R. Horton, T. R. Kashyap, D. Fushman, X. Cheng, M. T. Bedford and B. Wang (2019). "Crosstalk between Lys63- and Lys11-polyubiquitin signaling at DNA damage sites is driven by Cezanne." Genes Dev **33**(23-24): 1702-1717.

Yan, Y., X. Ding, K. Li, B. Ciric, S. Wu, H. Xu, B. Gran, A. Rostami and G. X. Zhang (2012). "CNS-specific therapy for ongoing EAE by silencing IL-17 pathway in astrocytes." Mol Ther **20**(7): 1338-1348.

Yang, Y., M. S. Islam, Y. Hu and X. Chen (2021). "TNFR2: Role in Cancer Immunology and Immunotherapy." Immunotargets Ther **10**: 103-122.

Yi, W., D. Schluter and X. Wang (2019). "Astrocytes in multiple sclerosis and experimental autoimmune encephalomyelitis: Star-shaped cells illuminating the darkness of CNS autoimmunity." Brain Behav Immun **80**: 10-24.

Yue, J. and J. M. Lopez (2020). "Understanding MAPK Signaling Pathways in Apoptosis." Int J Mol Sci **21**(7).

Zelic, M., F. Pontarelli, L. Woodworth, C. Zhu, A. Mahan, Y. Ren, M. LaMorte, R. Gruber, A. Keane, P. Loring, L. Guo, T. H. Xia, B. Zhang, P. Orning, E. Lien, A. Degterev, T. Hammond

and D. Ofengeim (2021). "RIPK1 activation mediates neuroinflammation and disease progression in multiple sclerosis." Cell Rep **35**(6): 109112.

DECLARATION OF ORIGINALITY

Hiermit erkläre ich, dass ich die von mir eingereichte Dissertation zu dem Thema

Astrocyte-specific function of OTUD7B

in experimental autoimmune encephalomyelitis

selbstständig verfasst, nicht bereits als Dissertation verwendet habe und die benutzten Hilfsmittel und Quellen vollständig angegeben wurden.

Weiterhin erkläre ich, dass ich weder diese noch eine andere Arbeit zur Erlangung des akademischen Grades doctor rerum naturalium (Dr. rer. nat.) an anderen Einrichtungen eingereicht habe.

Hannover, 10.12.2021

Wenjing Yi

DECLARATION OF HONOR

Ich versichere hiermit, dass ich die vorliegende Arbeit ohne unzulässige Hilfe Dritter und ohne Benutzung anderer als der angegebenen Hilfsmittel angefertigt habe; verwendete fremde und eigene Quellen sind als solche kenntlich gemacht.

Ich habe insbesondere nicht wissentlich:

- Ergebnisse erfunden oder widersprüchliche Ergebnisse verschwiegen,
- statistische Verfahren absichtlich missbraucht, um Daten in ungerechtfertigter Weise zu interpretieren,
- fremde Ergebnisse oder Veröffentlichungen plagiiert,
- fremde Forschungsergebnisse verzerrt wiedergegeben.

Mir ist bekannt, dass Verstöße gegen das Urheberrecht Unterlassungs- und Schadensersatzansprüche des Urhebers sowie eine strafrechtliche Androhung durch die Strafverfolgungsbehörden begründen kann.

Ich erkläre mich damit einverstanden, dass die Arbeit ggf. mit Mitteln der elektronischen Datenverarbeitung auf Plagiate überprüft werden kann.

Die Arbeit wurde bisher weder im Inland noch im Ausland in gleicher oder ähnlicher Form als Dissertation eingereicht und ist als Ganzes auch noch nicht veröffentlicht.

Hannover, 10.12.2021

Wenjing Yi